TECHNISCHE UNIVERSITÄT MÜNCHEN
Ingenieurfakultät Bau Geo Umwelt
Fachgebiet für Risikoanalyse und Zuverlässigkeit

Quantifying the Reliability and Effectiveness of Early Warning Systems for Natural Hazards

Martina Sättele

Vollständiger Abdruck der von der Ingenieurfakultät Bau Geo Umwelt der Technischen Universität München zur Erlangung des akademischen Grades eines

Doktor - Ingenieurs

genehmigten Dissertation.

Vorsitzender: Univ.-Prof. Dr. T. Wunderlich

Prüfer der Dissertation:
1. Univ.-Prof. Dr. D. Straub
2. Univ.-Prof. Dr. M. Krautblatter

Die Dissertation wurde am 18.03.2015 bei der Technischen Universität München eingereicht und durch die Ingenieurfakultät Bau Geo Umwelt am 31.05.2015 angenommen.

Abstract

Worldwide, early warning systems (EWS) are increasingly operated to prevent the damage and loss of life caused by natural disasters and smaller but destructive events. EWS are part of an integrated risk management approach, which comprises alternative mitigation measures to reduce risks imposed by natural hazards. Through timely information, EWS enable endangered persons and risk managers to set up preventive mitigation measures and avoid damage and loss of life. EWS are, compared to structural prevention measures such as dams, nets or galleries, cheap, flexible and have a minor impact on the environment. However, to identify optimal mitigation strategies, their effect on risk reduction and life cycle costs should be compared to alternative mitigation measures in cost-effectiveness analyses. Existing guidelines describe detailed procedures for the evaluation of structural mitigation measures, but not for the evaluation of complex and often human-centered EWS. The aim of this thesis is to close the existing gap and provide a framework approach for the evaluation of the effectiveness achieved with EWS. In addition, a guideline summarizes major findings in a simplified form to support practitioners in the development and operation of cost-effective EWS.

The development of a sophisticated and applicable framework approach is achieved in three main objectives, using theoretical and empirical methods. The first objective is to develop a novel, generic classification for EWS. This classification distinguishes between alarm systems (AS), warning systems (WS) and forecasting systems (FS) and enables a structured evaluation of EWS. AS are fully automated, threshold-based systems. They are installed to detect ongoing, spontaneously triggered processes such as earthquakes, debris flows and wildfires. WS use thresholds to detect precursors of processes that evolve over time, such as high-magnitude rockfalls, tsunamis and volcanic eruptions. This timely information enables experts to analyze the data in detail and set up intervention measures if necessary. FS have the lowest degree of automation. Here, experts analyze precursors at regular intervals to predict the occurrence probability of spontaneous events, such as snow avalanches and severe weather, on a regional scale. The novel classification is verified by applying it to a selection of modern EWS operated worldwide. The second objective is to identify those factors that have a major influence on the reliability and effectiveness in different EWS classes. In two detailed case studies, the reliability and effectiveness of an AS and a WS are assessed and optimized. For this evaluation, methods tailored to the individual EWS classes are developed. The reliability of automated AS can be modeled in Bayesian networks (BN) and depends on selected monitoring strategies, including sensor type, amount and positioning, of sensors, on thresholds and on the failure probabilities of system components. An evaluation of partly automated WS is more complex and must account for additional factors such as the accuracy of applied models and the influence of human decision-making. The third objective is to derive a framework approach for the evaluation of EWS, which constitutes the major result of this thesis.

In the novel framework approach, the effectiveness is measured as a function of the reliability, as is common practice for the evaluation of structural measures. The framework comprises three main parts: in the first two parts the reliability of EWS is quantified in a binary approach and expressed in terms of the probability that an event is detected (POD) and the probability that false alarms are issued (PFA). A reliability analysis of automated AS and the automated parts of WS and FS is conducted in the first part, before the reliability of the non-automated parts is assessed in the second analysis. In both reliability analyses, the technical and the inherent reliability are considered. The technical reliability accounts for the failure of system components and their configuration within the system. The inherent reliability describes the ability of the EWS to distinguish between hazard and noise. For the reliability analysis of automated parts, a tailored method is provided in which the reliability is modeled in a six step BN. The reliability analysis of complex, non-automated EWS parts is described in five steps. In the third part, POD and PFA (i.e. the reliability) are used to calculate the effectiveness. Hereby, both positive effects on risk reduction, due to timely information and negative consequences such as a reduced compliance caused by frequent false alarms, are considered.

In combination with the EWS classification and the case study results, this novel framework approach provides a valuable basis for the evaluation of EWS. In the future, this framework should be applied, tested and enhanced to create a convenient evaluation tool, enabling the optimization of EWS, their comparability with alternative risk mitigation measures and the identification of optimal warning strategies in the field of natural hazards.

Zusammenfassung

Weltweit werden Frühwarnsysteme (FWS) vermehrt zum Schutz vor Naturkatastrophen und vor kleineren aber zerstörerischen Ereignissen eingesetzt. Sie sind Teil eines ganzheitlichen Ansatzes für das Risikomanagement von Naturgefahren, welcher Massnahmen zur Vorbeugung, zur Intervention und Wiederherstellung beinhaltet. FWS wirken vorbeugend, indem sie durch frühzeitige Informationen vorwiegend Personenschäden in gefährdeten Siedlungen und auf Strassen und Schienen verhindern. Im Vergleich zu baulichen Massnahmen wie Dämmen, Galerien oder Netzen sind FWS kostengünstig, flexibel und verändern das Landschaftsbild nur wenig. Um optimale Strategien für den Schutz vor Naturgefahren zu entwickeln, müssen FWS in Kosten-Wirksamkeitsanalysen mit alternativen Massnahmen verglichen werden. Damit ein solcher Vergleich möglich ist, muss bewertet werden, inwieweit FWS ein bestimmtes Risiko minimieren. In bestehenden Leitfäden sind detaillierte Vorgehensweisen zur Bewertung der Wirksamkeit von baulichen Massnahmen beschrieben, aber nicht für FWS. Gegenstand dieser Arbeit ist es, ein allgemeingültiges Vorgehen zur Bewertung von komplexen FWS, die oft von menschlichen Entscheidungen abhängen, zu entwickeln. Zusätzlich wird eine Praxishilfe erstellt, die die wichtigsten Ergebnisse für Entscheidungsträger in einer vereinfachten Form zusammenfasst.

Die Entwicklung dieses Vorgehens beinhaltet das Erreichen von drei Teilzielen. Dabei werden sowohl theoretische als auch empirische Methoden angewendet. Das erste Teilziel ist die Entwicklung einer Klassifizierung für alle FWS weltweit. Diese neue Klassifizierung unterscheidet Alarmsysteme (AS), Warnsysteme (WS) und Vorhersagesysteme (VS) und ermöglicht eine strukturierte Bewertung von FWS. AS sind voll automatisierte Systeme, die auf Schwellenwerten beruhen. Sie werden installiert um spontane Ereignisse wie Erdbeben, Murgänge und Waldbrände nach deren Entstehung zu erkennen. WS basieren ebenfalls auf Schwellenwerten, allerdings erfassen sie Vorzeichen von Ereignissen, die sich wie z.B. grössere Felsbewegungen, Tsunamis und Vulkanausbrüche, über längere Zeit entwickeln. Experten erhalten zeitnah Informationen über relevante Veränderungen. Sie analysieren die Daten und leiten, wenn notwendig, Evakuierungen ein. VS besitzen den niedrigsten Automatisierungsgrad. Um die Eintrittswahrscheinlichkeit von spontanen Prozessen wie Lawinen und extremen Wettersituationen für bestimmte Warnregionen vorhersagen zu können, analysieren Experten regelmässig die aktuelle Lage. Diese neue Klassifizierung kann durch Anwendung auf eine Auswahl an aktiven FWS verifiziert werden. Das zweite Teilziel ermittelt Faktoren, welche die Wirksamkeit von FWS in den unterschiedlichen Klassen bestimmen. Dazu wird in zwei detaillierten Fallstudien die Zuverlässigkeit und die Wirksamkeit eines AS und WS mit speziell entwickelten Methoden bewertet und optimiert. Die Zuverlässigkeit von AS kann

in Bayesian Netzwerken (BN) quantifiziert werden und hängt massgeblich von der Art, Anzahl und der Position der Sensoren, von den voreingestellten Schwellenwerten und den Ausfallwahrscheinlichkeiten einzelner Komponenten ab. Die Bewertung des teilautomatisierten WS ist weitaus komplexer und muss Einflüsse wie Modellgenauigkeiten und die Qualität von menschlichen Entscheidungen berücksichtigen. Das dritte Teilziel ist die Entwicklung eines allgemein anwendbaren Vorgehens zur Bewertung von FWS.

Innerhalb dieses neuen Vorgehens wird die Wirksamkeit direkt von der Zuverlässigkeit des FWS abgeleitet. Ein solches Vorgehen wird üblicherweise zur Bewertung von baulichen Massnahmen angewendet und beinhaltet für FWS drei Teile. In den ersten beiden Teilen wird die Zuverlässigkeit binär, über die Wahrscheinlichkeit, dass ein Ereignis vom FWS detektiert wird (Probability of detection POD) und keine falschen Alarme ausgelöst werden (Probability of false alarms PFA), bemessen. In der ersten Zuverlässigkeitsanalyse werden voll automatisierte AS und automatisierte Teile von WS und VS und in der zweiten Analyse, nicht automatisierte Teile betrachtet. In beiden Analysen wird erstmals sowohl die technische als auch die inhärente Zuverlässigkeit berücksichtigt. Die technische Zuverlässigkeit hängt von der Ausfallwahrscheinlichkeit einzelner Komponenten und deren Anordnung im FWS ab. Die inhärente Zuverlässigkeit beschreibt die Fähigkeit des FWS, zwischen gefährlichen Ereignissen und Störsignalen zu unterscheiden. Die Bewertung der Zuverlässigkeit von automatisierten FWS erfolgt in einem BN in sechs Schritten. Die Bewertung von komplexen, nicht automatisierten Systemteilen erfolgt in fünf Schritten. Im dritten und letzten Teil wird die Wirksamkeit als Funktion von POD und PFA, also der Zuverlässigkeit, berechnet. Um das reduzierte Risiko zu bestimmen, werden sowohl positive als auch negative Effekte, die mit FWS einherkommen, berücksichtigt. Während zeitnahe Informationen eine positive Wirkung erzielen, da gefährdete Personen und Objekte evakuiert werden können, wirken sich häufige Fehlalarme oder zu kurze Vorwarnzeiten negativ auf das Befolgen von ausgesprochenen Warnungen aus.

In Kombination mit der Klassifizierung bildet dieses neu entwickelte Vorgehen eine wertvolle Grundlage zur Bewertung von FWS. Damit in Zukunft optimale Strategien zum Schutz vor Naturgefahren bestimmt werden können, sollte dieses Vorgehen weiter angewendet, getestet und in ein Softwaretool integriert werden.

Acknowledgements

First of all, I want to thank Michael Bründl, my supervisor at the WSL Institute for Snow and Avalanche Research (SLF), who developed the project idea and launched the whole project with the financial support of the Swiss Federal Office for Civil Protection (FOCP). He gave me the chance to enhance my engineering background and project and risk management skills in the area of "natural hazards". He gave me the opportunity to work in an area of personal interest, supported me and always believed in my skills.

I am particularly grateful to Prof. Daniel Straub, who decided to support me methodically and did an exceptionally great job. He supported and motivated me continuously and educated me in the field of reliability analysis and the application of methods. With his continuous and straightforward support, I was able to conduct a well-structured project and gain valuable results. I would also like to sincerely thank my second supervisor, Prof. Michael Krautblatter, who actively supported me in the Preonzo case study and the establishment of this thesis.

Christoph Werner from the FOCP did not only enable the project from a financial point of view, he has been actively involved in the development of the content and the structure of the guideline for practitioners. He also enabled a constant exchange of information with practitioners. In this context, I would also like to thank members of the expert group for their efforts: Estelle Grüter (MeteoSwiss), Markus Wüthrich (FOCP) and Hugo Rätzo (Swiss Federal Office for the Environment). In addition, I would like to thank Lorenz Meier, CEO of GEOPREAVENT AG, who collaborated closely with me and shared his great experience and knowledge about EWS.

I would also like to thank my numerous supporters: Christoph Graf, Giorgio Valenti and Marco Franzi, Nils Hählen, Christian Wilhelm, Marc Hauser, Urban Rieder, Christoph Nänni-Brun, Andreas Huwiler, Ueli Gruner, Hansueli Gubler, Sally Potter, Anton Lehnherr, Charles Schmid, Heinz Müller, Hans-Jörg Häberle, Marco Conedera, Willi Werlen, Lukas Eiholzer, Rudolf Krähenbühl, Josef Hess, Thomas Meisel, Karsten Jasper, Therese Bürgi, Massimiliano Zappa, Hans Bettschen, Daniel Streit, Bernhard Wehren, John Clinton, Stefan Brem and all those who contributed to my work.

For the great time I had at SLF and in Davos, I want to thank my friends and colleagues. Finally I would like to thank my mother, my sister and Sven Sturzenegger, who were always with me.

Martina Sättele March, 2015

Contents

List of Figures

List of Tables

Abbreviations

AS	**A**larm **S**ystem
BN	**B**ayesian **N**etwork
CDF	**C**umulative **D**ensity **F**unction
CPT	**C**onditional **P**robability **T**able
DG	**D**ecision **G**raph
EWS	**E**arly **W**arning **S**ystem
FOCP	**F**ederal **O**ffice for **C**ivil **P**rotection
FS	**F**orecasting **S**ystem
GLOF	**G**lacier **L**ake **O**utburst **F**lood
MC	**M**onte **C**arlo
MTBF	**M**ean **T**ime **B**etween **F**ailures
MTTF	**M**ean **T**ime **T**o **F**ailures
PDF	**P**robability **D**ensity **F**unction
PFA	**P**robability of **F**alse **A**larms
POD	**P**robability **o**f **D**etection
ROC	**R**eceiver **O**perator **C**haracteristic
RWS	**R**ockfall **W**arning **S**ystem
SLF	Institute for Snow and Avalanche Research
WS	**W**arning **S**ystem

Chapter 1

Introduction

1.1 Risk Management for Natural Hazards

Natural disasters cause increasing economic loss and affect larger parts of the population (Guha-Sapir et al., 2013; UNISDR, 2007a). Major disasters, such as the Indian Ocean earthquake and tsunami in 2004, the Atlantic hurricanes Katrina and Sandy in 2005 and 2012, the Haiti earthquake in 2010, the subsequent tsunami catastrophe in Japan in 2011 and recently, the typhoon in the Philippines in 2013, raised public awareness and forced decision-makers to invest into preparedness. In the future, climate change, economic growth and social shifts may reinforce this development (SwissRe, 2014). An increasing frequency and magnitude of extreme weather events is expected to increase the number of flood and landslide events (Van Aalst, 2006; Vellinga and van Verseveld, 2000). In areas affected by permafrost and rapid deglaciation, higher frequencies of rock slope failures may occur (Huggel et al., 2012; Krautblatter et al., 2013). In parallel, demographic changes resulting in increased exposure of persons to dangerous scenarios and the growing value of public infrastructures and economic assets will rise the risk potential (Lall and Deichmann, 2011).

For the management of risks imposed by natural hazards, comprehensive guidelines have been provided. In 2000, the Australian Geomechanics Society published one of the first guidelines for the risk management of landslides (AGS, 2000). The concept is aligned to the generic risk management concept AS/NZS 4360:1999 “Risk Management” and includes processes to analyze, assess and treat risks. In the meantime, different institutions adopted the concept and published similar frameworks or guidelines for the management of landslide risk (Dai et al., 2002; Fell et al., 2005; Safeland, 2011). A basic framework for the management of flood risks was developed in Germany (Schanze, 2006), including similar processes for risk analysis, assessment and reduction. In Switzerland, a comprehensive framework approach (Figure 1.1) was developed to manage and treat the risk imposed by landslides, snow avalanches, floods, storms, hail, earthquakes and heat waves (Bründl et al., 2009). This framework was recently adopted by e.g. Smith (2013) as a generic approach for risk management in the field of natural hazards.

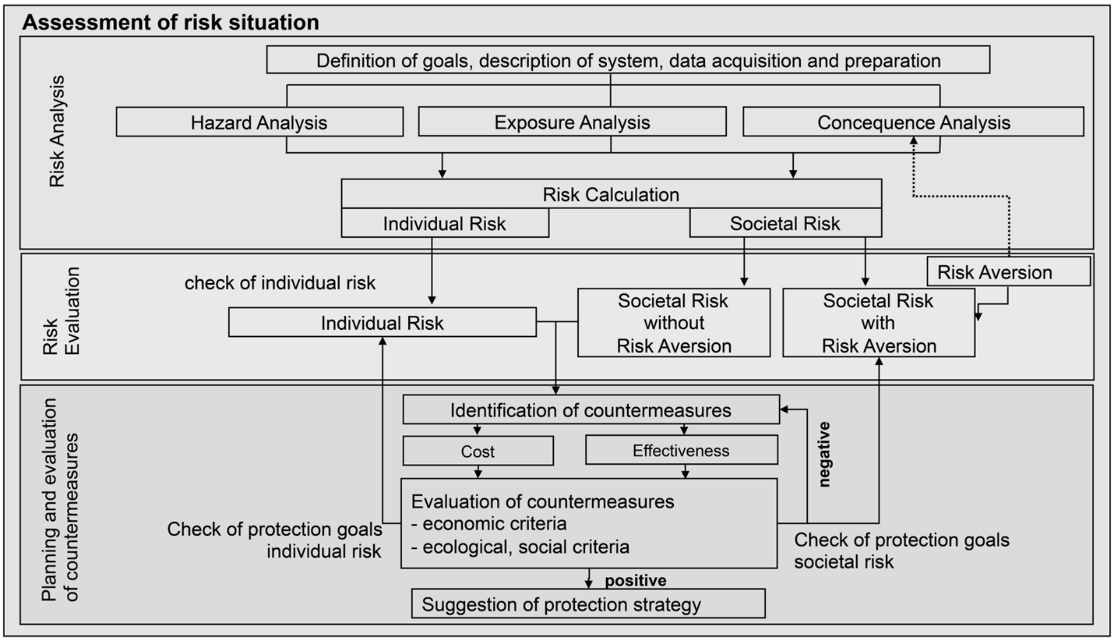

FIGURE 1.1: An Integrative Risk Management Concept: includes processes to analyze, evaluate and mitigate the risk (Bründl et al., 2009).

In modern risk management frameworks, the risk of natural hazards is quantified following an early definition developed by the former United Nations Office for Disaster Risk Reduction (UNDRO, 1980). They quantify the risk of natural hazards as the probability of the occurrence of an event and its consequences. The consequences of an event depend on the exposure probability and the vulnerability of elements at risk, and can be quantified from the associated damage. In modern approaches, the risk $R_{i,j}$ of an object i in a specific scenario j is calculated as:

$$R_{i,j} = p_j \times pe_{i,j} \times V_{i,j} \times A_i \tag{1.1}$$

The probability of the occurrence of scenario j is represented by p_j, $pe_{i,j}$ is the exposure probability of object i at risk in scenario j, $V_{i,j}$ represents the vulnerability of object i in scenario j; and A_i is the value of object i (Bründl et al., 2009; Fuchs et al., 2007). The overall risk R is evaluated by summing or integrating over all possible scenarios and exposed objects:

$$R = \sum_{j=1}^{n_{scen}} \sum_{i=1}^{n_{obj}} R_{i,j} \tag{1.2}$$

1.2 Risk Mitigation Strategies

To mitigate the risk of natural hazards, integrated risk management approaches comprise mitigation measures to prepare against, respond to and recover from disasters caused by natural hazards (FOCP, 2012). In the last few years, the focus of risk mitigation strategies has clearly shifted from response and recovery towards preventive mitigation strategies (UNISDR, 2007a). To increase the preparedness, early warning systems (EWS) are frequently applied as emergency provisions (Figure 1.2). They "provide timely and effective information and allow endangered individuals to take actions, prepare for effective response and avoid damage" (UNISDR, 2007b). In contrast to structural mitigation measures such as dams and galleries, EWS have low life-cycle costs, are highly flexible and have a low impact on the environment (Intrieri et al., 2012; Villagrán de Leon et al., 2013; Hattenberger and Wöllik, 2008).

The identification of an optimal risk mitigation strategy remains a major challenge for decision-makers. Existing guidelines recommend that the mitigation measures with minimal costs C_R leading to maximal risk reduction ΔR, are selected in a cost-benefit analysis (Penning-Rowsell et al., 2005; SafeLand, 2012; Špačková and Straub, 2014). This ratio between the risk reduction ΔR and costs C_R is referred to as the efficiency of mitigation measures E_M (SafeLand, 2012):

$$E_M = \frac{\Delta R}{C_R} \tag{1.3}$$

If the costs associated with the risk reduction are not explicitly measured in monetary terms, the effectiveness, which is the relative reduction of the overall risk achieved

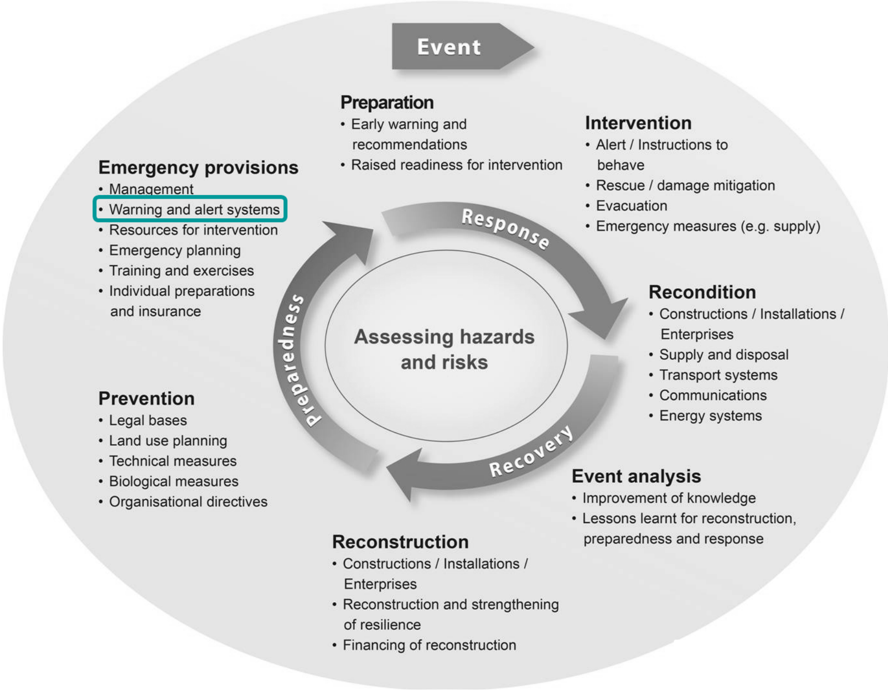

FIGURE 1.2: Cycle of Integrated Risk Management: includes mitigation measures to reduce the risk imposed by natural hazards to an acceptable level (FOCP, 2012).

due to a mitigation measure (Bründl et al., 2009), can be used as an evaluation criterion. A framework approach supporting decision-makers in evaluating the effectiveness of risk mitigation measures for a variety of natural hazard processes, such as avalanches, landslides, floods and debris flows, was provided by Romang (2008). In this framework, evaluation methods and examples for structural and biological measures are summarized. The application is demonstrated for the assessment of structural measures against snow avalanches by Margreth and Romang (2010) in detailed case studies, where the effectiveness is derived from the reliability of the snow structures. The reliability is evaluated semi-quantitative from the safety, serviceability and durability of the snow mitigation measures. EWS are not considered and in the field of EWS, an acknowledged framework approach for the quantification of the effectiveness achieved by EWS is currently missing.

The effect of EWS on risk reduction (effectiveness) is investigated and discussed in published literature and the reliability of EWS has been investigated and quantified in case studies. It is commonly accepted that EWS decrease the consequences of natural hazards (UNDRO, 1980). To this end, either the vulnerability (Einstein and Sousa, 2006) or the exposure probability of expected elements at risk (Dai et al., 2002; SafeLand, 2012) is reduced. A comprehensive evaluation of the effectiveness should address these positive effects and account for negative consequences associated with EWS. Elements at risk can only be protected through timely information if they comply with the warning. The compliance probability can be reduced through frequent false alarms and insufficient lead time (Pate-Cornéll, 1986; Schröter et al., 2008; Rogers and Tsirkunov, 2010). A high number of false alarms can reduce the compliance probability of persons at risk to an issued warning, due to a loss of trust that is known as the cry-wolf syndrome (Breznitz, 1989; Dejoy et al., 2006). Moreover, the lead time must be long enough that those willing to comply are able to do so.

As for structural mitigation methods, a comprehensive effectiveness evaluation, including positive and negative consequences, can be derived from the reliability (Schröter et al., 2008; Margreth and Romang, 2010). Recently, Balbi et al. (2014) published an approach where the effectiveness of a flood EWS is modeled from the reliability, the lead time and the coverage of persons reached by the EWS. In the field of EWS, the reliability has been investigated in several case studies and is commonly quantified as the ability of EWS to detect events and avoid frequent false alarms (Pate-Cornéll, 1986; Krzysztofowicz et al., 1994; Simmons and Sutter, 2009; Rheinberger, 2013). This reliability depends among other factors on the failure probabilities of technical system components. In two case studies, Bründl and Heil (2011) and Sturny and Bründl (2013) assess the technical reliability of two active EWS and identify the most critical components. These and other approaches on the quantification of the reliability and effectiveness achieved with EWS have been published (see Chapter 3), but no comprehensive framework is available.

1.3 Research Goal and Objectives

To support decision-makers in the selection of optimal risk mitigation measures a novel framework approach for the quantification of the effectiveness achieved with EWS is developed in this thesis. It enables the evaluation and optimization of the effectiveness and makes EWS comparable to alternative measures of an integrated risk management approach. A comprehensive approach provides methods enabling a structured analysis of the effectiveness directly from the reliability of an EWS. This framework and a guideline for practitioners are the main achievements of this thesis, which is financially supported by the Swiss Federal Office for Civil Protection (FOCP) within the project REliability

WARNing and Alerts (ReWarn) founded in 2011. The guideline summarizes important findings on the reliability of EWS to assist practitioners in developing and operating reliable EWS. To achieve these main goals, three major objectives are defined (Figure 1.3):

Objective I: Development and verification of a generic classification for EWS as the basis for a structured evaluation of EWS.

Objective II: Quantification and optimization of the reliability and the effectiveness achieved with EWS in two detailed case studies to identify class-specific needs.

Objective III: Development of a novel framework approach for the evaluation of EWS that is generically applicable to different EWS classes.

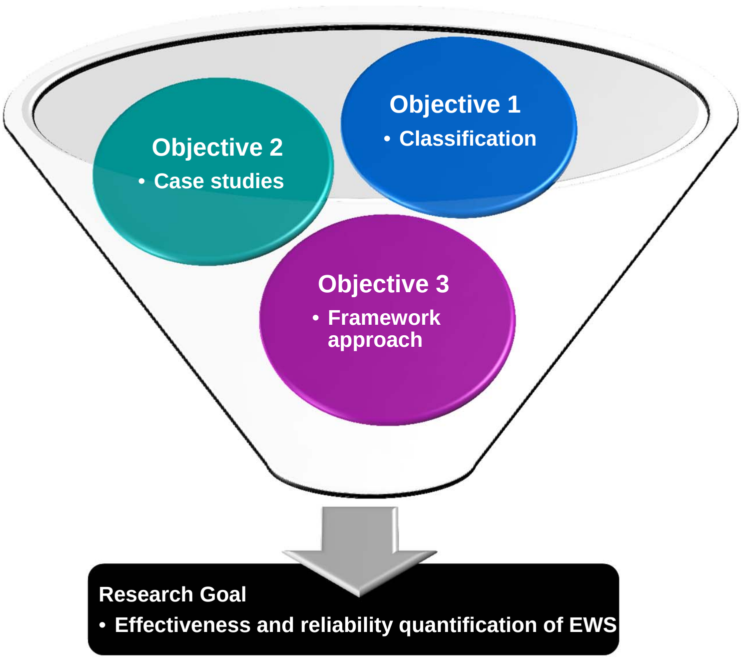

FIGURE 1.3: Research Goal and Objectives: defined to ensure a structured conduction of the research project.

1.3.1 Research Approach

To develop a framework approach that will be accepted and is applicable in practice and has a solid scientific research background, several theoretical and empirical methods are combined.

Objective I: First an overview of active EWS is generated in a literature review and field observations. The literature review enables the identification of modern EWS technologies that are operated worldwide for different kinds of natural hazard processes. The field observations are conducted in four cantons of Switzerland, located in alpine terrain (Bernese Oberland, Grisons, Ticino and Valais) and focus on site-specific EWS installed for gravitationally driven, alpine, natural hazard processes. Within the field inspection, existing EWS, their components and information flow are depicted in system sketches. The generic classification is developed based on the literature review, the field inspection and information collected in structured interviews with system operators and manufacturers. The classification is verified by applying it to a selection of modern EWS. To receive feedback from researchers and practitioners the classification is published in papers and presented at conferences and workshops (Sättele et al., 2012a,b; Sättele and Meier, 2013; Sättele et al., 2013b; Stähli et al., 2015).

Objective II: Firstly, quantitative evaluation criteria and methods for the evaluation of EWS applied in existing approaches are summarized in a literature review. Secondly, two existing EWS are assessed in detailed case studies and new evaluation methods are developed. In one case study, the reliability and the effectiveness of an automated EWS installed for the detection of spontaneous debris flow events is evaluated and optimized. Main results were presented at a conference (Sättele et al., 2013a) and published in a journal paper (Sättele et al., in press). In the second case study, the same evaluation criteria are assessed and optimized for a partly automated EWS installed to forecast the event timing of a slowly evolving rock slope failure (Sättele et al., accepted,b). In both case studies, not only are criteria and methods for the evaluation of EWS identified, but also those factors that influence the effectiveness and reliability of a certain EWS class.

Objective III: Firstly, a guideline for practitioners is developed that summarizes findings from both case studies in a simplified form. To define the degree of detail and the content with the end users, two workshops are conducted. The final guideline for practitioners is presented and published at several workshops and conferences (Sättele et al., 2014a,b; Sättele and Bründl, in print). The novel framework approach for the quantification of the effectiveness and reliability achieved with EWS is based on the classification and includes complex results that could be derived from the findings of the case studies. To establish a generically applicable framework approach, regular meetings with an expert group are conducted. The expert group includes members from different management disciplines, such as risk and natural hazards management and system stakeholders, including manufacturers, operators and user. The final framework approach will be published in a conference paper (Sättele et al., accepted,a) and a journal paper (Sättele et al., in preparation).

1.3.2 Thesis Outline

The structure of this thesis is aligned to the three objectives and organized into eight chapters, in addition to the introduction (Figure 1.4).

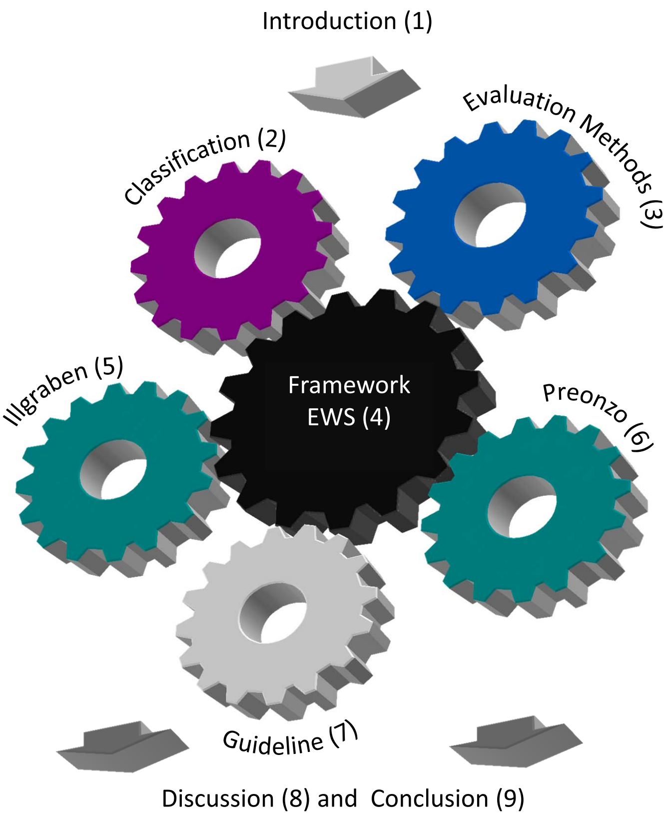

FIGURE 1.4: Thesis Outline: the structure is aligned to the objectives and organized into nine chapters.

Chapter 2 is related to Objective I; here, the novel classification for EWS is presented. First, the classification, which distinguishes EWS in three classes, is introduced and typical system characteristics are summarized for each class. Then, modern EWS operated worldwide and active on-site EWS for alpine processes in Switzerland are presented and assigned to the classification.

Chapter 3 is related to Objective II; here, methods and evaluation criteria that have been applied for the quantification of the effectiveness and reliability of EWS are introduced and discussed. The terms effectiveness and reliability are defined and methods for the quantification of EWS are presented.

Chapter 4 is related to Objective III; here, the main result, the novel framework approach for the quantification of the effectiveness and reliability achieved with EWS, is presented and specific needs for different EWS classes are discussed.

Chapter 5 is related to Objective II; here, detailed results of the Illgraben case study are presented to demonstrate the applicability of the framework on automated EWS. In addition, factors that influence the effectiveness and reliability of automated EWS are summarized and possibilities for system optimization are presented.

Chapter 6 is also related to Objective II; here, detailed results of the second Preonzo case study are presented. In addition, factors such as human decision-making and the accuracy of forecasting models that influence the effectiveness and reliability of partly automated EWS are evaluated and optimized.

Chapter 7 is strongly related to Objective III; here, the aim and structure of the guideline for practitioners, which was developed during the thesis, are presented and recommendations for practitioners are summarized.

Chapter 8 includes the final discussion; here, the applicability of achieved results and findings are addressed in the context of existing work and further needs are discussed.

Chapter 9 includes the final conclusions; here, the main achievements are summarized and an outlook on next steps is presented.

Chapter 2

Classification of Early Warning Systems for Natural Hazards

In the last decade, EWS have undergone a rapid technical development and are applied to prevent damage imposed by different natural hazard processes (Grasso and Singh, 2009). The improvement of EWS technology has been strongly supported in international projects, such as the Hyogo Framework (UNISDR, 2007a) and is financially supported by governments and NGOs. Modern EWS are designed according to project specific needs and are commonly installed as prototypes with a low degree of standardization. In practice, EWS are unambiguously referred to as alarm, alert, early warning or early alert, detection, forecasting, monitoring and warning systems.

Although a sophisticated classification for EWS could not be found in the literature, several institutions developed definitions for the terms alarm, alerts, warnings, prediction and forecast (Villagrán de Leon et al., 2013). In Switzerland, alarms are directly issued to endangered persons or public, in contrast to warnings which are issued to inform responsible authorities about potential risks (FOCP, 2013b). Alarms are acoustic or optical signals issued to protect endangered persons from imminent or existing hazardous conditions. Warnings are issued by EWS when the possibility of a catastrophic event exists in the near future: either if the event is occurring, is imminent or has a very high probability (Villagrán de Leon et al., 2013). Those warnings include recommendations or orders to take actions, such as evacuations (Hamilton, 1997). Alerts are not the same as alarms; they are low-level warnings and typically used to summarize several warning levels. E.g. in the U.S., levels become more serious from Outlook to Watch to Warning (USGS, 2014). Those alerts are mainly issued by institutions to warn the public if certain thresholds have been exceeded (Villagrán de Leon et al., 2013). Forecasts include the probability of a hazard event to occur during a certain time-frame in a prescribed geographical (Hamilton, 1997). They are definite statements or statistical estimates of the occurrence of future events (Grasso and Singh, 2009).

A sophisticated classification for EWS that is consistent with existing definitions could not be found. Nevertheless, some authors discuss or propose partly diverse ideas on possible classifications. For example, Bell et al. (2010) distinguish between monitoring, expert and alarm systems. Monitoring systems are operated to investigate and understand the underlying hazard process, expert systems support decision-makers in data interpretation and alarm systems are based on predefined thresholds. In contrast, Schmidt (2002) and Glantz (2004) state that monitoring systems are not stand-alone EWS because they do not issue timely information. However, they are a valuable part of every EWS in increasing the general understanding of dangerous processes. The term expert system is already used to signify an established system type in the field of artificial intelligence for computer systems that imitate the decision abilities of humans (Jackson, 1990).

Our novel approach classifies EWS into alarm systems (AS), warning systems (WS) and forecasting systems (FS) (Sättele et al., in preparation). This classification is originally developed for EWS installed for gravitational-driven alpine processes (details in Chapter 2.4), but is generally applicable to EWS operated worldwide (Chapter 2.3) and consistent with existing definitions. It is based on different monitoring strategies for natural hazards and addresses associated lead times and system designs.

2.1 Monitoring Strategies of EWS

EWS differ strongly in their monitoring strategies (Figure 2.1a). Before the event has started, precursors, such as trigger events and changes in the disposition, can indicate a future event. When the event has already started, typical process parameters can be observed. Trigger events are precursors that activate main hazard events, such as extreme precipitation, earthquakes and snow melt (Keefer, 1999). Changes in the disposition include time-dependent parameters, such as state of vegetation, availability of loose material, and determine when and how often events take place (Zimmermann et al., 1997). Process parameters are those that can be measured when the natural hazard event has already started, such as increased flow heights, speed, pressure and ground motions that are associated with debris flows. The lead time is directly determined through the choice of monitoring parameters. Two main monitoring strategies can be distinguished. If the EWS monitors process parameters of already ongoing hazard events, the information content of the measured data is high, but the associated lead time is short. If the EWS monitors precursors before a hazard event starts, the information content of the monitored data is lower, but the lead time is extended.

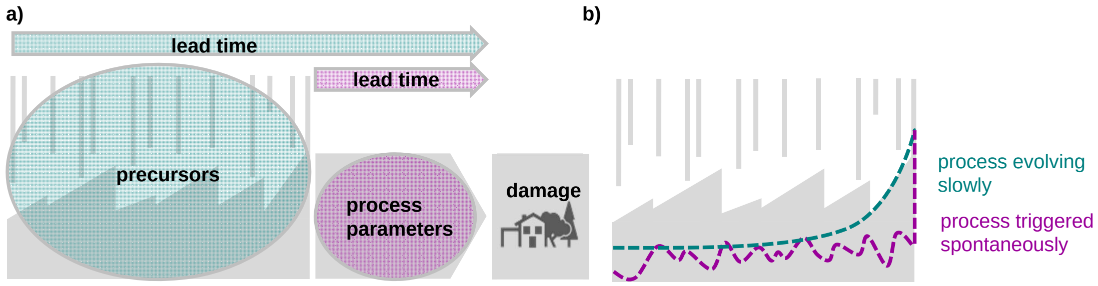

FIGURE 2.1: Monitoring Strategies: a) EWS can monitor precursors or process parameters leading to different lead times; aligned to (Zimmermann et al., 1997); b) dependent on the process type, the information content of precursors varies.

The choice of the monitoring strategy includes a trade-off between lead time and the information content of the monitored data, and depends on the occurrence type of the underlying hazard processes (Figure 2.1b). Processes that may be rapidly triggered, such as flash floods, debris flows, snow avalanches, spontaneously triggered slope failures and earthquakes, provide data with high uncertainty before the event starts. For example, a debris flow is triggered after heavy local rainfall, depending on the availability of loose material (Badoux et al., 2009). In contrast, processes that evolve slowly, such as mid- and high-magnitude rockfalls, deep-seated landslides and river floods, enable the monitoring of precursors with high information content in two phases (Sättele et al., accepted,b). In the first phase, slope failures, for example characteristically evolve over long time scales, typically weeks to several years, until a critical path of detachment is developed (Krautblatter and Moore, 2014). In the final phase, velocities increase significantly before the final failure occurs (Hungr and Evans, 2004). With respect to the occurrence type of a natural hazard process, three monitoring strategies can be distinguished:

- precursors of processes that evolve slowly are monitored: the information content is high and the lead time is extended.
- precursors of processes that are triggered spontaneously are monitored: the information content is lower and the lead time is extended.
- process parameters of processes that are triggered spontaneously are monitored: the information content is high but the lead time is short.

2.2 Classification of EWS into Alarm, Warning and Forecasting Systems

A novel, generic classification for EWS was derived directly from the monitoring strategies and divides EWS into AS, WS and FS. Each class has a certain degree of automation and can be described through a typical system design in three main units: monitoring, interpretation and dissemination unit (Figure 2.2). In addition, EWS incorporate devices for power supply and diagnosis tools, which detect critical failures of system components and report them to system operators. Operations plans summarize responsibilities and procedures for daily operation, maintenance and in the case of an event.

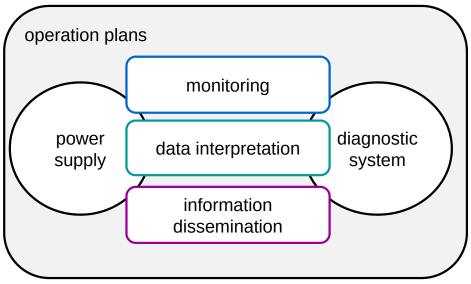

FIGURE 2.2: Units of an EWS: similar, independent of the EWS class, including components for monitoring, data interpretation and the information dissemination.

Figure 2.3 illustrates the main components of each EWS class and the degree of automation. The monitoring unit incorporates sensors, which continuously monitor the environment to detect typical changes. The data interpretation unit is the interface between the units and includes those components and resources necessary to analyze, transmit and manage the measured data for decision-making. The information dissemination unit covers those components and resources necessary to issue information to endangered persons. Remote EWS components are supplied autonomously, for example by batteries charged with solar panels, while less remote components are typically connected to power networks. Diagnosis systems monitor the availability of sensors and the data transmission devices, such as the mobile network or radio connections.

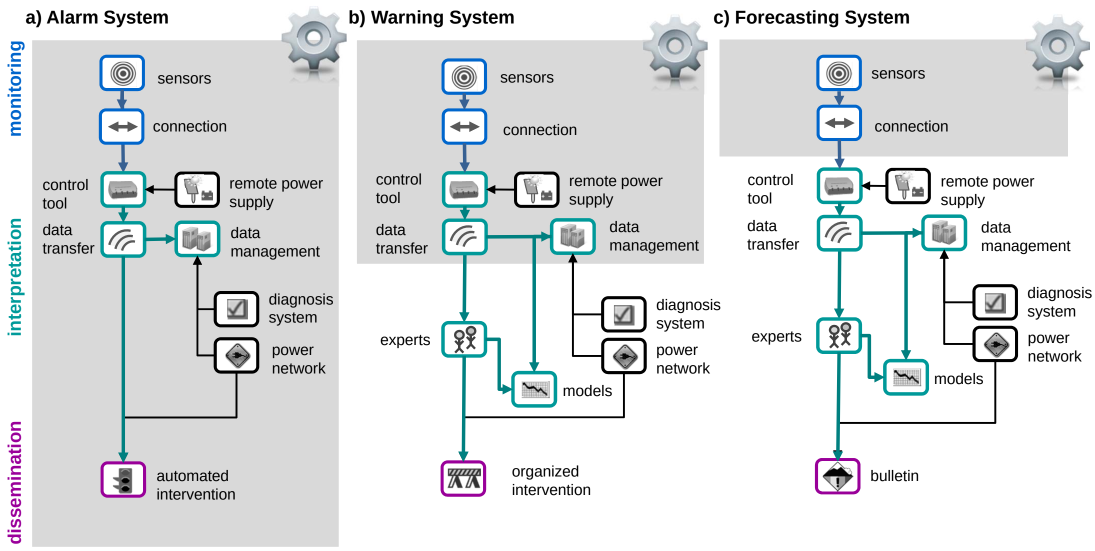

FIGURE 2.3: Classification of EWS: each EWS class incorporates different system components and degree of automation. Automated parts are illustrated in gray boxes.

2.2.1 Alarm Systems

In the monitoring unit of AS, sensors detect process parameters of already ongoing hazard events (Figure 2.3a). The information content of the measured data is high, but the lead time is short. To deal with this short lead time, AS are fully automated. The data interpretation unit includes data control, transfer and management tools as well as components for diagnosis and power supply. The control tool is the heart of the data interpretation unit and is often installed in the form of a data logger that controls the sensor measurements and analyzes the data with respect to predefined thresholds. The alarm is transferred directly to the dissemination unit, where automated intervention measures, such as optical or acoustical signals and barriers are activated. In parallel, system operators and responsible risk managers receive information and can access and analyze the measured sensor data.

2.2.2 Warning Systems

In the monitoring unit of WS, sensors monitor, precursors such as trigger events or changes in the disposition, before the event releases (Figure 2.3b). The information content of the data is often lower in this early stage, but the lead time is extended. The data interpretation unit incorporates two levels and is partly automated. The initial warning is automatically released whenever predefined thresholds are exceeded. The final decision is made by experts analyzing the measured sensor data with models. Within the information dissemination unit, intervention measures, such as evacuations, are initiated.

2.2.3 Forecasting Systems

In the monitoring unit of FS, precursors are observed by sensors or persons to obtain extended lead times (Figure 2.3c). The degree of automation is significantly lower compared to threshold-based AS and WS. In data interpretation units, experts analyze sensor data and apply models on a regular basis. The information is disseminated in the form of bulletins, in which the regional danger levels are assigned to forecast the occurrence probability of hazardous events for predefined regions. The bulletins are available for authorities and the public on the internet, radio and television. If certain danger levels are exceeded, information is send to authorities and endangered persons.

2.3 Application of the Novel Classification for EWS

Worldwide, EWS are operated to prevent damage caused by meteorological disasters, including flood, earthquakes and tsunamis, wildfires, volcanic eruptions and gravitational-driven alpine processes, such as debris flows, flash floods, snow avalanches, small- to high-magnitude rockfalls and landslides. Depending on the underlying natural hazard process, its predictability, the competences and requirements of those operating and the needs of those endangered by the hazard, different EWS are operated. They vary in their spatial dimensions, lead time, design and associated degree of automation. In the following sections, modern EWS are exemplary assigned to the classification and system components are described for the monitoring, data interpretation and dissemination unit.

2.3.1 EWS for Meteorological Hazards

Meteorological processes differ strongly in their predictability. While small-scale features, such as hail, heavy local precipitation and tornadoes, occur spontaneously, large-scale weather patterns, such as long-term precipitation causing floods, provide longer lead times. To prevent damage caused by meteorological processes, FS are mainly operated.

In most countries, national weather services run FS, such as the Met Office in England. In the monitoring unit, data is collected from different sources and enables atmospheric observations before hazard events occur (MetOffice, 2014b). Surface data is collected offshore with buoys and on land with networks of weather stations. In England, more than 200 stations measure meteorological parameters, including air temperature, atmospheric pressure, precipitation, wind speed and direction, humidity, cloud height and visibility. In addition, technologies such as weather satellites, balloons and aircraft measurements are applied. The data interpretation is conducted daily by forecasters running numerical weather prediction models multiple times to obtain ensemble weather models (Legg and Mylne, 2004). A major challenge remains the prediction of small features, such as local storms, heavy rainfall or hailstorms. With nowcasting methods, only short-term event predictions for a few hours ahead can be made by extrapolating weather data measured in real-time (Mass, 2011). In the dissemination unit, the Met Office publishes forecasts for rain, wind, snow, ice and fog on the internet, radio, TV, social media, smart phone apps, RSS and via email alerts. The warnings are released in four levels, where the highest level includes the implementation of predefined preventive procedures and instructions for the public from emergency services and local authorities (MetOffice, 2014a).

For the protection of coastal regions, the Tropical Cyclone Program was established to coordinate the development of national and regional warning services for tropical cyclones (WMO, 2014). These FS are operated by regional, specialized meteorology centers for hurricanes or tropical cyclone warning. A prominent example is the U.S. National Hurricane Center, responsible for the Eastern Pacific and Atlantic that is part of the National Centers for Environmental Prediction since 1995 (Rappaport et al., 2009). In the monitoring unit, data is mainly obtained from satellites, including geostationary satellite intensity estimates, passive microwave imagery, and rainfall and wind measurements. Data is also provided by ships and reconnaissance aircrafts. In the data interpretation unit, forecasters are supported by software tools displaying modeled data, which has improved the operational efficiency of forecasters in analyzing and forecasting dangerous events. In the dissemination unit, hurricane forecasts are published every six hours in the hurricane season. Figure 2.4 shows a cyclone track and intensity forecast, for the next 2, 24, 36, 48, 72, 96, and 120 hours. When the lead time decreases, the track and intensity errors decrease. In 2011, a very good track forecast could be achieved twelve hours before the actual hurricane caused damage. Similarly, the predicted intensity accuracy was significantly higher twelve hours than it was ninety-six hours before the event (Blake and Kimberlain, 2013).

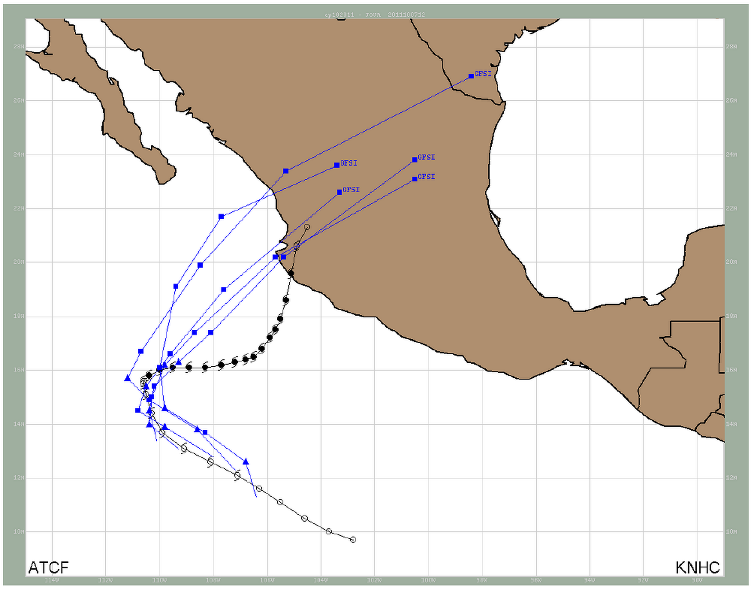

FIGURE 2.4: Hurricane Forecast: five day track forecast model for the hurricane Jova (Brennan, 2012)

FS for severe weather are currently undergoing a clear trend towards automated procedures in the data interpretation and dissemination units. In Germany, the AutoWARN system was developed by the Deutscher Wetterdienst to support a centralized and automated warning process (Reichert, 2010). The system combines all available meteorological information from observations, radar products, nowcasting products, statistical forecast products, and model forecasts of numerical weather prediction to generate automated warning status proposals that support forecasters in decision-making. In England, the National Severe Weather Warning Service was enhanced when a risk-based approach was adopted. An ensemble-based, first-guess tool for severe weather was developed to support forecasters in short range (1-2 days) warnings. The tool generates automated early warnings and provides the opportunity to increase the lead time. Moreover, the tool follows a risk-based approach, where the risk is evaluated from the probability of an event to occur and the impact on the society in a risk matrix (Neal et al., 2013). Similar efforts are undertaken by the NOAA National Severe Storms Laboratory within the project FACET, which consists of seven interrelated functions: including, for example grid-based probabilities, advanced forecast of tornadoes, large hail or local rain events by real-time statistical projections of indicators such as intensity, and support tools for forecasters.

2.3.2 EWS for Floods

Flood forecasts depend directly on meteorological predictions generated for severe rainfall events. Lead times of floods vary significantly for river and for flash floods. While river floods occur, the water level raises over long periods, often between days and weeks. In contrast, flash floods are triggered fast after severe precipitation, typically in smaller catchments within minutes or hours. Modern flood warnings are primarily generated with FS.

Most national or regional flood FS are coupled hydro-meteorological systems. For example, in Finland, the monitoring unit of the national FS includes measuring stations and manual measurements for precipitation, water level, discharge, runoff and snow water equivalent, ice thickness, water temperature, etc. (SKYE, 2013). In the data interpretation unit, these observations are combined with meteorological forecasts (Wetterhall et al., 2013). To generate probabilistic forecasts for floods, forecasters increasingly apply Hydrological Ensemble Prediction Systems (see Table 1 in HEPEX (2013)). With this ensemble method, uncertainties associated with the forecasts can be addressed and an improved performance even for extreme events can be achieved (Wetterhall et al., 2013). The detection of local flash floods, triggered by local heavy rainfall and the reaction of small catchments remains a major challenge. In recent years, radar-based and pluviometer-based nowcasts have been used to generate short-term forecasts up to six hours (Liechti et al., 2013). In the data dissemination unit, flood bulletins are disseminated on the internet in predefined danger levels on the regional scale. In addition, warnings are sent to regional centers responsible for flood management, municipalities and emergency services which prescribe preventative measures involving residence (SYKE, 2013).

To support the development of a global scale FS, the European Flood Awareness System has been tested on other continents and could successfully forecast flood events in large basins. This would have saved lives across the world, including major events such as Pakistan in 2010 (Alfieri et al., 2013). In the monitoring unit, hydrological and meteorological data is collected by responsible centers. The interpretation of the data is executed in the European Centre for Medium-Range Weather Forecasts (UK) where forecasters analyze data to identify and evaluate endangered areas. In Figure 2.5, the predicted discharges for a river in Romania in July 2007, modeled by the European Flood Awareness System, are illustrated (Cloke and Pappenberger, 2009). In the dissemination unit, information is published in the form of maps, including flood probabilities for members up to ten days in advance (Thielen et al., 2009). In these maps, critical river sections are assigned to three warning levels that are specified for predefined thresholds and disseminated to authorities across Europe.

With ensemble methods, national or site-specific FS are able to provide reliable predictions several days ahead of critical discharges (Cloke and Pappenberger, 2009). Despite these progresses, event analysis of major past disasters revealed shortcomings of operational FS, which are partly similar to those that come along with meteorological FS. Thus, a similar trend towards a higher degree of automation (e.g. support decision-makers with proposals in identifying adequate preventive action and mitigation measures) and an increased use of probabilistic analyses tools can be observed. Information on uncertainty is increasingly used to assess forecast skills and improve the system performance. For floods, the improvement of forecasting accuracies depends on additional hydrological processes such as snow melting, debris blocking and ice melting (Cloke and Pappenberger, 2009). The timely prediction of flash floods remains a major

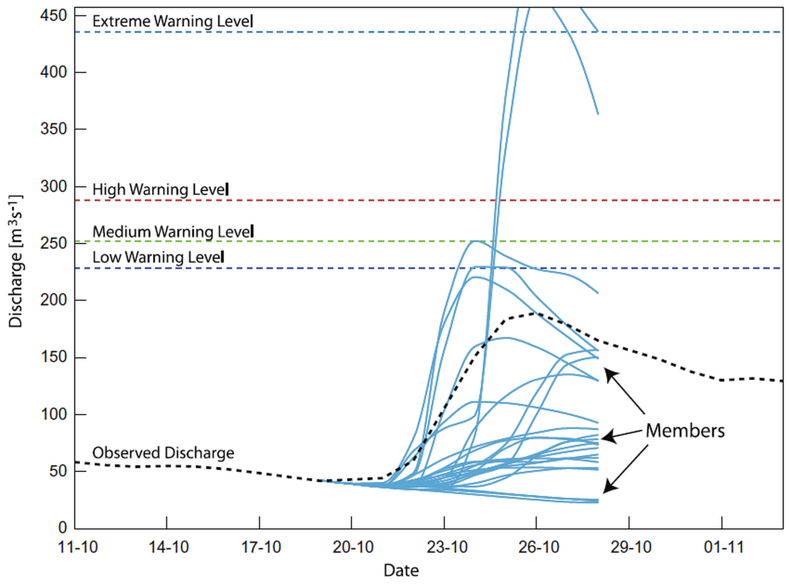

FIGURE 2.5: Ensemble Flood Prediction: modeled predictions (solid lines), observed discharge (black dashed line) and four flood discharge warning levels (Cloke and Pappenberger, 2009)

challenge. Currently, first efforts undertaken in Africa, Taiwan, the U.K. and U.S. could be made with probabilistic models leading to increased lead times (Poolman et al., 2014; Yang et al., 2014; Price et al., 2014; Hardy et al., 2013). In the future, such efforts have to be incorporated in a comprehensive risk management framework in which local warnings, in combination with additional risk mitigation measures for flash flood EWS, are conducted within these short lead times (Obrusnik, 2011; Borga et al., 2011).

2.3.3 EWS for Earthquakes

Earthquakes occur spontaneously without precursors and are the most challenging process for prediction. They offer minimal lead times, depending on the distance to the epicenter, usually mere tenths of seconds, allowing for a limited conduction of mitigation measures to prevent damage (Grasso and Singh, 2009). Most systems are operated on a regional or national scale to detect earthquakes in real-time, but they are not EWS because they do not provide timely information enabling the implementation of mitigation measures. These systems produce so-called shake maps, which graphically illustrate measured ground vibrations immediately after an event to establish and organize emergency measures in areas in need of help (Gasparini and Manfredi, 2014). Only in some earthquake-prone countries, such as Japan, Mexico, Taiwan and Turkey, AS are developed and operated to prevent damage caused by earthquakes.

The first AS, the Urgent Earthquake Detection and Alarm System UrEDAS, was implemented in 1982 in Japan to protect the fast transport system Shinkansen railway (Nakamura and Saita, 2007; Saita and Nakamura, 2003). A monitoring unit, consisting of seismic sensor networks, is installed along the rails measuring p-waves. Those primary waves are faster and arrive first, before destructible s-waves occur (Figure 2.6). In the data interpretation unit, seismic signals are automatically analyzed in real-time, without data storage, to obtain maximal lead time. Software estimates the magnitude, the position and the depth of the epicenter to identify endangered areas and estimate the destructiveness of the earthquake. Based on predefined thresholds, alarms are released or not. In the data dissemination unit, alarms are issued in the form of automated power cut-offs to stop trains that are close to endangered areas.

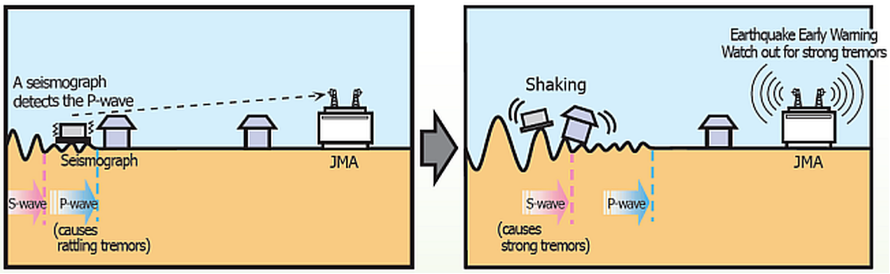

Figure 2.6: Wave Forms of Earthquake: fast and less destructive p-waves can be monitored to increase the lead time (JMA, 2014).

In Japan, it is not only the railway lines but the whole country that is equipped with one of the most advanced AS for earthquakes. In the monitoring unit, about 800 high sensitivity seismic sensors are placed in boreholes (deeper than 100 m). In the interpretation unit, data is processed in real-time to estimate relevant earthquake parameters within a few seconds after p-waves arrive at the closest station (Nakamura et al., 2009). This information is merged with the results of Japan Meteorological Agency's nowcast system, which is based on $4,000$ seismic intensity meters, to issue timely earthquake and tsunami information. In the dissemination unit, prevention measures are activated automatically for areas that are more than 30 km away from the epicenter. Besides automated control measures for trains, factory buildings and other safety critical infrastructures are shut down.

In the U.S., an earthquake AS is under development for the West Coast. The United States Geological Survey and several partners are working on the development of ShakeAlert. The monitoring unit consists of a network with approximately 400 high-quality, ground motion sensors. Since 2012, test alarms are sent to users if predefined thresholds in the data interpretation unit are exceeded. In the dissemination unit, users receive a map showing the epicenter, waves moving towards the user and the remaining time to arrival (Figure 2.7). In the future, this AS will provide seconds, or even minutes of lead time before dangerous waves arrive (Burkett et al., 2014).

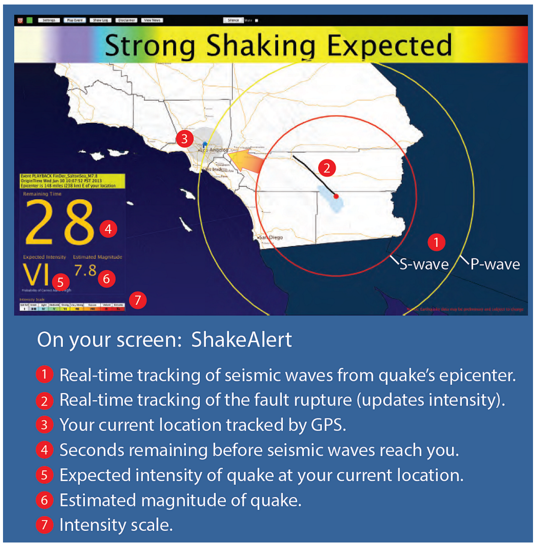

FIGURE 2.7: Information Dissemination of the Earthquake Alarm System: map shows the epicenter, waves moving towards the user and the remaining time to arrival (Burkett et al., 2014)

The main shortcoming associated with earthquake AS is the lead time. Currently, several projects are conducted to develop technologies and procedures that maximize the lead times. For example, the Collaboratory for the Study of Earthquake Predictability runs test centers in Japan, Switzerland, New Zealand and the U.S. and has testing regions in California, Italy, Japan and the North and Southwest Pacific to support earthquake prediction experiments (CSEP, 2015). A new approach that combines advantages of regional (accuracy) and on-site concepts (speed) was presented by Böse et al. (2007). Within this concept, alarms can be issued from one station in a network before seismic waves arrive in all stations. Also, Nakamura et al. (2009) proposed that borehole data in combination with on-site processing at each station could lead to a significant improvement and increase the lead time for areas close to the epicenter. Other institutions work on the improvement of probabilistic forecast methods for earthquake EWS. For example, the ElarmS methodology enables an estimation of the occurrence probability and the associated lead time available from different earthquake scenarios (Allen, 2007).

2.3.4 EWS for Tsunamis

In coastal regions prone to tsunamis, earthquake AS are enhanced including prediction capabilities for tsunamis. Lead times depend on the distance of the earthquake to the coastal region. Thus, far-field and near-field tsunamis are distinguished. Far-field tsunamis are characterized by the long travel distance of the tsunami compared to the earthquake rupture length. Additionally, forecast is less complex compared to near field-tsunamis, where the tsunami travel distance is short compared to the earthquake rupture length. To predict tsunami timing and size after the detection of major earthquakes, WS are operated to protect affected coastal regions.

After the 2004 near-field tsunami in the Indian Ocean, which killed about 250,000 people, the German Indonesian Tsunami WS was set up (Lauterjung et al., 2010). To deal with short lead times (20-40 minutes) between earthquake and tsunami impact, new monitoring technologies have been developed to generate timely forecasts 5-10 minutes after the earthquake (Figure 2.8).

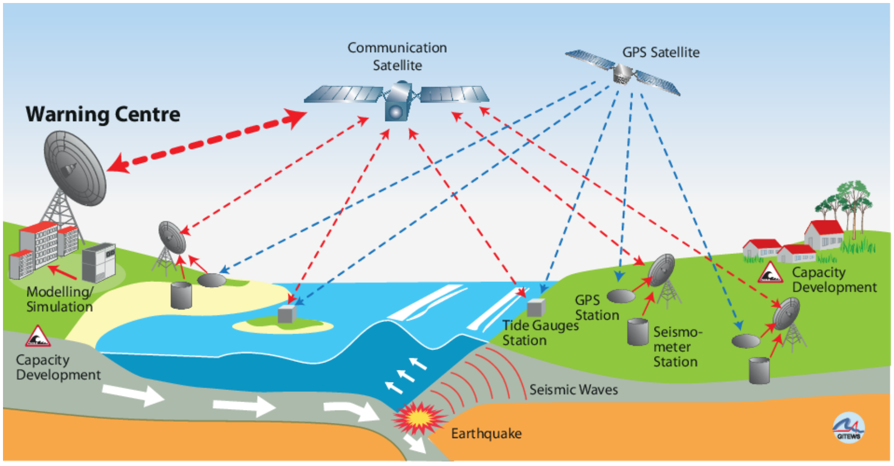

FIGURE 2.8: Indian Ocean Tsunami Warning System: includes modern monitoring technologies (GITEWS, 2015)

The monitoring unit includes a seismic broadband network of 150 sensors. In the sea, sensors such as buoys connected with ocean bottom pressure units are used and at the coastline, tide gauges are installed. In the data interpretation unit, experts are informed automatically when predefined thresholds are exceeded. To decrease the number of false alarms and obtain maximal lead times, a combination of thresholds for warning release is specified. Whenever predefined thresholds are exceeded, tsunami scenario simulations and decision-support systems are operated automatically to receive fast results. Figure 2.9 illustrates two tsunami simulations based on a certain location and magnitude (M_w 8.4) of a hypothetical earthquake generated with the new EWS In the dissemination unit, responsible staff members have to issue warnings to authorities. Evacuations are then conducted following pre-established plans. To increase the awareness of endangered persons towards tsunami danger, the WS operators conduct regular training in coastal regions. Similar WS are installed in Chile, Greece, Japan and the U.S.

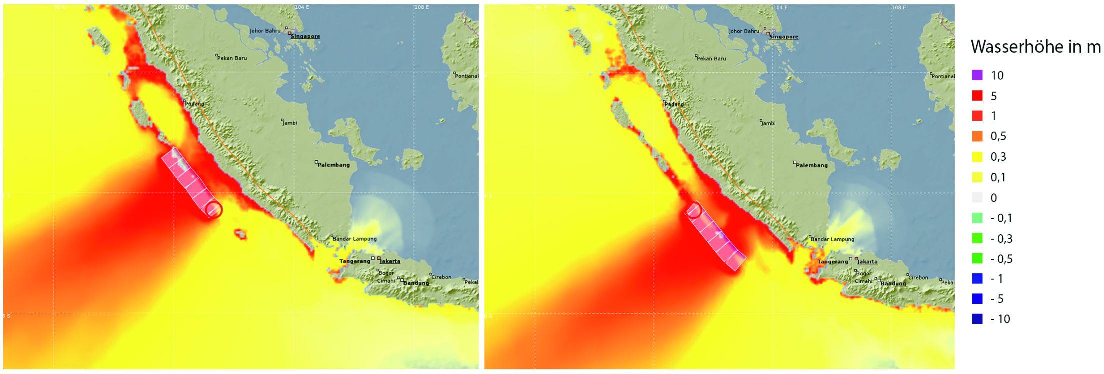

FIGURE 2.9: Modeled Tsunami Scenarios: two tsunami simulations based on a certain location and magnitude (M_w 8.4) of a hypothetical earthquake (Lauterjung et al., 2010); scenario for rupture running from epicenter north (left) and running south (right).

The tsunami in Japan in 2011 demonstrated the difficulties that WS for near-field tsunamis have to deal with. A first tsunami warning was generated by the Japan Meteorological Agency three minutes after the earthquake based on seismic measurements (Ozaki, 2011). When more data from offshore GPS buoys was available, the predicted tsunami heights and affected areas were increased continuously, as was the predicted magnitude of the earthquake. Unfortunately, the earthquake and the tsunami disrupted data transmission and sensors close to the epicenter that would have been necessary to generate more accurate and timely predictions and would have supported the decision-making for changing and closing the tsunami warnings (Wei et al., 2013). To generate reliable warnings in the future, technical components and social aspects, such as the timely compliance to warnings, need to be improved.

2.3.5 EWS for Wildfires

Wildfires appear spontaneously without clear precursors. They are typically induced in dry areas by natural processes, such as lightning, or more often by humans, who are the main reason for their ignition. Modern EWS technologies differ strongly and both AS and FS are operated.

To prevent damages related to wildfires, so called fire danger rating systems are operated on regional or on national levels. These systems enable the prediction of danger levels on a regional scale based on fire indexes, which have been adapted from Canada, the U.S. and Australia (Groot et al., 2015). The Canadian Forest Fire Weather Index FWI was developed already in the 1960s and is the most widely used one. It is a weather-based approach, considering temperature, rainfall, relative humidity and wind speed. In the U.S. National Fire Danger Rating System, additional parameters, such as cloudiness, min. and max. temperatures and precipitation durations are considered to estimate the moisture content of fuels. To support national and regional fire management, especially in countries were fire danger rating systems are actually missing, a global system was released in 2011 (De Groot et al., 2010). This system is based on the Canadian Forest Fire Weather Index and provides forecasts up to one week ahead.

Modern fire FS are enhanced danger rating systems (Groot et al., 2015). In the monitoring unit, humidity and temperature sensors are directly inserted in so-called fuel sticks to gain important data, enabling the estimation of the moisture content for a range of fuel complexes. In addition, satellite data is used to estimate the water content of vegetation. In the data interpretation unit, forecasters combine information on moisture content with weather forecasts and information about fire activity monitored with remote sensing technology (mainly satellites). In the U.S., forecasters of the Storm Prediction Center run short-range ensemble methods to quantify the probability of fire weather parameters exceeding critical thresholds specified within the national fire rating system to identify critical areas (Taylor et al., 2003). The dissemination of forecasts is provided regularly for one day, two days and for the next three to eight days, separately.

In Switzerland, the experimental project FireLess2 was initiated to test the applicability of wireless sensor technology to automatically monitor the humidity of the main components of dead fuel on forest soils (Conedera et al., 2011). In the monitoring unit, sensors deliver near-real-time data on litter and humus moisture content of different forest types (Figure 2.10). Weather sensors provide data, such as rainfall, air humidity and temperature, wind speed and direction. In the data interpretation unit, measured sensor data and additional information, such as weather forecasts, are combined to specify the danger levels. The automated configuration worked reliably and delivered valuable information during the test phase. This technology could be used to enhance FS and support decision-makers in evaluating fire danger in the future.

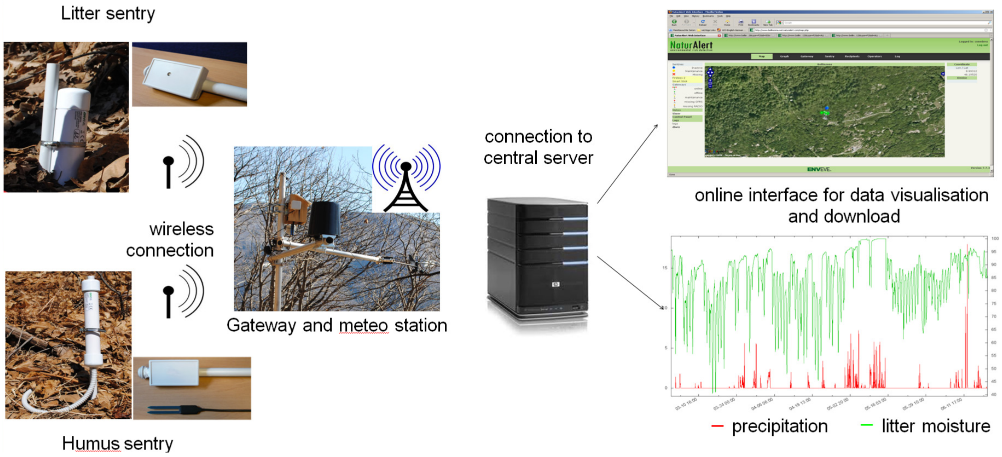

FIGURE 2.10: FireLess Wildfire EWS: sensors delivered data on litter and humus moisture content of different forest types (Conedera et al., 2011).

AS are operated to detect ongoing fires before they cause damage to infrastructures and persons. For South Africa, the Advanced Fire Information System was developed (Davies et al., 2008). In the monitoring unit, satellite technology is used to detect ongoing fires. Whenever a fire is detected, alerts are issued automatically in the data interpretation. In the dissemination unit, alarm information is sent to the public via cell phones. A similar worldwide AS was funded by NASA. The Fire Information for Resource Management System is used to send satellite-derived fire information to inform users all over the world in near-real-time or as daily or weekly summaries. Users can select any area of the world for notification by drawing on an interactive map. Underlying real-time information about active fires is obtained from the Webfire Mapper from NASA and the University of Maryland (Davies et al., 2009) (Figure 2.11).

AS provide reliable information on dangerous events, while FS can estimate the danger level and the associated probability of dangerous events, thus preventing damage. With

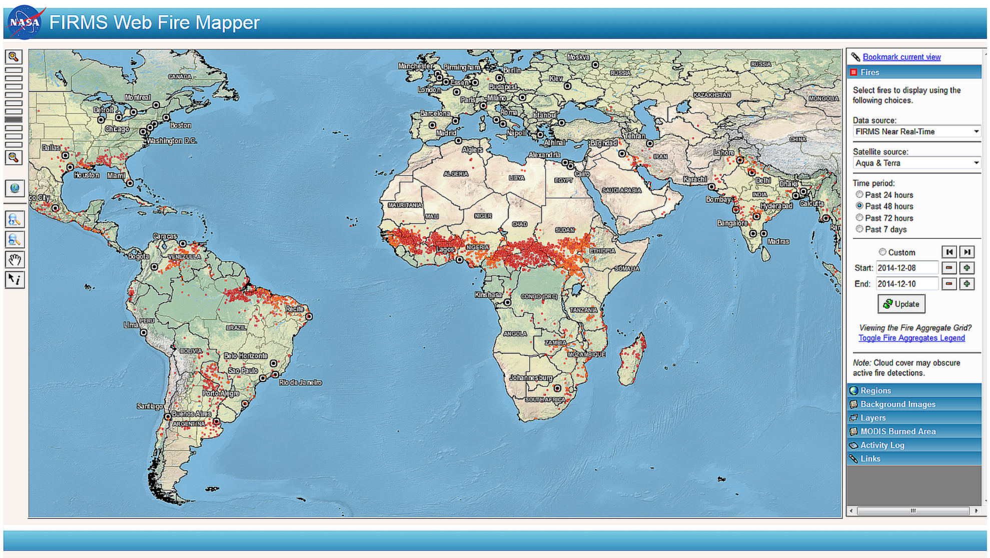

FIGURE 2.11: Web Fire Mapper for Central Africa: displays current fires (NASA, 2015).

AS, damage can only be prevented when lead times are sufficient, which depends on the distance between the fire and endangered persons and infrastructures.

2.3.6 EWS for Volcanoes

Volcano eruptions are typically announced by precursors, such as geophysical and geochemical phenomena, hours to days in advance. On several dangerous volcanoes, EWS are installed to provide timely warnings and prevent damages from associated explosions, flying rocks, fast-moving, hot ash clouds, lava flows, lava domes, landslides, ash, volcanic gases, lightning, lahars (mudflows), tsunami, and/or earthquakes (GeoNet, 2014). In countries such as Japan, the U.S. and New Zealand, volcanoes with a high risk potential are equipped with AS and WS, and in Central and South American countries and Africa, volcanoes are monitored frequently (Grasso and Singh, 2009).

Two AS are installed to protect the ski area on Mt. Ruapehu in New Zealand from lahars and provide automated information within seconds (Sherburn and Bryan, 1999; Leonard et al., 2008). One AS detects eruptions that are big enough to cause damage at the ski area. In the monitoring unit, seismic and acoustic (microphones) sensors are installed to distinguish volcanic earthquakes with eruptions from tectonic earthquakes. Earthquakes with dangerous eruptions, typically produce airwaves that can be recorded by acoustic microphones. In the data interpretation unit, thresholds for seismic and acoustic data are combined to detect events and avoid false alarms. In the dissemination unit, warnings are automatically issued via sirens and loud speakers issuing instructions for visitors. The other AS detects lahars in the channel. Before a dam at the crater lake collapsed, the monitoring unit consisted of geophones, tripwires and a lake level sensor. The data interpretation unit is based on thresholds and in the dissemination unit pagers and phones are automatically activated, following an emergency response plan. Similar AS for lahar detection are installed in Ecuador, Indonesia, Japan, Mexico, the Philippines and the U.S. (USGS, 2015a).

Some countries or institutions run WS, such as the one operated by the Alaska Volcano Observatory. They are based on monitoring techniques, allowing for a timely identification of unrest that may lead to future events (Moran et al., 2008). In the monitoring unit, sensors monitor the occurrence of seismic signals, deformations, gas occurrences, and hydrological or geophysical changes (Figure 2.12). In addition, remote-sensing technologies are applied to observe volcanoes. In the interpretation unit, system operators receive automated information whenever predefined thresholds are exceeded. They analyze the data and assign and communicate danger levels for persons on ground and to worldwide standardized levels for aviation (Figure 2.13).

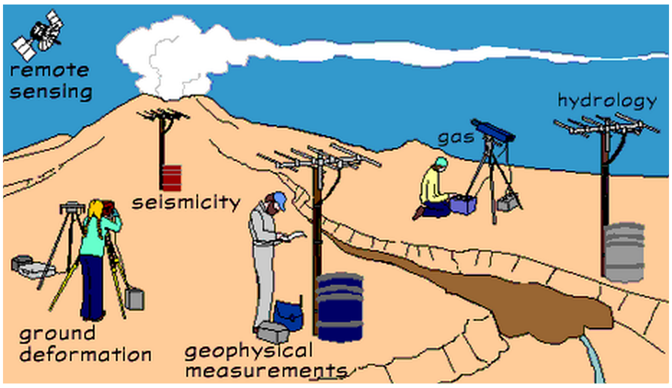

FIGURE 2.12: Monitoring Techniques for Volcano Warning Systems: include seismic, deformation, gas, hydrological and geophysical measurements as well as remote sensing techniques (USGS, 2015b).

The operation of WS is associated with risks because precursors vary strongly for different volcanoes. At some volcanoes, eruptions are indicated by increased seismic activity, while at others an increased gas production can be observed. At Mt. Ontake warnings could not be generated in time to protect the life of thirty-six victims in September 2014, although a new WS was implemented in 2007 for 110 active volcanoes (Cyranoski,

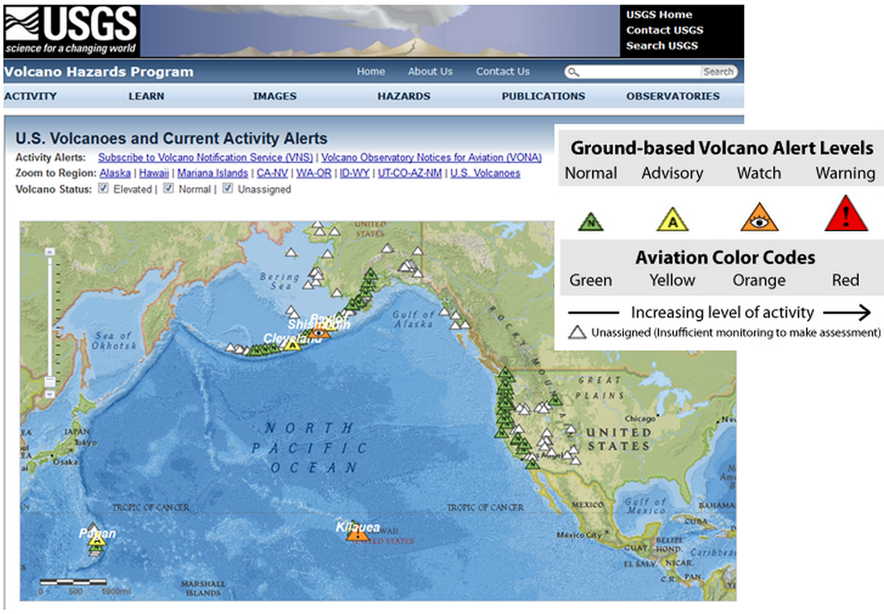

FIGURE 2.13: U.S. Volcanoes and Current Activity Alerts: maps volcanoes and alert levels (USGS, 2014).

2014). The five GPS stations and the tiltmeter showed no changes before and during the eruption. Only the twelve seismometers indicated increased activity several days before the main event and a high activity eleven min before the event. A warning was not issued because of the missing deformation activity and because similar seismic activities could be observed on other sites that did not lead to an event. In the future, reliable warnings with sufficient lead time can be made when on-site specific characteristics are understood and considered in the warning procedures. To support the forecasters, probabilistic tools, such as a Bayesian Belief Network and Hidden Markov Models (Marzocchi et al., 2008; Oliveros et al., 2008; Hincks et al., 2014) are increasingly applied to generate long- or short-time forecasts for volcanic eruptions.

2.3.7 EWS for Mountain Hazards

Gravitationally driven mass movement processes occur in mountain regions and vary strongly in their spatial and temporal dimension. While mid- and high-magnitude rockfalls and deep-seated landslides evolve slowly over years, processes such as debris flows and snow avalanches are triggered spontaneously. To cover the variety of process types, AS, WS and FS are operated (Thiebes, 2011; Michoud et al., 2013).

WS are commonly installed to predict the timing of mid- and high-magnitude rockfalls, which typically evolve over long periods (years) and provide longer lead times (between days and weeks). In Åknes (Norway), a large rockslide of possible 30-40 million m^3 can trigger a tsunami in the underlying fjords (Blikra, 2008). In the monitoring unit, sensors measure precursors, typically displacement rates with extensometers, single lasers, GPS and a total station. In addition, seismic sensors, a climate station and borehole instrumentation (inclinometers and piezometers) are installed. In the data interpretation unit, automated warnings are generated and send data to experts if predefined thresholds, such as displacements, are exceeded. To support decision-makers the data interpretation is implemented in an integrated web-based system and five warning levels are defined for displacement rates and accelerations of different instrumentation (Figure 2.14) (Kristensen et al., 2010). The dissemination unit includes sirens that can be activated to warn endangered persons in case of imminent slope failure. Similar WS are described in Froese and Moreno (2011), summarized by Thiebes (2011), and further system details are presented in Chapter 2.4.

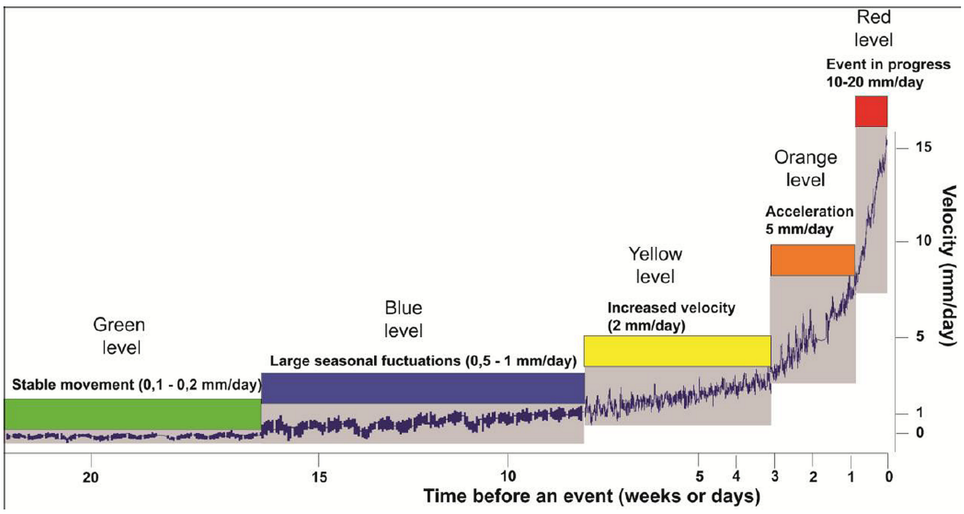

FIGURE 2.14: Warning Levels Åknes Rockslide: thresholds and associated warning levels for the total station (Kristensen et al., 2010).

In many countries, such as Canada, China and the U.S., WS and FS are operated on a regional scale to predict the danger level of spontaneous debris flows and scattered landslides based on rain thresholds (Thiebes, 2011). A prominent example is the Rio Watch, a WS that was installed in 1996 in Rio, Brazil on a regional base for landslides (D'Orsi et al., 2004). In the monitoring unit, rainfall patterns are observed to predict landslide probabilities. To this end, about thirty rain gauges are installed. In 1998, weather and hail stations were added to detect storms earlier. In the interpretation unit, warnings are released to experts if predefined thresholds for rain are exceeded. In the second step, experts analyze the data to assign four danger levels defined for expected spatial densities of landslides to four warning regions (Calvello et al., 2014). Information is disseminated by radio and TV stations to warn and evacuate endangered persons. Through the integration of weather and hail stations, the lead time could be increased and the implementation of preventive, emergency measures improved. In Italy, the first national FS was installed for rain-induced landslides (Brunetti et al., 2009). In the monitoring unit, 1,950 sensors deliver continuous rainfall measurements. This measured rainfall data is combined with weather forecasts and compared to predefined thresholds in the interpretation unit. The information is disseminated in five levels that represent probabilities of landslide occurrences. These forecast maps are published in a WebGIS interface and a daily report is delivered via e-mail to the Italian Department for Civil Protection (Rossi et al., 2012).

To prevent damages from spontaneous events and avoid false alarms on-site, AS are operated to detect spontaneous debris flows, rockfalls and snow avalanches (Gubler, 2000; McClung and Schaerer, 2006; Arattano and Marchi, 2008; Badoux et al., 2009). In the monitoring unit, ongoing processes are detected with sensors, such as seismic sensors, tripwires, radars. In the data interpretation unit, predefined thresholds determine if alarms are issued. In the dissemination unit, alerts are automatically released in the form of, for example red lights when predefined thresholds are exceeded. Detailed examples of AS for mountain processes are presented in Chapter 2.4.

Both WS and FS, especially for the prediction of spontaneous processes, have to deal with high uncertainties and are prone to false alarms. To decrease the uncertainty, precursors such as precipitation and other failure mechanisms should be further investigated and assessed probabilistically (Stähli et al., 2015). With stochastic disaggregation methods, radar measurements or models obtained from numerical weather predictions are downscaled before a large numbers of outcomes are produced. Modern approaches generate probabilistic estimations of areas most vulnerable for rain events (Schleiss and Berne, 2012). Advances have also been made in modeling (e.g. the hydro-mechanical properties) and in monitoring early slope failures of snow avalanches with seismic and acoustic sensors (Van Herwijnen and Schweizer, 2011; Reiweger et al., 2014) and could improve the forecast ability of WS and FS for spontaneous mass movement events.

2.4 Application of EWS Classification to Alpine Processes in Switzerland

The geography of Switzerland dictates that natural hazards often involve water and gravitationally driven alpine processes. The landscape is characterized through rivers and more than 1,500 lakes; and the Alps cover 60% of the country. Floods, (thunder) storms, forest fires, snow avalanches, debris flows, rock and ice falls, landslides, flash floods and glacier lake outburst floods (GLOF) are frequent events. The highest property damages in the last ten years have been caused by floods, hail and storm (IRV, 2014). Those numbers are strongly dominated by major flood events, which were triggered through long-lasting rainfall and caused over 50% of the total damage. Between 1972 and 2007, most fatalities have, however, been caused by debris flows, landslides, rockfalls and snow avalanches (Hilker et al., 2009).

Due to this geographical situation, EWS have a long history in Switzerland. The first automatic AS was operated in Mahnkinn in 1937 to detect spontaneous snow avalanches above an endangered railroad (Sättele and Meier, 2013). In 1967, the same company built an AS to protect railway sections prone to rockfalls (Figure 2.15). An automated earthquake detection system was installed in the early seventies and has been enhanced with the latest seismic sensor and data management technology operated today by the Swiss Seismological Service (Clinton et al., 2011). Automated rain measurements were first implemented in 1978. Since that, a modern measuring network with a large coverage has been developed by the Swiss Office for Meteorology and Climatology (MeteoSwiss) (Spreafico et al., 2005). In 1980, forty-six automated stations to measure the river levels and five flood AS were introduced (Spreafico, 1972). These technologies have been the first step towards the development of the flood FS operated by the Federal Office for the Environment, today. The first automatic snow measuring station was tested and developed in 1985 near Zermatt. In 1996, the WSL-Institute for Snow and Avalanche Research (SLF) began, in collaboration with the authorities to construct an automated measuring network, which provides an important part of the data basis for the Swiss Avalanche FS today (Lehning et al., 1998). The first on-site AS for debris flows was installed in 1995. Since that, a variety of on-site AS and WS for landslides, rockfalls, snow avalanches, floods and debris flows have been installed (Rageth, 1998; Gubler, 2000).

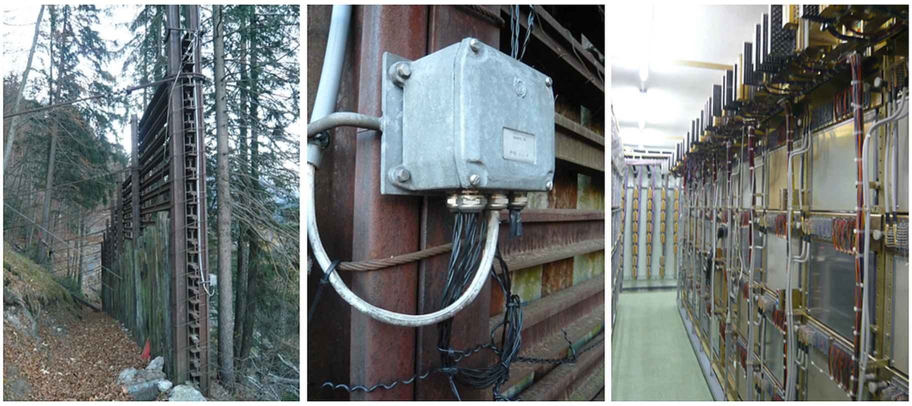

Figure 2.15: Early EWS for Rockfall Processes: fences with wires that are destroyed if rockfall hits the fence (left); wire connection to traffic control center that initiates disruption of the contact line and stops the train (middle); traffic control center (right).

After the major flood catastrophes in 2005 and 2007, in which unexpectedly high damages were caused, clear responsibilities were assigned to departments and the improvement of EWS technology was officially supported by the Swiss Government. A program for the Optimization of Early Warning and Alerting of Natural Disasters was initiated, in which procedures and responsibilities were defined and assigned to four departments (Hess and Schmidt, 2012). The Federal Office for the Environment operates a flood FS for main rivers and MeteoSwiss publishes a daily bulletin for severe weather; in winter, the SLF provides a daily bulletin for snow avalanches and the Swiss Seismological Service provides real-time earthquake information. To improve the collaboration of the four institutes, the common information platform GIN was established (Heil et al., 2014). In addition, warning procedures have been defined. Whenever warning level four, out of five levels, is exceeded, warnings are actively issued to authorities and to the public. The dissemination of the information is coordinated from a warning center and published via radio and television.

A prominent example of a national FS is the Swiss avalanche system operated by the SLF (Figure 2.16). The monitoring unit consists of a network with about 160 snow and weather stations in the Alps (Techel and Darms, 2014). These stations measure parameters such as the snow height, the amount of fresh snow, air and snow temperature and humidity, solar radiation, wind direction and wind speed. The sensors are controlled by data loggers and measurements are conducted at regular intervals. The power at these remote locations is supplied via solar panels and batteries. Data measured by the stations is sent via mobile networks or radio from remote stations to a central server.

The data interpretation is conducted by experts on a daily basis. During a briefing, two experts analyze measured sensor data, data from observers, and data from weather stations operated by MeteoSwiss, and consult meteorological forecasts as well as complex snowpack models. The forecasts are disseminated in the form of a bulletin, in which warning regions are assigned to five danger levels. The bulletin is published via radio, TV and internet, and if danger level four is exceeded, warnings are actively communicated to the warning center, which disseminates the information to persons responsible for safety and the public.

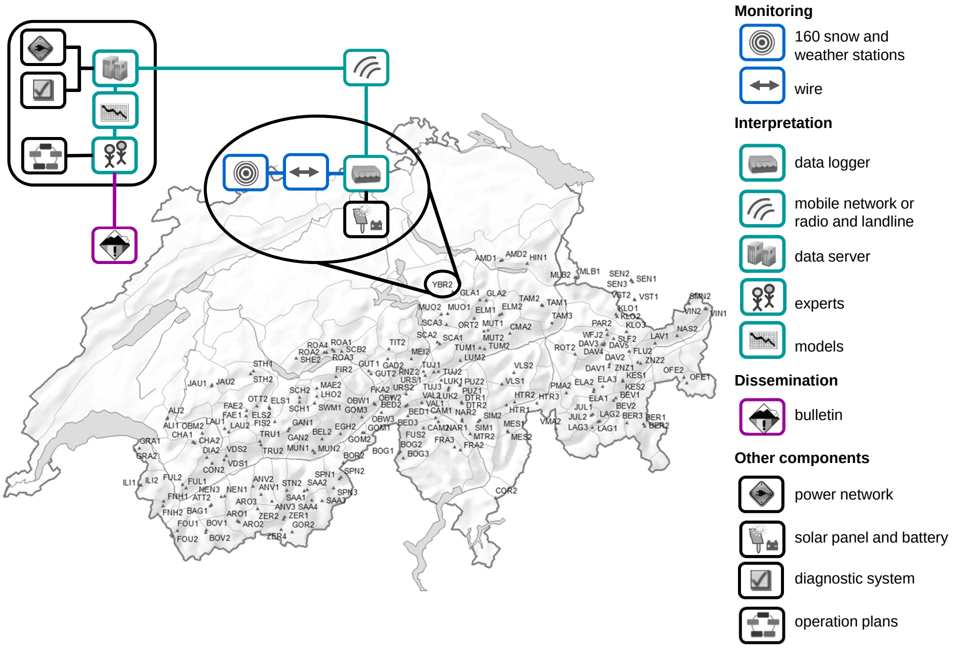

FIGURE 2.16: The Swiss Avalanche Forecasting System: incorporates an automated snow and weather measuring network, based on pixmaps©2015 swisstopo (5704 000 000).

Besides those national efforts, a variety of on-site WS and AS are operated by authorities or private companies in alpine regions. Within structured interviews and detailed field investigations, forty-eight on-site AS and WS operated in four cantons (Bernese Oberland, Grison, Ticino and Valais) could be identified by the end of 2011 (Figure 2.17). The range of EWS identified covers the variety of technologies operated for snow avalanches, debris flows, GLOFS, different magnitudes of rockfalls and landslides in Switzerland. Within the field investigation, all systems and their components have been documented in their three main units for monitoring, data interpretation and information dissemination, and assigned to the novel classification (Figure 2.2).

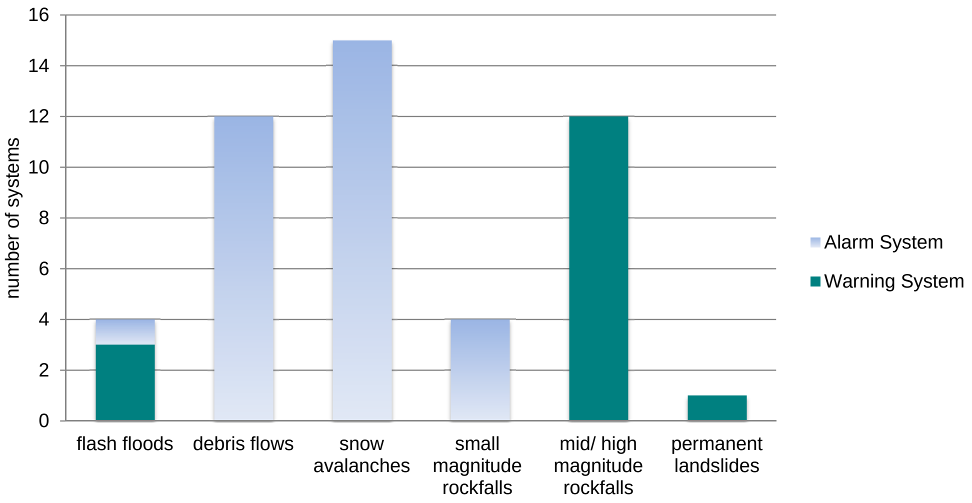

FIGURE 2.17: On-site EWS for Alpine Processes in Switzerland: identified within the field investigation are EWS mainly installed for snow avalanche, debris flow and rockfall processes.

2.4.1 On-site EWS for Snow Avalanche and Debris Flows

Debris flow processes and snow avalanches both build up spontaneously without clear precursors and flow fast. For the detection of snow avalanches there are fifteen on-site AS close to endangered road or railway sections within the field investigation, and twelve for debris flows. Two of those AS are operated for both processes and detect avalanches in the winter and debris flows in the summer.

In the monitoring unit, tripwires, seismic sensors and radars are used to detect ongoing events. The alarm decision in the interpretation unit is based on predefined thresholds or a combination of thresholds. The alarm information is transmitted directly via radio or mobile network to a dissemination unit, where acoustic or optic alarms are triggered to inform endangered persons. If trains are affected, either contact lines are disconnected or responsible traffic controllers are informed.

As an example, the Höfijbach AS is installed to protect traffic on a road from spontaneous debris flow events (Figure 2.18). The monitoring unit consists of two parts (GEOPRAEVENT AG, 2009). In the upper catchment, two tripwires are controlled by a data logger. In the lower part, another logger controls one tripwire and one echo sounding device to measure the flow depth (Figure 2.19). In the data interpretation unit, the status of the sensors is analyzed. Whenever tripwires in the upper catchment are pulled out, the upper logger sends information via radio to the lower logger. The lower logger activates an automated alarm when it receives a signal from the upper logger or when the lower tripwire is pulled out and the flow depth exceeds a predefined threshold. In the dissemination unit, optical signals at the underlying road are activated automatically and information is sent to system operators via mobile network. System operators who conduct the analysis can access a webcam to evaluate the situation.

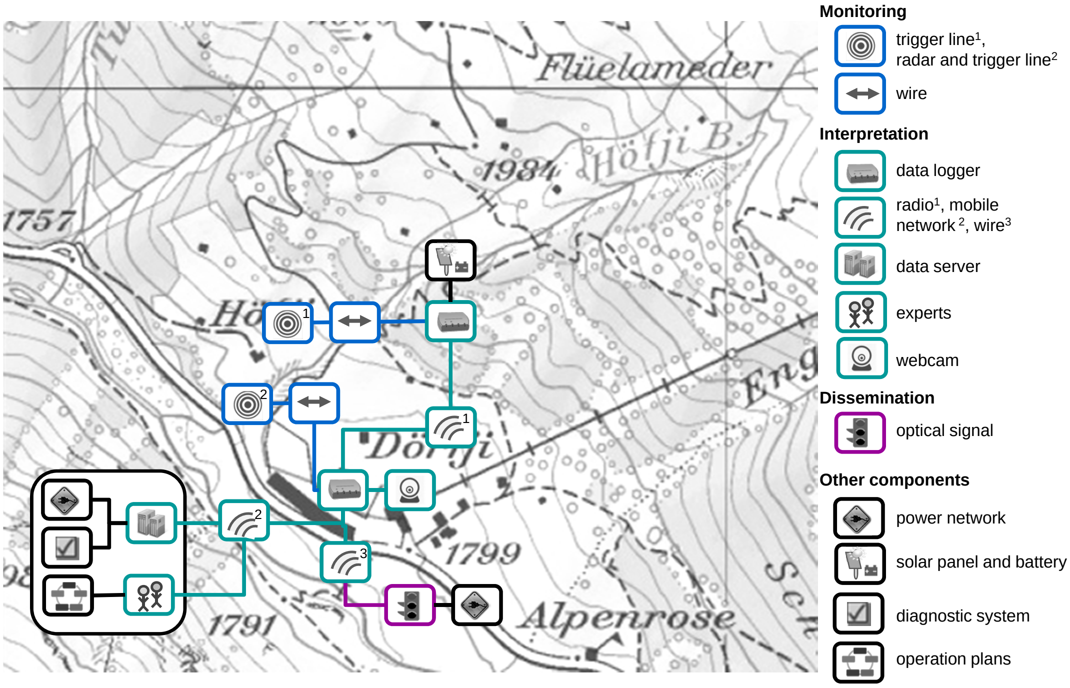

FIGURE 2.18: System Sketch Höfijbach Alarm System: installed for automated detection of debris flows, based on pixmaps©2015 swisstopo (5704 000 000).

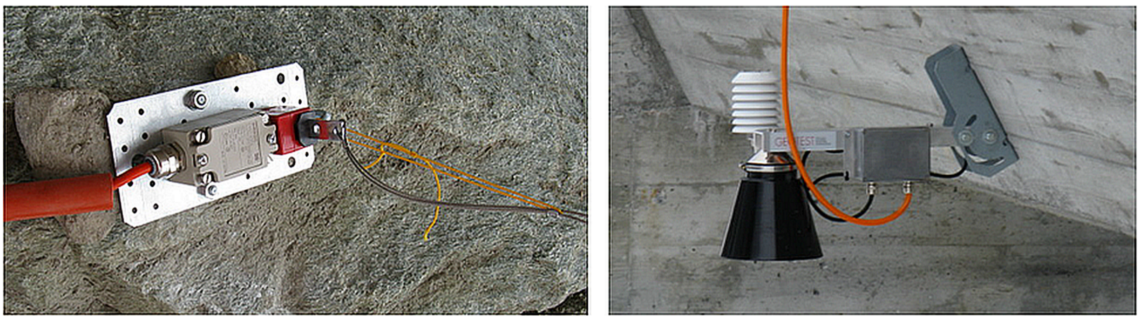

FIGURE 2.19: Sensors of the Höfijbach Alarm System: tripwire (left), echo sounding device to measure to flow height (right), (GEOPRAEVENT AG, 2009).

2.4.2 On-site EWS for Flash Floods

While river floods impose a significant danger in flat areas, flash floods arise from heavy rain or can occur from glacier lakes (GLOF) in alpine regions. For the detection of rain-induced floods, the Federal Office for the Environment operates an AS with measuring stations all over Switzerland, and for GLOF three WS are operated.

The monitoring unit of the AS includes thirty-eight measuring stations all over Switzerland. The data interpretation is based on predefined water level thresholds. Dependent on the location of the measuring station, river floods and flash floods can be detected. The information is disseminated with automated alarms issued to customers.

To detect flash floods from GLOF, three WS are installed. In Plaine Morte, a WS is installed to prevent damage from flash floods triggered in three glacier lakes regularly in the summer months (Figure 2.20). The monitoring unit consists of sensors installed to detect precursors of the flood event. To monitor precursors, pressure sensors in each lake detect significant changes in water level (Figure 2.21). To detect dangerous floods, a sensor to measure the flow height is installed further down in the catchment. The data interpretation consists of two levels; the first level is based on thresholds that are specified to send automated warnings to system operators; in the second instance, data is analyzed and pictures regularly taken by three webcams are consulted to decide on appropriate prevention measures. In the information dissemination unit, evacuations are conducted and mobile flood protection is established following intervention plans.

2.4.3 On-site EWS for Rockfalls and Landslides

Dependent on their magnitude, rockfalls appear suddenly or evolve over a long time. For the prediction of mid- and high-magnitude rockfalls and deep-seated landslides, WS are operated and spontaneous events are detected with AS.

For the prediction of mid- and high-magnitude rockfalls and rockslides twelve WS could be identified. In the monitoring unit, displacements are measured. Extensometers are installed in the tension cracks or total stations measure the distance to reflectors on the front face at regular intervals. Whenever specific thresholds are exceeded, automated information is send to the authorities as the first step of the data interpretation. In the

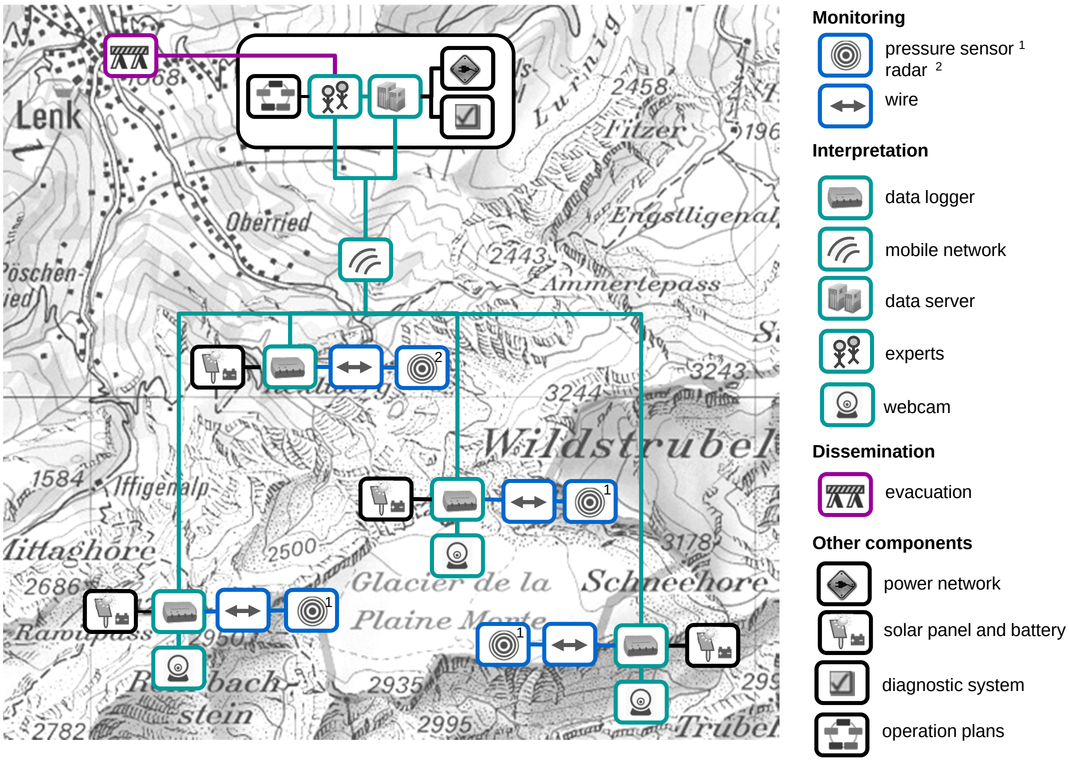

FIGURE 2.20: System Sketch of the Plaine Morte Warning System: installed to generate warning for GLOF, based on pixmaps©2015 swisstopo (5704 000 000).

FIGURE 2.21: Sensors of the Plaine Morte Warning System: a radar detects floods in the catchment (left), pressure sensors monitor the lake levels (right), (GEOPRAEVENT AG, 2015).

second step, a decision about evacuation is made by experts, who apply forecast models on measured sensor data. Often the inverse velocity model (see Chapter 6) is used to predict critical failure time. In the dissemination unit, evacuation plans summarize procedures and responsibilities for evacuations. The potential risk imposed by a deep seated landslide is mitigated with a similar WS.

AS for rockfall are installed to discover spontaneous, small-magnitude rock- and blockfall events endangering persons in cars or trains. In the monitoring unit, falling rocks are detected through nets equipped with pressure and seismic sensors or tripwires. The data interpretation is automated and an alarm is issued when thresholds are exceeded or when tripwires are pulled out. To stop cars or trains immediately, the dissemination unit is automated. Whenever an event is detected, contact lines are interrupted to stop arriving trains. Alternatively, signals or barriers are activated to warn traffic on endangered road sections. The Swiss Federal Railway Company SBB operates an advanced AS, where experts in a control center investigate the situation and confirm the alarm before trains are stopped (SBB, 2011). Through that additional decision-instance, the AS is able to avoid false alarms and unnecessary traffic interruptions (Figure 2.22).

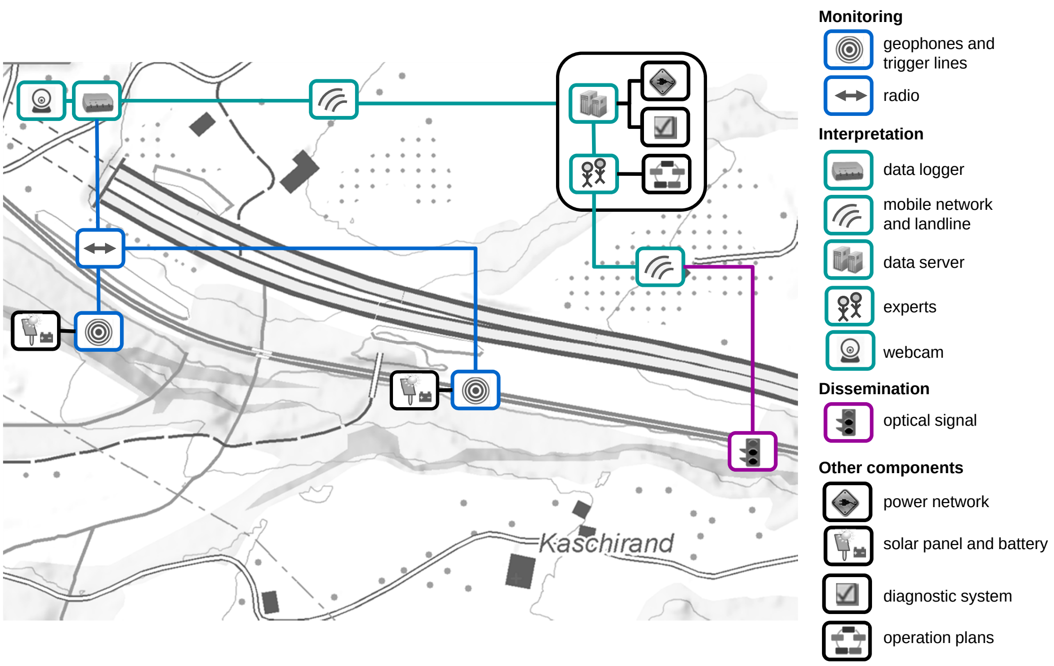

FIGURE 2.22: System Sketch of the SBB Alarm System: installed in Kaschirand to detect rock- and blockfalls on rails, based on pixmaps©2015 swisstopo (5704 000 000).

In the monitoring units of the AS installed in Kaschirand, there are two nets close to critical railways sections. Each net is equipped with twenty-one sensors (Figure 2.23). The sensors include two techniques to detect events. Seismic sensors measure ground vibrations and tripwires are pulled out when the net is hit. In the data interpretation unit, threshold combinations are stored in the logger and alarm information is issued automatically to a traffic control center. The responsible traffic controller analyzes the data and confirms the alarm within ninety seconds if the data indicates a dangerous event. In the dissemination unit, train stops are only initiated, if the traffic controller has not classified the alarm as a false alarm.

FIGURE 2.23: Sensors of the SBB Alarm System: seismic sensors detect ground shaking (left), tripwires are pulled-out when nets are hit by rocks (right), (SBB, 2011).

2.5 Summary

EWS are installed worldwide to prevent damages and loss caused by natural hazards and can be classified following our novel approach into AS, WS and FS. Each class can be described through typical characteristics, which depend on the process, the selected monitoring strategy and the associated lead time and system design (Table 2.1).

In practice, certain EWS classes are commonly applied for different natural hazard processes (Figure 2.24). AS are mainly installed for the detection of processes that have no precursors or precursors that are complex to interpret. These are processes that build up fast, such as earthquakes, debris flows, snow avalanches, wildfires, floods and volcano eruptions. To deal with short lead times, AS are fully automated.

TABLE 2.1: Characteristics of EWS Classes: depending on the selected monitoring strategy.

system class	alarm system	warning system	forecasting system
monitoring parameter	process parameters	precursors	precursors
lead time	short	extended	extended
prediction accuracy	high	medium	low to medium
decision instance	threshold	threshold/ experts	experts
automation	fully	partly	partly

WS are typically installed for processes that have clear precursors, such as volcanoes, tsunamis and GLOF, or for processes that evolve slowly, such as mid- and high-magnitude rockfalls and deep-seated landslides. The extended lead time, which can be in the range of days to weeks, enables experts to analyze the data and initiate appropriate mitigation measures.

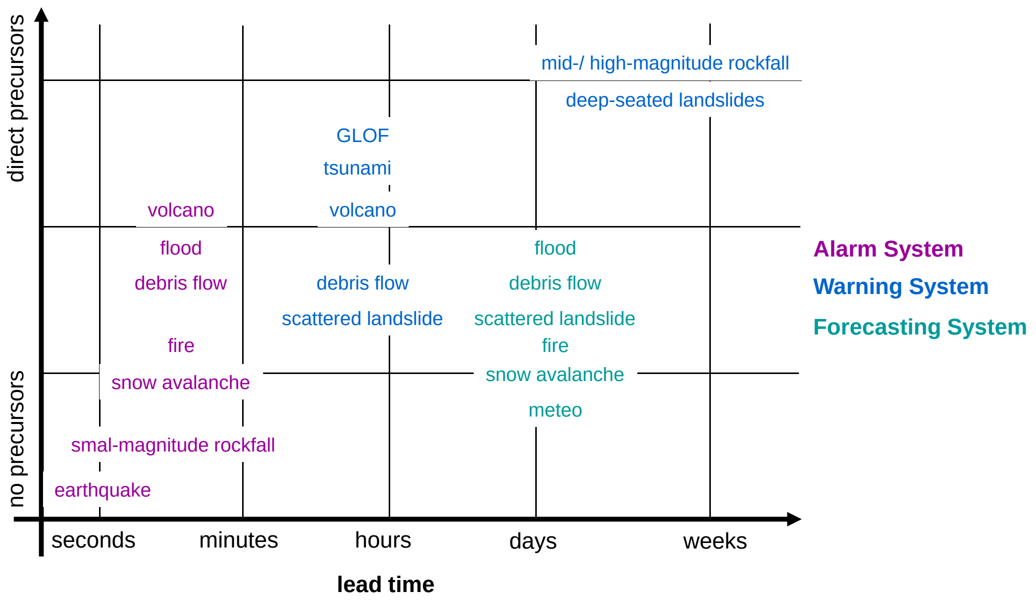

FIGURE 2.24: Overview EWS: type of occurrence influences type of EWS and lead time.

FS are often operated to increase the potential lead time of processes that appear spontaneously and do not come along with clear precursors, such as meteo, flood, wildfire, snow avalanche, debris flow and scattered landslide processes. The data interpretation is complex and conducted on a regular basis to provide danger level forecasts on a regional scale.

Currently, a clear trend towards automated processes and probabilistic methods can be observed to be able to increase the lead times and increase the prediction accuracy, especially for the prediction of spontaneous natural hazard processes. An important step towards improved EWS for natural hazards is thereby the enhancement of meteorological forecasts, because weather forecasts are the basis for the prediction of floods, wildfires, landslides, etc. In Switzerland, a great number of on-site AS and WS are installed to avoid uncertainties and associated false alarms that come along with regional WS and FS.

Chapter 3

Criteria and Methods for the Evaluation of Early Warning Systems

With the classification presented in the last chapter, the basis for a structured evaluation of EWS is provided. In the present chapter, possible criteria and methods for the evaluation of EWS are summarized. Together they should enable a quantitative assessment of EWS to integrate them in existing risk management approaches, in which alternative risk mitigation measures are compared to identify the optimal risk mitigation strategy. In Chapters 5 and 6, selected criteria and methods are then applied in case studies to test their applicability and to identify those parameters that influence the performance in different classes. In Chapter 4, selected methods are enhanced and a novel framework for the evaluation of EWS is provided.

3.1 Evaluation Criteria for EWS

Evaluation criteria for EWS should be consistent with the criteria commonly used in risk management for natural hazards to enable their comparability with alternative measures. At the same time, these criteria should address specific characteristics associated with complex technical and often human-centered EWS.

3.1.1 Efficiency and Effectiveness of EWS

In existing risk management approaches, it is common practice to identify optimal mitigation measures by comparing the effect on risk reduction and related cost of alternative measures in cost-benefit analysis (Penning-Rowsell et al., 2005; SafeLand, 2012; Špačková and Straub, 2014). In Switzerland, the conduction of cost-benefit analysis is even obligatory for financial support to be offered by authorities (Bründl, 2012). A software tool for the assessment of the economic efficiency achieved with varying mitigation measures is provided by the Federal Office of the Environment to support practitioners in applying for financial contributions.

The efficiency of mitigation measures is assessed when monetary values are assigned to the risk reduction achieved with a mitigation measure. Following SafeLand (2012), the efficiency of landslide mitigation measures can be expressed as a function of the total risk reduced divided by the cost of the measures (see Eq. 1.3). To assess the efficiency of EWS, monetary values have to be assigned to both benefits and negative consequences of EWS (Pate-Cornéll, 1986; Grasso et al., 2007; Schröter et al., 2008; Rheinberger, 2013). If the cost associated with the hazard and its consequences is not explicitly measured in monetary terms, instead of a cost-efficiency analysis, a cost-effectiveness analysis can be carried out. This less time consuming cost-effectiveness analysis is commonly used to assess and identify optimal structural mitigation measures for natural hazards in Switzerland (Bründl et al., 2009; Margreth and Romang, 2010). In a cost-effectiveness analysis, the life-cycle cost of the mitigation measures are compared against the effectiveness of the EWS. The effectiveness is a measure of the risk reduction achieved with the EWS, and a comprehensive evaluation addresses positive and negative consequences associated with EWS (Pate-Cornéll, 1986; Einstein and Sousa, 2006).

The consequences of risk reduction achieved by EWS are commonly evaluated using the framework of signal detection theory. This approach is based on a binary model in which a classifier is used to determine if correct rejections, hits, misses or false alarms are generated (Figure 3.1) (Swets, 1996). For EWS, a correct rejection means that no alarm is issued in situations where no hazard event occurs, a hit is achieved if a hazard event is detected and an alarm is issued, a false alarms means that an alarm is issued but no event occurs and a miss means that an event occurs, but no alarm is issued (Einstein and Sousa, 2006). The classifiers are, in the case of EWS, predefined warning criteria based on thresholds and combinations of threshold or human-decision instances.

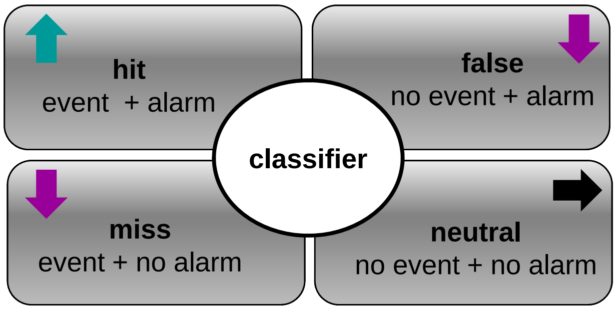

FIGURE 3.1: Signal Detection Theory: a perfect EWS detects all events and produces no misses or false alarms.

A perfect EWS detects every natural hazard event and never produces false alarms or misses (Intrieri et al., 2013). However, in the work environment of EWS, false alarms are commonly triggered by noise. For example in the case of a debris flow AS equipped with geophones to measure ground vibrations associated with dangerous debris flow events, noise can be induced by animals or side events, such as rockfalls in the catchment.

To identify an optimal trade-off, the benefits associated with a hit and the negative consequences of false alarms and missed events are compared in decision analysis. EWS achieve benefits by reducing the consequences of natural hazard processes. To this end, they mitigate the vulnerability (Einstein and Sousa, 2006) or the probability of exposure for endangered elements at risk (Dai et al., 2002; SafeLand, 2012). These benefits can be tangible/intangible and direct/indirect (Carsell et al., 2004). Tangible benefits are those to which monetary values can be assigned; for intangible benefits, monetary values are more difficult to define. Direct benefits are those that accrue for people and property profiting from mitigation measures implemented by the EWS; indirect benefits are economic benefits to those outside the area covered by the EWS. Likewise, negative consequences associated with false alarms and misses should be considered and quantified to ensure a comprehensive decision-making procedure. A high number of false alarms can e.g. reduce the probability that persons comply with an issued alarm, due to a loss of trust, which is known as the cry-wolf syndrome (Breznitz, 1989; Dejoy et al., 2006). This is associated with the financial loss caused by evacuations and interruption of business processes. For the evaluation of some EWS, the lead time is a crucial factor. If the lead time is too short, persons willing to comply are not able to do so (Pate-Cornéll, 1986) and if the lead time is too long, unnecessary costs for intervention measures are created.

Grasso et al. (2007) present a decision procedure, in which an optimal trade-off between false alarms and misses for an earthquake AS is determined in cost-efficiency analysis. In this study, costs are assigned to benefits of correct decisions (hit, neutral) and to wrong decisions (false alarm, miss). The costs in the case of a correct detection are those expected due to the earthquake, minus the savings due to the mitigation measures. Moreover, costs for taking mitigation measures are considered. In their study, they update the sensor data to predict the magnitude of the event when lead time decreases and illustrate that trade-off between prediction accuracy and lead time. As lead time decreases, the probability of false alarms and misses decreases. They conclude that the expected loss associated with a predicted magnitude is an important decision criterion that should be considered in decision analysis. In Grasso et al. (2007), the negative, intangible consequences associated with false alarms are not considered, as suggested by Pate-Cornéll (1986). In her analysis, she assessed the effectiveness of an EWS applied to fire detection in buildings, as the risk reduction achieved through early event detection and the probability that endangered persons comply with the warning. To quantify the compliance probability to a warning, the long-term effect of false alarms and the lead time are addressed.

For the evaluation of EWS, it is common practice to consider the probability that an event is detected (POD) and the probability of false alarms (PFA). E.g. Simmons and Sutter (2009) express the tornado warning performance of the U.S. National Weather Service in terms of the number of detected events and the false alarm ratio. Similarly, Rheinberger (2013) models the performance of two avalanche warning services based on the trade-off between POD and PFA. More recently, Liechti et al. (2013) describe the performance for probabilistic flash flood forecasts, generated with ensemble methods (see Chapter 2) with POD and the ratio of false alarms.

To summarize the relation between the POD and PFA, receiver operator characteristic (ROC) curves are used as simple graphical tools. This approach has seen widespread application, e.g., to represent the accuracy of diagnostic tests in medicine (Fawcett, 2006), and is increasingly applied in the field of EWS. POD and PFA are both influenced by the interpretation of the measured data. The basic relation of POD and PFA as a function of the threshold is illustrated in Figure 3.2. The measured signal can be either due to a hazard event H or due to noise N. The decision to issue a warning (detection, alarm) is based on the threshold t. If the measured signal is larger than t, a warning is issued. With increasing threshold t, both the POD and the PFA decrease. With $f_{(S|H)}(s)$ being the conditional probability density function (PDF) of the signal S given a hazard event H, and $f_{(S|\bar{H})}(s)$ being the conditional PDF of S given no hazard event $\bar{H}$, it is (Peterson et al., 1954; Swets, 1996):

$$POD(d) = \int_t^\infty f_{(S|\bar{H})}(s)ds \tag{3.1}$$

$$PFA(d) = \int_t^\infty f_{(S|\bar{\bar{H}})}(s)ds \tag{3.2}$$

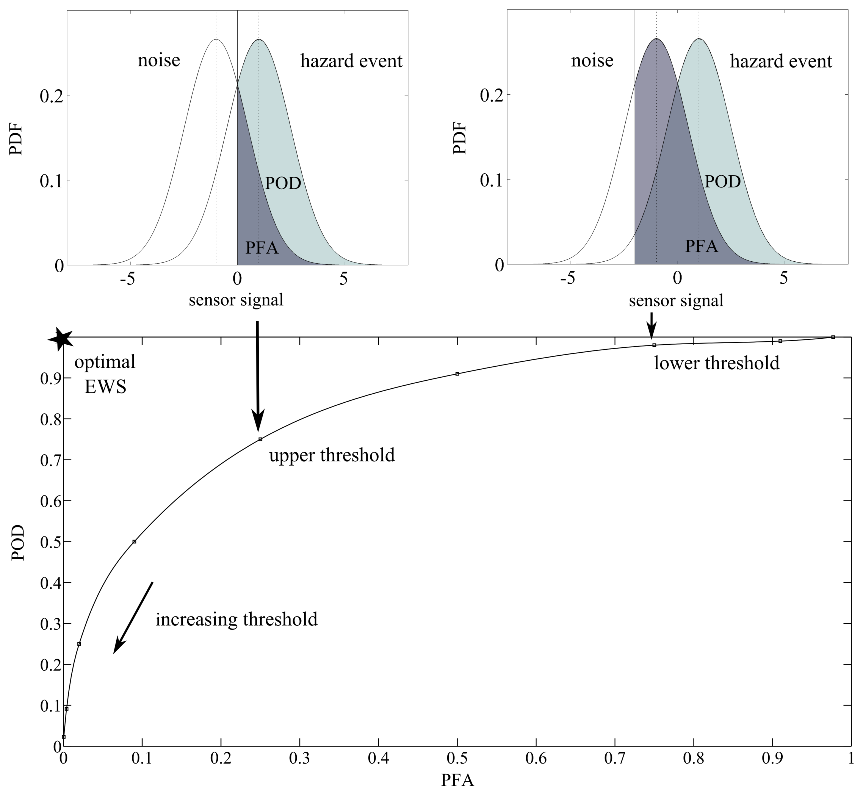

FIGURE 3.2: Components of Signal Detection Theory and Related ROC Curve: with an increasing threshold, POD and PFA decrease. A perfect EWS has POD = 1 and PFA = 0 (upper left corner).

POD and PFA are commonly used to determine the reliability of EWS, which is introduced in the next chapter as the second evaluation criteria. Reliability analysis has been identified as an accurate basis for a comprehensive effectiveness evaluation of structural risk mitigation measures and EWS (Margreth and Romang, 2010; Balbi et al., 2014).

3.1.2 Reliability of EWS

Reliability is defined as the "ability of an item to fulfill a required function under stated conditions for a stated period of time" (IEEE, 2010). In classical reliability analysis, the reliability of systems and components is expressed by failure rates (Blanchard and Fabrycky, 2011). The failure rate $\lambda(t)$ can be calculated following Eq. 3.3 from the expected number of failures $E[N]$ during a given time period t for s components:

$$\lambda(t) = \frac{E[N]}{t \times s} \tag{3.3}$$

Failure data can be collected from field data, incidents and records or it can be gathered in expert interviews (Stewart and Melchers, 1997). Depending on the industry, failure data is obtained in laboratory tests or observed in practice. This data is used to specify mean time to failure (MTTF) values, or for repairable parts from mean time between failure (MTBF). If values for MTTF or MTBF are specified, the failure rate of a system or its components can be calculated following Eq. 3.4:

$$\lambda = \frac{1}{MTTF} \quad \text{or} \quad \lambda = \frac{1}{MTBF} \tag{3.4}$$

In some industry sectors, such as automotive, electronics, nuclear power plants, offshore platforms and telecommunications, tailored handbooks provide constant failure rates for components and guidance for their quantification. Most of those guidelines are adapted from the first official handbook, the MIL-HDBK-217 - Reliability Prediction of Electronic Equipment, published by the U.S. Department of Defense (IEEE, 2002).

Failure rates vary during the system lifetime. Following the so-called Bathtub curve, three phases can be distinguished (Figure 3.3). In the first phase, manufacturing imperfections lead to initial failures and the hazard rate decreases with time. In the second phase, which represents the majority of the lifetime, the failure rate is constant. In the third phase, failures due to wear-out and aging increase and so does the failure rate.

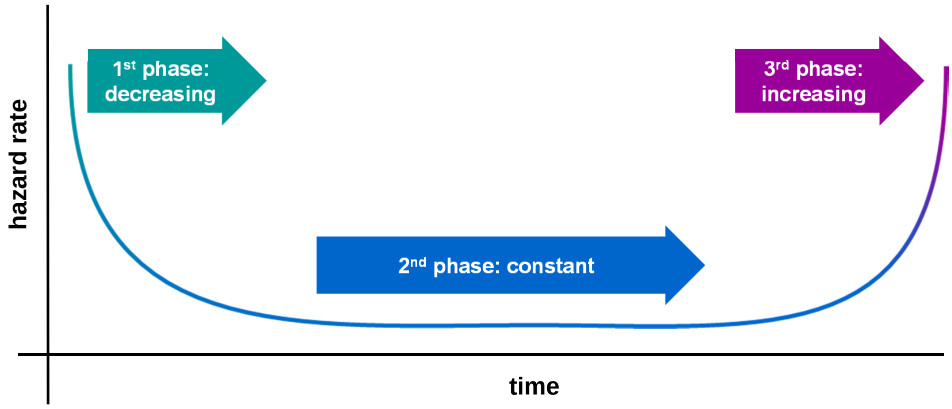

FIGURE 3.3: Bathtub Curve: describes three phases of failure rates during the life-cycle.

The failure probability over time t can be described in statistical distributions, which are fitted to experimental data. Exponential distributions are commonly used to describe the second phase, where failure rates are constant. In risk analysis for civil and environmental engineering, failures are often expected to occur randomly in time and independently of each other (Straub, 2012). The failure probability is thus calculated based on a Poisson process (Eq. 3.5).

$$Pr(F(t)) = 1 - exp^{-\lambda t} \tag{3.5}$$

To describe the failure probability in these phases, where the failure rate increases or decreases with time t, Weibull and Lognormal distributions are often used; e.g. Weibull distributions to describe the wear-out process when the shape parameter of the distribution is larger than one (IEEE, 2002). In civil engineering, non-homogeneous Poisson processes are applied, in which λ is a function of time (Straub, 2012). In the Preonzo case study, the probability of n_F failures out of n sensors on a given day is described through a binomial distribution (see Chapter 6.2.3).

The technical reliability of a system depends on the failure probabilities of single system components, but also on their arrangement in the system. Distinctive components can be connected in series, in parallel or as combinations thereof (Stewart and Melchers, 1997; Straub and Der Kiureghian, 2010). When components are connected in series, the failure of a single component will cause a system failure (Figure 3.4 a). The system reliability decreases with the number of components connected in series. In contrast, the system reliability increases when components are designed parallel (Figure 3.4b). In such a redundant system configuration, a system is available as long as only one component works.

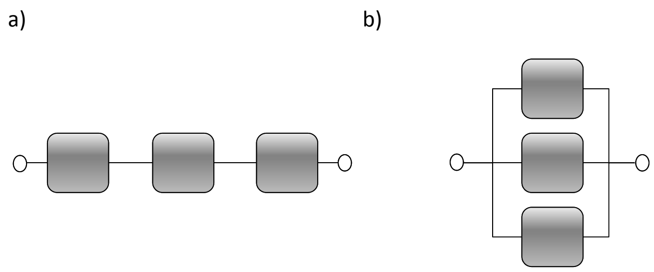

FIGURE 3.4: Reliability-Block Diagram: a) serial; b) parallel/ redundant system configurations.

In the majority of published reliability analyses in the field of EWS for natural hazards, not the technical but the inherent reliability is evaluated. The inherent reliability is then typically quantified as the probability of a correct forecast POD (Pate-Cornéll, 1986; Rheinberger, 2013; Balbi et al., 2014) alone or as a function of both POD and PFA (Krzysztofowicz et al., 1994). If the reliability is quantified as a function of POD and PFA, results are often graphically illustrated in ROC curves (see Figure 3.2). However, in some analyses, the reliability is quantified as the prediction accuracy and demonstrated as a function of the lead time of the EWS (Grasso et al., 2007; Schröter et al., 2008). As lead time increases, more data is collected and the prediction accuracy increases. The prediction accuracy accounts not only for the ability of the system to distinguish between noise and hazard, but also assesses its ability to predict the location and the severity of the event. In published reliability analyses of EWS, either the technical probability or the inherent reliability is considered. Analysis in which both aspects are addressed could not be found.

To ensure a comprehensive evaluation of EWS in the framework approach (see Chapter 4), reliability analysis will consider both, the inherent and the technical reliability. In the next section, methods used to quantify and optimize the reliability and the effectiveness of EWS are presented.

3.2 Quantitative Evaluation Methods for EWS

To evaluate the reliability and effectiveness, different methods are applied in the field of EWS. In this chapter, quantitative methods are summarized to provide an optimal basis for the framework approach and the case studies in the next chapters. Some of these methods can be applied to evaluate both criteria; the reliability and the effectiveness. First, methods primarily applied for reliability assessment (fault trees and Bayesian networks (BN)) are presented. Then, methods that support decision-makers in the identification of an optimal trade-off between positive and negative consequences associated with EWS (decision trees and influence diagrams) are summarized.

3.2.1 Fault Tree Analysis

To assess the failure probability of systems, classical quantitative methods, such as event trees, fault trees, bow tie or failure mode and effect analysis, are applied (Stewart and Melchers, 1997). Fault trees are Boolean logical diagrams that consist of an undesirable top event and a logical order of possible events connected via AND and OR gates (Figure 3.5). In this illustrative example, the top event is used to describe the case when the *alarm is not issued* by an EWS. That could be either because of a *technical system failure* OR because *no event is indicated* by the EWS. An event is not indicated if in a redundant sensor unit both *sensor 1 failed* AND *sensor 2 failed*.

With such a fault tree, Bründl and Heil (2011) assess the technical reliability of the Swiss avalanche FS in a case study (system details, see Figure 2.16). First, they depict all system components and their dependencies in a system sketch. Second, they constructed the fault tree to identify the most critical system components in a semi-quantitative way. However, they do not address all possible system failures and the inherent reliability of the FS. In recent publications, complex and human-centered EWS are evaluated with BN, which are used in the reliability analysis community as a novel tool to assess the reliability of systems (Langseth and Portinale, 2007; Bensi et al., 2012).

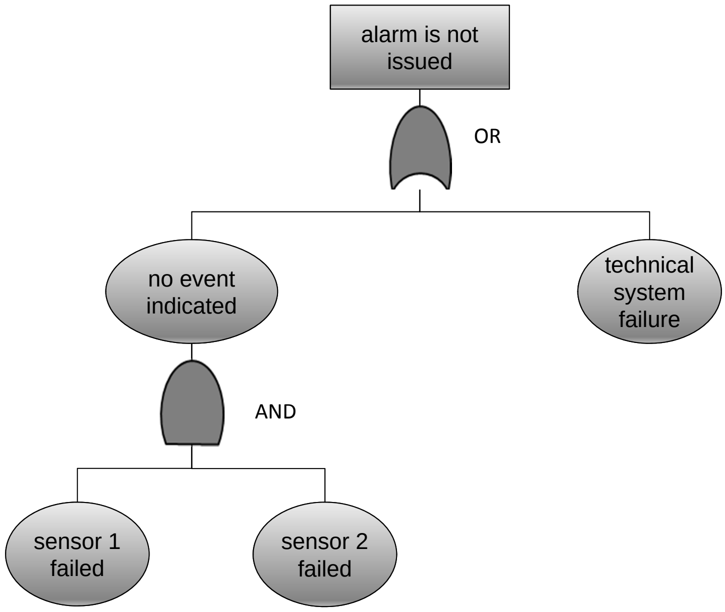

FIGURE 3.5: Fault Tree: with an undesirable top event and AND and OR gates.

3.2.2 Bayesian Networks

In recent years, BN have been increasingly applied for environmental modeling and for the evaluation of natural hazard risks. Aguilera et al. (2011) and Vogel (2014) summarize suitable applications of BN for environmental modeling. Straub (2005) states reasons why BN have a large potential for assessing natural hazard risks. They allow the incorporation of expert knowledge, deal with rare data and are based on an intuitive modeling approach. Applications of BN for modeling EWS are presented by Medina-Cetina and Nadim (2008), who present a BN of a landslide EWS and apply it to determine optimal thresholds, and by Blaser et al. (2011), who use BN to assess a Tsunami EWS in Sumatra.

A BN is a graphical probabilistic model consisting of nodes and arcs. Each node represents a random variable and the arcs among the nodes characterize the stochastic dependence among these (Jensen and Nielsen, 2007). In many instances, the arcs can be constructed following the causal relations between the random variables (Straub and Der Kiureghian, 2010). In discrete BN, each node has a finite set of mutually exclusive states. Conditional probability tables (CPT) are attached to each node, specifying the probability of the random variable conditional on its parent nodes. The joint probability distribution $P(U)$, in which $U = \{A_1, A_2....A_n\}$ is the universe of variables A_i, is calculated from all CPT $P(A_i \mid pa(A_i))$ in the BN, in which $pa(A_i)$ are the parents of A_i, following the chain rule:

$$P(U) = \prod_{i=1}^{n} P(A_i \mid pa(A_i)) \tag{3.6}$$

An illustrative example is depicted in Figure 3.6. In this BN, the probability of *alarm* A issued through an EWS through timely *indication* I of a dangerous avalanche *event* E can be modeled. In addition, an avalanche *event* can generate *damage* D. The joint probability distribution for this avalanche example (Eq. 3.7) can be obtained following the chain rule (Eq. 3.6).

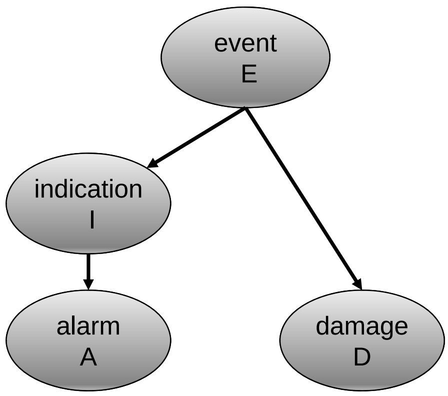

FIGURE 3.6: Illustrative Example of a Bayesian Network: to model the avalanche problem.

$$P(E, I, A, D) = P(E)P(I \mid E)P(D \mid E)P(A \mid I) \tag{3.7}$$

In the example BN, probabilities for $P(E)$ and conditional probabilities for $P(I \mid E)$, $P(D \mid E)$ and $P(A \mid I)$ are described in the CPT of child nodes. In Table 3.1, the probabilities of *damage* conditional on an *event* are specified. If no *event* occurs, the probability of *damage* is zero; if an avalanche *event* occurs, the *damage* probability is 0.8 because smaller events may not cause *damage*. If similar probabilities and conditional probabilities are defined for all nodes, the BN can be used to compute the conditional probability of all random variables. In the BN, the joint probability for all possible scenarios can be modeled, e.g., for the case of an avalanche *event* that is not *indicated* by the EWS and no *alarm* is issued, which causes *damage*.

Table 3.1: CPT of the Node Damage: to specify the probability of damage conditional on an event.

		probability conditional on	
event		no	yes
damage	no	1	0.2
	yes	0	0.8

For the reliability analysis of EWS, BN have first been applied in our case studies (see Chapter 5 and 6) and in a study of Sturny and Bründl (2014), who used BN to probabilistically model the technical reliability of a glacier lake WS. In this analysis, they follow findings from Sättele et al. (2012a) and estimate the failure probability of components, such as *battery, logger, station, sensor*, considering both *internal failure* causes due to e.g., aging, and *external failure* sources due to e.g., lightning and humidity (see Figure 3.7). In the CPT of the nodes that represent system components, conditional failure probabilities are specified (see Table 3.2). With this BN, they model the overall technical reliability and identify those system components that are most critical to system failures but do not cover the entire complexity of the EWS. The inherent reliability of the WS is not addressed. In the following (see Chapters 4 and 5), an enhanced BN is applied to model the technical and inherent reliability of EWS.

Table 3.2: CPT to Specify Conditional Failure Probabilities: due to internal and external failure causes.

external failure		yes		no	
internal failure		yes	no	yes	no
component	functioning	0	0	0	1
	failure	1	1	1	0

3.2.3 Decision Trees

Decision trees are graphical constructions for quantifying the probabilities and consequences associated with possible outcomes of decision-making (Friedl and Brodley, 1997). Between an initiating decision (squared node) and possible outcomes (triangles),

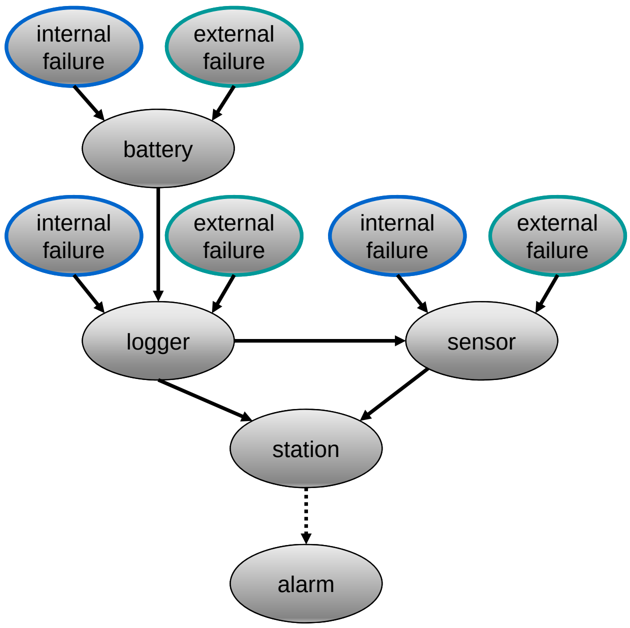

FIGURE 3.7: BN to Model Failure Probability of an EWS: includes components of the EWS (here battery, logger, station and sensor), which can fail due to internal and external failure causes.

subsequent random outcomes or chances (circles) can be defined in a logical order. The chances at each branch need to be mutually exclusive and collectively exhaustive. Rheinberger (2013) adapted a decision tree (Figure 3.8) originally developed for the evaluation of fire warning systems in buildings by Pate-Cornéll (1986) to analyze and compare the performance of two Swiss snow avalanche warning services.

Based on the *National Avalanche Forecast* F, local risk managers have to decide if the endangered roads are *closed* ($C = 1$) or not ($C = 0$). After the closure, an avalanche *event* can occur ($E = 1$) or not ($E = 0$). The decision tree leads to four possible outcomes (neutral, a hit, a miss or false), see Chapter 3.1. The consequences of these outcomes are described in utility functions, including costs and positive and negative short- and long-term effects on risk reduction achieved with the EWS. Moreover, all decisions are associated with the life-cycle costs for acquisition, operation and maintenance of the EWS. To identify an optimal decision rule D the expected utilities for each decision outcome $U(C, E)$, the probabilities of an avalanche (non-)occurrence $P(E)$ and the probabilities to decide appropriately, conditional on the (non-)occurrence of an event $P(C \mid E)$, are minimized following Eq. 3.8. The probabilities of avalanche (non-)occurrences are approximated from avalanche frequencies stored in a database. The

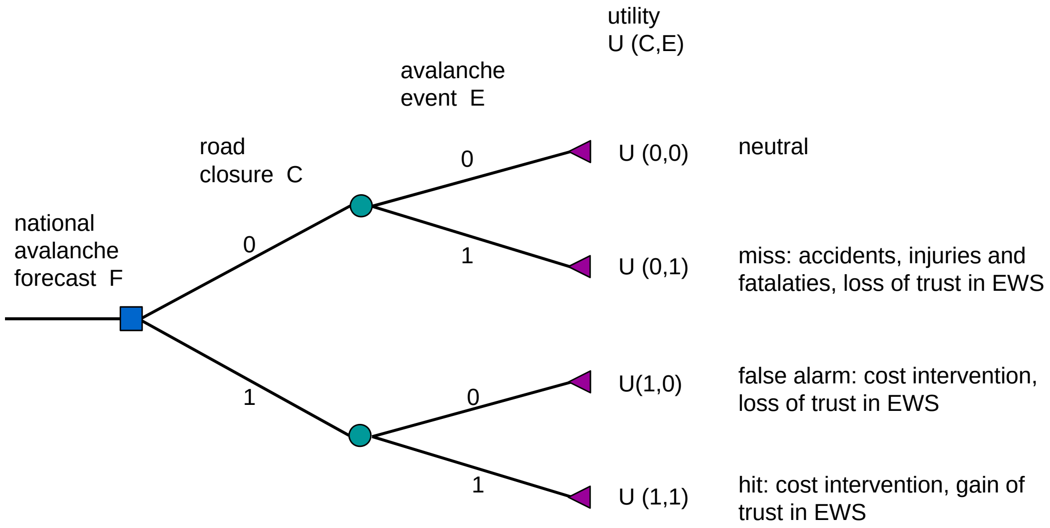

FIGURE 3.8: Decision Tree Avalanche Problem: can lead to neutral decision, hit, misses and false alarms.

conditional probability of making a right decision (hit, neutral) and of wrong decisions (false alarm, miss) are derived from the past performance of the two systems under consideration.

$$E[(D)] = \sum_C \sum_E P(E) \times P(C \mid E) \times U(C,E) \tag{3.8}$$

A similar approach is presented by Martina et al. (2006), who identify the optimal threshold of a flood EWS by minimizing the expected value of a Bayesian cost utility function. In this utility function, the decision conditional on the occurrence of a flood event (POD/ PFA) is considered. The decision tree originally developed by Pate-Cornéll is more complex and addresses the long-term memory-effect of false alarms on the response probability of individuals to a warning. The decision tree can be updated whenever a new event occurs and is used to model the response at a certain lead time, given individual risk attitudes, cost of the event and of response. This decision tree and two alternative models to quantify the response probability are then used to identify the optimal threshold and associated optimal trade-off between POD, PFA and the lead time. Another decision tree for the evaluation of EWS is presented by Einstein and Sousa (2006). They calculate the utilities (costs) caused by an EWS in the event of multiple damage levels. The utilities include costs of consequences, costs for passive countermeasures and the effectiveness of the EWS for certain hazard danger levels. Through an additional sensitivity analysis, they identify the effectiveness, which is expressed by conditional probabilities, as a significantly influential factor on the achieved risk reduction. However, to identify a maximal risk reduction associated with minimal costs for complex EWS, the authors recommend the application of influence diagrams.

3.2.4 Influence Diagram

BN can be extended to influence diagrams, which enable decision-making under uncertainty, whereby the strategy that maximizes the expected utility is sought (Shachter, 1986; Jensen and Nielsen, 2007). Influence diagrams are essentially BN, extended with decision nodes (squared) and utility nodes (rectangle), wherein the latter describe the preferences of the decision-maker. In Figure 3.9, the BN illustrated in Figure 3.6 is enhanced to an influence diagram that enables the choice of the optimal decision rule of the avalanche EWS.

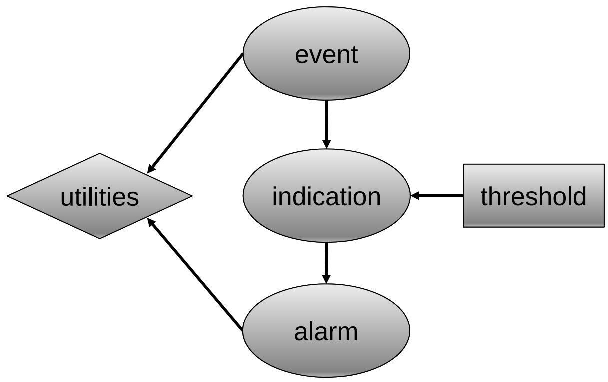

FIGURE 3.9: Illustrative Example of an Influence Diagram: based on the BN (Figure 3.6) to identify the optimal decision rule.

In the decision node *threshold*, two decision rules are modeled as warning thresholds. A low threshold represents a less risk-tolerant decision-maker and a upper threshold represents a more risk-tolerant decision-maker. The probability of the occurrence of an *event* is specified in the top node with 0.05. The probability that the EWS *indicates* an event is specified conditional on the *threshold* and the occurrence of an *event* (see Table 3.3).

TABLE 3.3: CPT of the Node Indication: to assign conditional probabilities to an indication of the EWS.

event		yes		no	
threshold		low	high	low	high
indication	yes	0.99	0.7	0.1	0.01
	no	0.01	0.3	0.9	0.99

In the node *utility* (see Table 3.4), monetary values are assigned to possible outcomes (hit, miss, neutral, false alarms). If one computes the influence diagram, the expected utilities for both thresholds are modeled. For the less risk-tolerant decision-maker (low threshold) a utility value of -167 is achieved and for the more risk-tolerant decision-maker (upper threshold) the utility is -209. In that case, a lower threshold would be the more optimal warning strategy. A more detailed application of an influence diagram is demonstrated in the Illgraben case study (see Chapter 5).

TABLE 3.4: CPT of the Node Utility: to assign monetary values to neutral decisions, misses, hits and false alarms.

event	yes		no	
alarm	yes	no	yes	no
value	- 5000	-10000	-1000	0

3.3 Summary

The effectiveness and the reliability are valuable evaluation criteria for EWS and enable their comparison to alternative risk mitigation measures in an integrated risk management approach. The effectiveness is the reduced risk reduction achieved with the EWS and can be quantified from positive consequences achieved through timely detection (POD) and negative consequences, such as decreased compliance due to false alarms (PFA). The reliability of EWS is commonly expressed as a function of POD and PFA and an adequate basis for effectiveness considerations. A comprehensive reliability evaluation includes both the technical failure probabilities of system components and the inherent reliability of EWS. In existing studies, fault trees and Bayesian approaches are applied to assess the reliability and effectiveness of EWS. Decision trees are applied to identify an optimal trade-off between the POD, PFA and the lead time. In the field of EWS, BN have not been previously applied to model the reliability. In the following chapter, a novel framework approach, in which the reliability of EWS is modeled with a BN as the basis for the effectiveness evaluation, is demonstrated. In two case studies (see Chapter 5 and 6), the BN is applied to model the reliability and enhanced to identify optimal warning strategies.

Chapter 4

Framework for the Evaluation of Early Warning Systems

In the previous chapters, a classification, evaluation criteria and methods for the quantitative assessment of EWS were introduced. In this chapter, a novel framework approach, enabling the quantification of the effectiveness achieved with EWS, is presented. The framework approach addresses needs and requirements associated with different EWS classes, identified in the classification and in two detailed case studies, in which EWS for alpine processes were investigated (see Chapter 5 and 6). However, it is generically applicable for all kinds of natural hazard processes. Figure 4.1 illustrates the three main parts, in which the effectiveness is derived from the reliability.

Part I: Reliability analysis to quantify the automated parts of EWS: The technical reliability depends on failures of components and dependencies among them. The inherent reliability depends on the monitoring strategy (type, number and positioning of sensors) and automated decision instances (thresholds and their combinations). The reliability is expressed in terms of POD and PFA.

Part II: Reliability analysis to quantify the non-automated parts of EWS: The technical reliability depends on failures of components and dependencies among them and influences the ability of decision-makers to make accurate event forecasts. The inherent reliability of WS and FS depends on human decision-making based on models and their accuracy. The reliability is expressed in terms of POD and PFA and depends on the lead time.

Part III: Effectiveness Analysis of the EWS: The effectiveness of EWS can be quantified in terms of the risk reduction achieved through timely detection of an event POD and the probability that persons comply to the warning (POC), which can be decreased due to frequent false alarms (PFA) or insufficient lead time provided by the EWS.

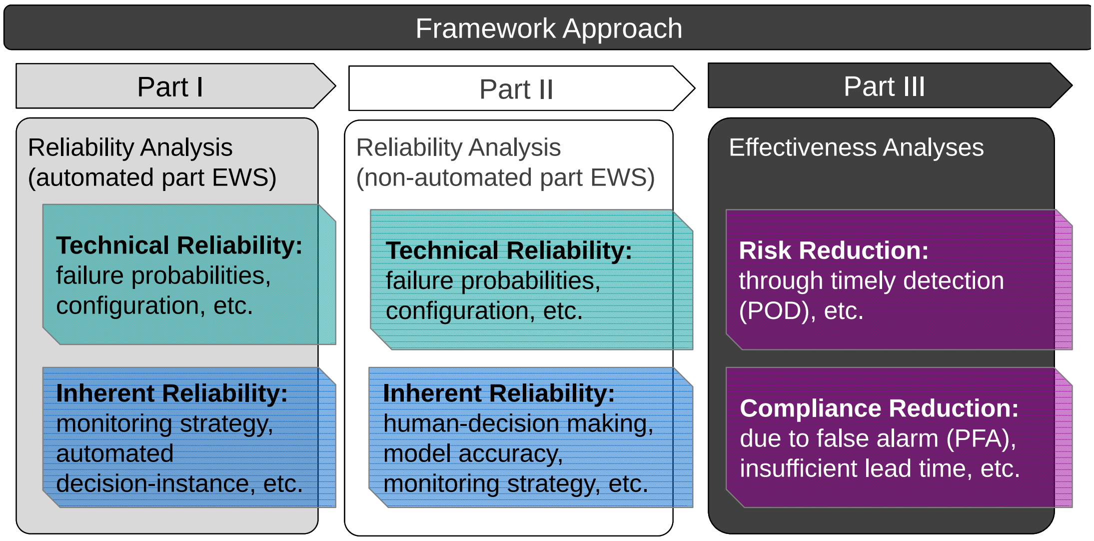

FIGURE 4.1: Framework Approach for Quantification of EWS: includes three main processes.

In function of the EWS class and the degree of automation, different parts of the framework approach need to be conducted. In Figure 2.3, parts typically automated in each EWS class are illustrated. Fully automated AS can be quantified within part I and III; partly automated WS and FS require a more complex analysis, including all three parts. In the following sub-chapters, steps, equations and factors necessary to evaluate EWS in those three main parts are described. For part I, a tailored method to assess the reliability is introduced.

4.1 Reliability Analysis of the Automated EWS

The reliability achieved by fully automated AS and the automated part of WS and FS can be determined in a comprehensive analysis, including both the technical and inherent reliability (Figure 4.2). The reliability analysis is conducted within six steps, in which the reliability is modeled probabilistically in a BN and expressed in terms of POD and PFA.

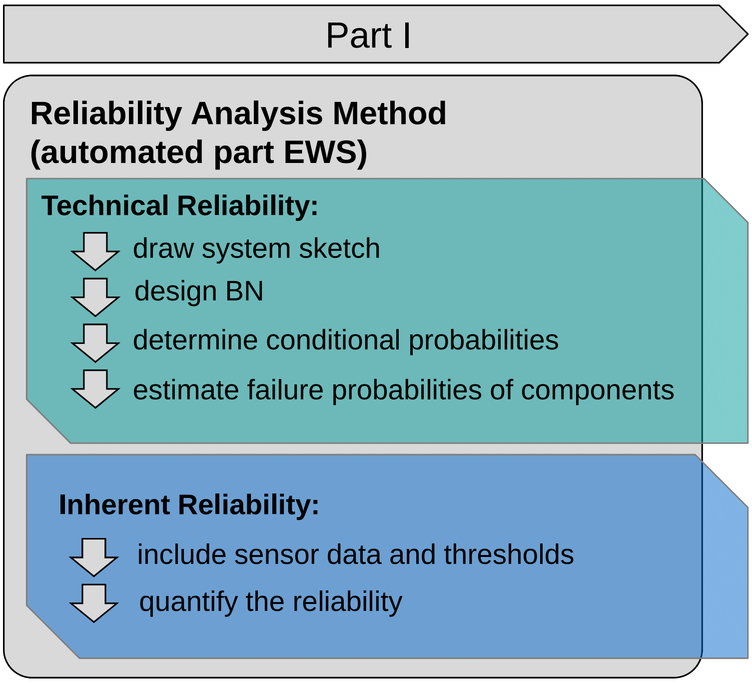

FIGURE 4.2: Reliability Analysis for Automated Parts of EWS: includes six steps to model technical and inherent reliability in a BN.

In the context of EWS, the POD and the PFA can be defined within an expectation operator $E[\cdot]$ as:

$$POD = E\left[\frac{\text{number of detected events}}{\text{number of events}}\right] \tag{4.1}$$

$$PFA = E\left[\frac{\text{number of days with false alarms}}{\text{number of event free days}}\right] \tag{4.2}$$

Note that the PFA must be defined using a reference unit, e.g., days, as illustrated in Eq. 4.2. To ensure the comparability, it is important to use the same unit consistently throughout all parts of the framework.

4.1.1 Draw System Sketch

A system sketch is an essential basis to understanding the design and the dependencies among the components in an EWS (Figure 4.3). It can be constructed according to the three main units of an EWS: monitoring, data interpretation, information dissemination and contains all EWS components, including those for power supply, data management and diagnostic tools (see Fig. 2.3). Diagnostic tools are important as they deliver timely information on failures of components and should be considered when estimating failure probabilities of system components (see Chapter 4.1.4). The degree of detail is limited to main components, e.g., the data logger includes the software or the mobile network includes the devices for data transmission, the modem and the availability of the mobile phone. Redundant system parts, which are duplications in the form of identical or different system components fulfilling the same function, are depicted redundantly in the system sketch. To understand the EWS and prepare for the next step, all the components essential for the warning chain are highlighted.

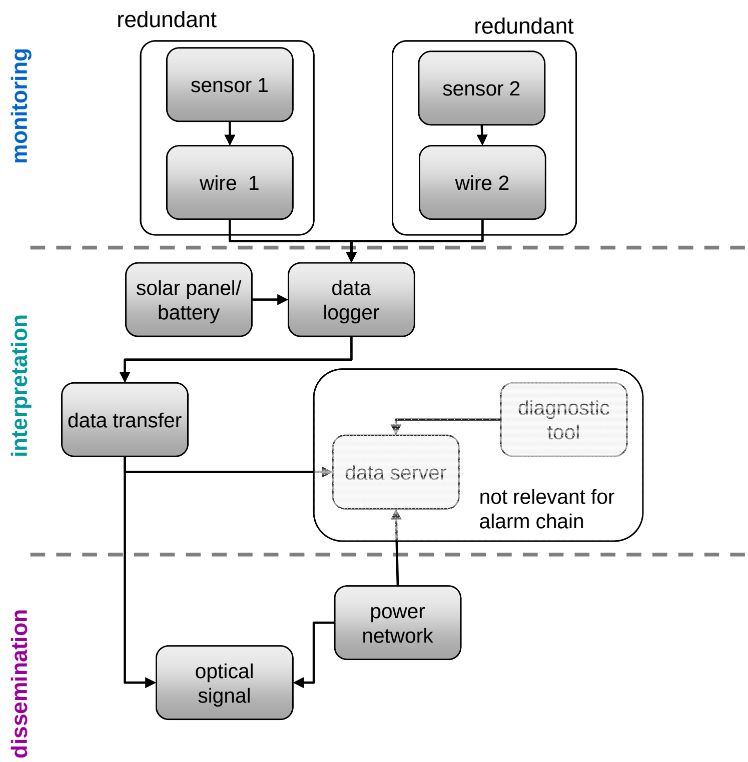

FIGURE 4.3: System Sketch of EWS: constructed according to the three main units and including all components of the EWS.

4.1.2 Design BN

The BN is constructed according to the three main units of an EWS and can be derived from the system sketch. It consists of arcs and three different node types, shown as black, white and grey in Figure 4.4.

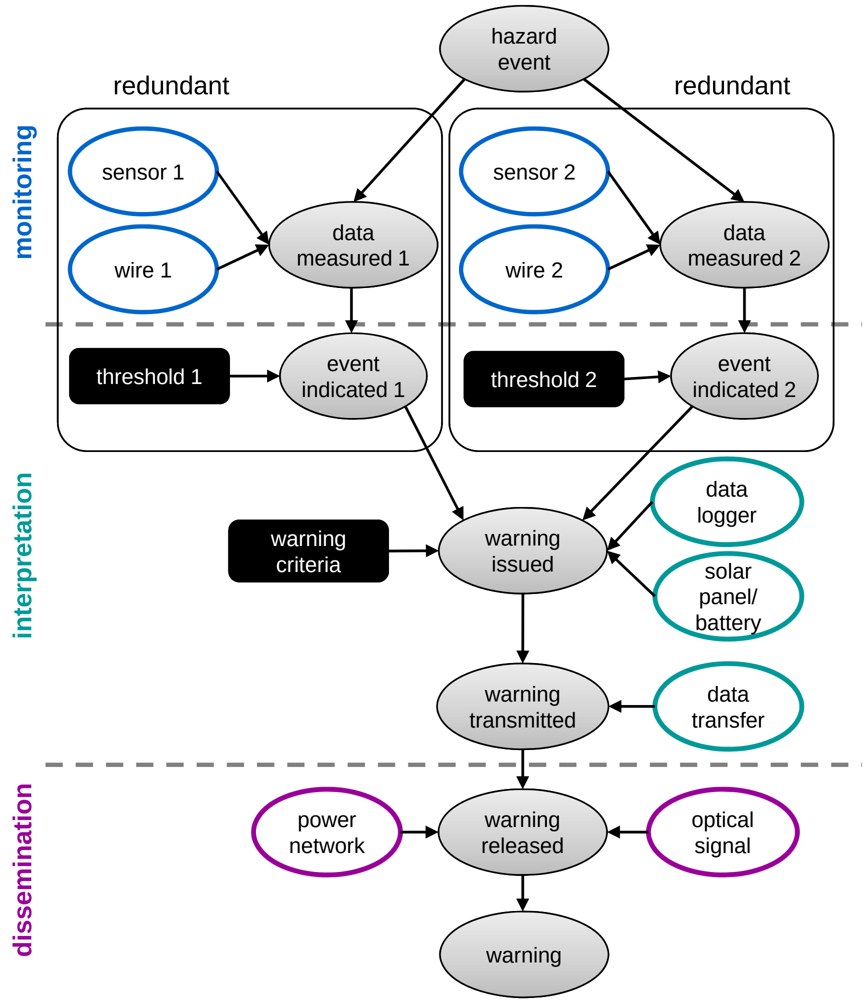

FIGURE 4.4: BN for EWS Reliability Analysis: consists of arcs and three node types.

Grey nodes depict the causal chain from the *hazard event* to the *warning*. In the top node *hazard event*, mutual states can be assigned to indicate the occurrence of an event. Two states (*yes* and *no*) are necessary to model the reliability of the EWS as a measure of POD and PFA, in the node *warning* (see Chapter 4.1.6). Additional states can be defined in the top node to assess the POD achieved for different event magnitudes. The other nodes of the causal chain represent main functionalities, such as *data measured* and *event indicated*. Redundant system parts require redundant nodes in the causal chain. The information flow between those main functionalities is represented with arcs. Individual EWS components are integrated as white nodes in the BN and their failure probabilities are specified in the CPT (see Chapter 4.1.4). To each grey node of the causal chain, those components that influence its functionality are connected via arcs. Dependencies between the nodes are described by these arcs and in the CPT of grey nodes (see Chapter 4.1.3). Black decision nodes, *threshold* and *warning criteria*, as well as *data measured* by sensors, conditional on the occurrence of an event, are added in the causal chain to incorporate the inherent reliability into the BN (see Chapter 4.1.5).

The reliability of the automated part of WS and FS can also be modeled in a BN, as illustrated in Figure 4.5. WS are typically automated in the monitoring and the data interpretation unit; and the BN is constructed to model the probability that the system operators receive timely warnings (POD) and false alarms (PFA) in the node *warning*. Often, the *thresholds* used in WS are set low to ensure that small changes are detected as soon as possible. This implicates high values for POD and PFA. This PFA can be neglected for WS if one assumes that the compliance of the experts does not decrease when regular, automated warnings are issued. In these cases, the decision nodes *threshold*, necessary to model the PFA, can be excluded from the BN. This simplified consideration can be adopted to model the automated part of FS, where the reliability is independent of thresholds. For FS, the BN is a valuable tool to model the probability that system operators receive data on a regular basis in the data interpretation unit.

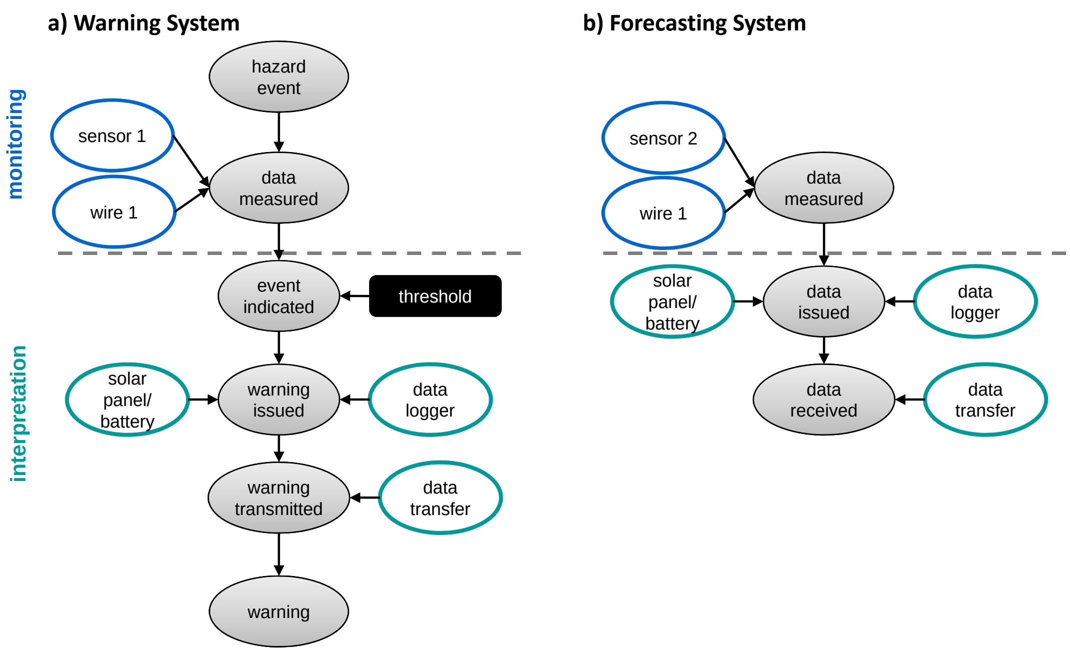

FIGURE 4.5: BN to Model Warning and Forecasting Systems: BN to model reliability of automated parts of Warning and Forecasting Systems.

4.1.3 Determine Conditional Probabilities

The reliability of an EWS depends on the configuration of EWS components and their interdependencies. Besides arcs, which are used to determine the information flow between the individual components of the EWS, conditional probabilities can be specified in the CPT of child nodes. In the CPT, dependencies are typically modeled deterministically as AND or OR relations. AND relations are used to specify serial connections and OR relations are used to model redundancies. In Table 4.1, the CPT of components connected in series is illustrated. In Figure 4.4, a *warning is released* when both the *power network* AND the *optical signal* in the non-redundant dissemination unit are functioning. Table 4.2 is used to present the CPT of redundant system parts. In the causal chain, a *warning is issued* if an *event is indicated* by senor unit 1 OR by sensor unit 2.

TABLE 4.1: CPT of the Node Warning Released: used to model AND relation.

power network		yes		no	
optical signal		yes	no	yes	no
warning released	yes	1	0	0	0
	no	0	1	1	1

TABLE 4.2: CPT of the Node Warning Issued: used to model OR relation.

event indicated 1		yes		no	
event indicated 2		yes	no	yes	no
warning issued	yes	1	1	1	0
	no	0	0	0	1

4.1.4 Estimate Failure Probabilities of Components

The failure probabilities of individual EWS components influence the technical reliability of the EWS and have to be specified for each component in the BN. The technical EWS components are represented in the white nodes of the BN and are modeled by binary random variables, with states *functioning* and *failed* in the CPT (Table 4.3). These

TABLE 4.3: CPT of the Nodes Representing Components: used to incorporate failure probabilities.

component	functioning	0.9995
	failure	0.0005

failure probabilities include both the failure probabilities associated with internal failure, such as aging, and those with external failure sources, such as lightning, humidity and extreme temperatures.

Specified MTTF and MTBF values are often available and can be used to determine the internal failure rate λ_{IF} following Eq. 3.4. This failure rate λ_{IF} is associated with a reference unit (e.g. failures per day or per year) that should comply with the one selected above for PFA.

Following, Eq. 4.3, λ_{IF} can be combined with the external failure rate λ_{EF} to obtain λ.

$$\lambda = \lambda_{IF} + \lambda_{EF} \tag{4.3}$$

Values for λ_{EF} are rarely specified by suppliers and need to be approximated in the same unit as λ_{IF}, based on repair records and expert estimates. EWS are primarily installed in remote areas. As an example, EWS for volcanoes and alpine hazards are installed in mountain regions, close to rivers and glaciers, in high altitudes, steep catchments and are thus prone to numerous external failure causes. Lightning, humidity, storm and extreme temperatures are the most frequent external factors that cause failures on system components. Rockfalls, snow avalanches and snow load, ice blocks, flood, vegetation, mud, dust and fog are site- or system-specific causes that can lead to failures of system components. Additional potential failure causes, such as construction, vandalism and animals, must also be considered. Automated parts of EWS for tsunamis and hurricanes are installed under water or on its surface and have to withstand destructive impacts such as strong waves and aggressive salt water.

From the overall failure rate λ, failure probabilities can be derived in probability distributions. If failures occur following a Poisson process, i.e., if they occur randomly in time and independently of each other, the probability of a component failure at time t is calculated as (Straub, 2012):

$$Pr(F(t)) = \lambda \times E[T_r] \tag{4.4}$$

λ is the failure rate of the component and $E[T_r]$ is the expected time it takes to detect and repair a failure. The approximation holds for small values of λ, i.e., for $\lambda \ll 1/(E[T_r])$. How fast component failures are detected, depends on whether a diagnostic system is integrated in the EWS or not and on the speed of detection if one is installed. How fast components are repaired depends on the type of failure, the availability of service personnel and spare parts, and on additional operational measures taken to ensure that hazardous events are detected. If a diagnostic tool is installed to send daily reports, failures are detected within one day. If spare parts are available for all parts and can be implemented within one day, $E[T_r]$ is two days. If failures probabilities cannot be quantified following a Poisson process, more suitable probability distributions can be used (see Chapter 3.1.2).

4.1.5 Include Sensor Data and Thresholds

To model the ability of an EWS to distinguish between hazard and noise, the nodes *threshold*, *warning criteria* and *data measured* are added in the BN. This step should be conducted for all AS and can be skipped for the automated part of FS. For WS this consideration is relevant if frequent false alarms are expected to decrease the compliance of the information recipient. In the BN black decision nodes *threshold* are added to each node *event indicated* to specify a warning threshold. An additional decision node, called *warning criteria*, is added to the node *warning issued* if warnings are based on the indication from individual sensors. In Figure 4.4, the warning is only issued when both sensors indicate an event. In the CPT of nodes *data measured*, the probabilities of the sensor signal exceeding the defined threshold, conditional on whether or not an event occurs, are specified.

For the evaluation of existing AS and WS, past sensor data can be used to estimate the probability of sensor signals to exceed a threshold conditional on an event during the selected reference unit. The selected period should be similar to the reference unit chosen for the calculation of failure rates (as defined in 4.1.3). To obtain scalar sensor signals, the maximum or mean values measured in each time unit are determined first.

Then, signals recorded on days with events and days without events are assigned into two groups. In each group, probability distributions are fitted to measured sensor signals to obtain the PDF. The ground motions and flow heights conditional on debris flow events in the Illgraben are described, e.g., in lognormal distributions (see Chapter 6). The selection of the distribution depends on the process and has to be identified site-specifically. In Figure 4.6, a threshold and two cumulative density functions (CDF) fitted to sensor signals measured on days with and without events, are illustrated. The intersections between the CDF and the threshold indicate both the probability of the threshold being exceeded on event days (0.99) and on days without events (0.01). Similar consideration can be made for varying thresholds to specify the probabilities in the node *data measured*.

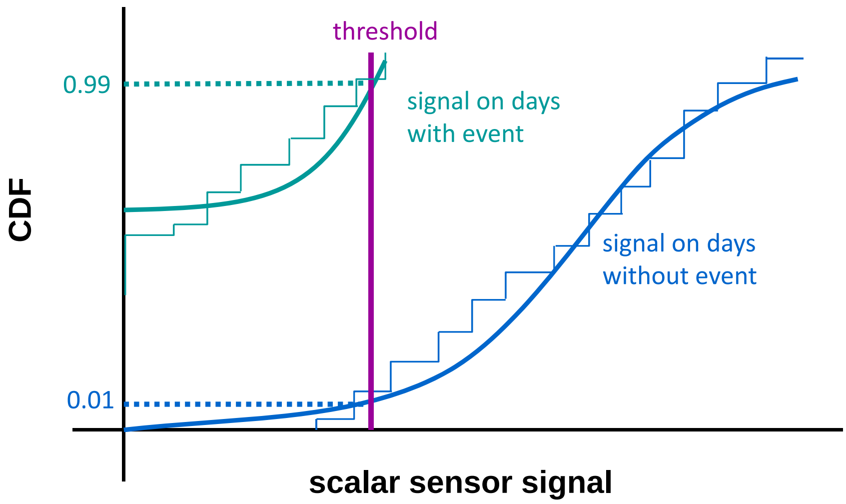

FIGURE 4.6: Fitted Sensor Signal Conditional on Event: and threshold to identify probabilities in the CPT of the nodes *data measured*.

If sensor data is not scalar, it is typically transformed into scalar signals that are comparable to thresholds. For example, earthquake AS, measure time series of ground vibrations with different sensors to model the expected magnitude in real-time, which is then compared to a predefined threshold (see Chapter 2.3.3). In this case, the probability of the modeled senor data, here expected magnitude, to exceed a certain threshold is specified in the CPT.

If the EWS are installed for the detection of rare events, such as volcanic eruptions and high-magnitude rockfalls, signals measured on days with events may be rare. In this case, probabilities have to be estimated by experts. That must be done carefully and with respect to the positioning of the sensor; as demonstrated for similar sensors installed to detect debris flows, the performance can vary significantly (see Figure 5.6).

4.1.6 Quantify the Reliability

In the last step, the BN is used to probabilistically model the reliability of automated AS and the automated part of WS and FS. For AS and WS values for POD and PFA can be obtained by changing the status of the top node and evaluating the BN. To compute the POD in the node *warning*, the top node *hazard event* can be set to the state *yes*; likewise, the PFA is obtained by setting the top node to state *no*. The same BN allows the technical or inherent reliability to be modeled separately. Therefore, the probability of measured sensor data to exceed the threshold is set to 1 or failure probabilities of system components are set to 0. For FS and WS, whose reliability is measured in terms of POD alone, the top node *hazard event* can be set to the state *yes* to model the reliability.

The BN can be extended to an influence diagram to optimize the reliability for utilities defined for hits, false alarms, misses and neutral decisions. In Chapter 5, the threshold which maximizes the system reliability is defined in an influence diagram. The reliability analysis of non-automated parts of WS and FS is less time critical and includes more complex decision procedures as illustrated in the following.

4.2 Reliability Analysis of the Non-Automated EWS

The second reliability analysis for the non-automated part of WS and FS has to address both the technical and the inherent reliability to evaluate the ability of the decision-maker in setting up intervention measures and avoiding damage. The inherent reliability depends on the ability of the model to forecast the event and the ability of the decision-makers to interpret the model. The technical reliability influences the ability of the EWS to support the decision-makers in creating an event forecast that directly depends on the availability and quality of the measured sensor data. In the novel framework approach, the technical and the inherent reliability achieved in the non-automated parts of EWS are quantified in five steps (Figure 4.7). The reliability is evaluated in a binary approach and expressed in terms of POD and PFA. The POD is the probability that the intervention measures are in place when the event occurs to avoid damage. The PFA means that intervention measures are in place and no event occurs.

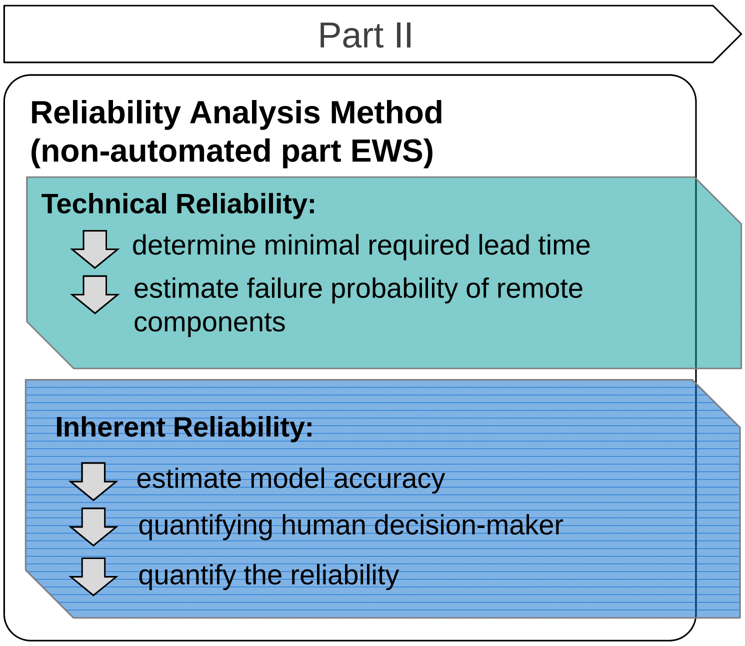

FIGURE 4.7: Reliability Analysis for Non-Automated Parts of EWS: includes five steps to model technical and inherent reliability.

4.2.1 Determine Minimal Required Lead Time

In the non-automated part of WS and FS, experts analyze precursors to obtain extended lead times up to several days (see Figure 2.24). In this case, the reliability should be evaluated as a function of the lead time. Typically, the reliability increases when the lead time decreases, as illustrated in Figure 4.8. To simplify the subsequent reliability analysis, it can be useful to quantify the reliability at a fixed lead time Δt. For WS, the minimum lead time required to conduct the intervention measures, can be chosen to ensure that interventions are conducted successfully and no additional costs are caused through unnecessary long interventions. In the Preonzo case study, the reliability of the EWS is evaluated one day before the event (see Chapter 6). For FS, the lead time is equal to the release frequency; for a daily bulletin, the lead time would be one day.

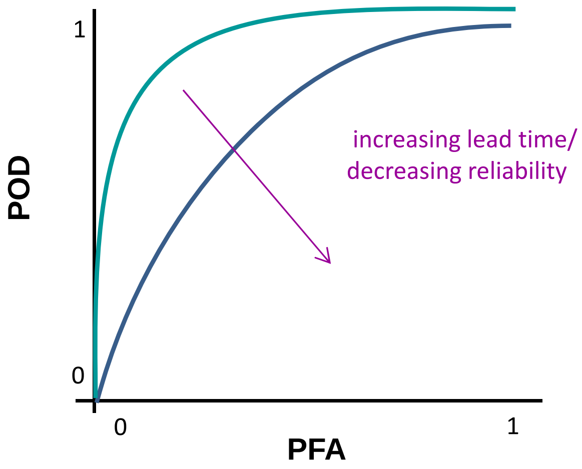

FIGURE 4.8: Reliability vs. Lead Time: typically the reliability decreases when the lead time increases.

4.2.2 Estimate Failure Probability of Remote Components

The failure probability of remote components, such as sensors, typically increases when the event gets closer for WS because destructive side-events arise in the release area. The increased technical failure probability $P(F)$ at a certain lead time Δt before the event can be quantified by fitting probability distributions, such as the Weibull or a binomial distribution (see Chapter 3.1.2 and Chapter 6.2.3.), to failure records of past events. In cases, where records are not available, the failure probability $P(F)$ for a certain lead time Δt before the event has to be estimated by experts or adapted from experience made at similar sites.

If an increased number of failures are expected, the number of remaining sensors at the lead time Δt should be determined and used in the next step, where the accuracy of the model is estimated. If a WS is constructed in a way that increased failure probabilities are not expected, this step can be neglected. This is typically the case for FW where forecasts are made on a regular basis and not only when hazardous events are expected in the near future.

4.2.3 Estimate Model Accuracy

The model accuracy depends on varying parameters, such as on the underlying monitoring strategy, the technical failure probability and on the applicability of the model itself. The monitoring strategy is important because the type, the number and the positioning of the sensors determines the data base quality. An increased technical failure reliability may have a negative effect on the quality of the data base. The applicability of the model can vary significantly for different natural hazard process types. While brittle rockfalls with high-magnitudes can be, for example, forecasted reliably with the inverse velocity model (Wegmann et al., 2003; Petley and Petley, 2006; Krähenbühl, 2006; Rose and Hungr, 2007), small-magnitude rockfalls occur typically spontaneously. Similarly, volcanic eruptions are characterized trough site-specific precursors and warning criteria are often not transferable (see Chapter 2.3.6).

For natural hazard events that occur frequently, values for POD and PFA can be quantified in post-analysis to evaluate models following Eq. 4.1 and 4.2. Models used within WS are typically applied to predict site-specific events and can be evaluated by their application on recorded pre-event data. To this end, the model is applied at the fixed lead time (see Chapter 4.2.1) on data measured by individual sensors before that lead time to obtain event forecasts. In Figure 4.9, the forecasted number of days to the event modeled at lead time $\Delta t = 1$ by grouped sensors are illustrated and fitted with a probability distribution. In this example 0.95% of the sensors predict the event to occur at the expected lead time $\Delta t = 1$ and thus the POD is 0.95. To obtain values for PFA, the model is applied to make forecasts on days not equal to the lead time (for the example, more than one day before the event). Then those forecasts, in which sensors predict the event for the next day but no event occurs are identified and compared to the number of non-event days. A detailed evaluation of the inverse velocity model is demonstrated in Chapter 6. In this study, the model becomes more reliable with an increasing number of sensors.

In published literature, models used in FS for meteorological hazards and floods, are evaluated as a measure of POD and PFA (Simmons and Sutter, 2009; Liechti et al., 2013). Evaluation of these models can be more complex, because not only the ability to predict a specific hazard event but the ability of the model to predict the occurrence probability of hazardous events on a regional scale needs to be evaluated.

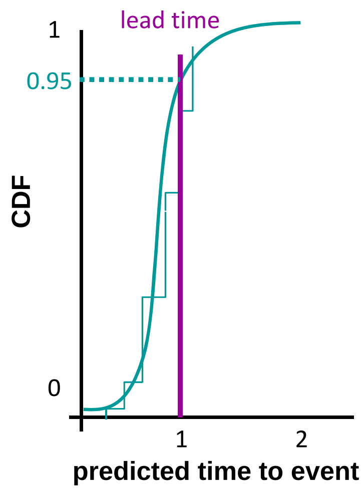

FIGURE 4.9: Forecasted Days to Event: modeled by grouped sensors at lead time $\Delta t = 1$.

If event data for the evaluation of models used in WS and FS is not available, values for POD and PFA can be adopted from event analysis of similar EWS or from expert estimates. Besides the ability of the model, the ability of humans to make accurate decisions should be evaluated in the next step.

4.2.4 Quantifying Human Decision-Makers

The reliability achieved in the non-automated parts of both WS and FS depends strongly on the ability of humans to make correct decisions. To quantify this ability, decision-makers can be characterized through different risk types. Each risk type is specified through different criteria, which must be fulfilled when intervention measures are set up. These criteria can be inherent or technical. An inherent criterion could, for example, mean that an evacuation is set up if the model predicts an event with a probability higher than a predefined value. A technical criterion would mean that an evacuation is initiated if, for example, a predefined percentage of sensors are left. In case of the inherent criteria, the POD could be derived from the model accuracy. If the model predicts the event to occur within the specified lead time with a probability of 0.95 and the decision-makers evacuate if the probability is higher than 0.8, intervention measures are set up.

In practice, decision-making procedures which are conducted in both WS and FS are complex and not determined by simple decision rules. Decisions are made by expert teams, who apply models on measured sensor data and consult additional information sources. As an example, the danger levels of snow avalanches, which are published daily in the bulletin of the Swiss FS, are selected by an expert team, who consult snowpack and weather models as well as information from local observers (see Chapter 2.4). A comprehensive evaluation of decisions made in that expert team would has to account for varying factors, such as the model accuracies, the effect of group dynamics and the risk tolerance and experience of the individuals.

4.2.5 Quantify the Reliability

The reliability achieved in the non-automated part of WS and FS depends, among other factors, on the lead time, the monitoring strategy, the technical failure probabilities, the model accuracy and complex human, decision-making procedures. The reliability should, as for automated EWS (see reliability analysis, part I), be expressed in terms of POD and PFA. These measures are then used in the last part to quantify the effectiveness of EWS.

For FS and WS, the reliabilities of both analyses are combined to obtain one value for POD and one for PFA as input parameters for effectiveness evaluation. To obtain an overall POD, the values modeled in the first reliability analysis POD_1 and in the second analysis POD_2 are combined following Eq. 4.5:

$$POD = POD_1 \times POD_2 \tag{4.5}$$

POD_1 and POD_2 are multiplied because the overall POD cannot exceed single values of POD. If, for example, the POD_1 calculated for the automated part is 0.95, the overall POD cannot exceed this value. To determine the overall PFA, values calculated in both reliability analyses are summed up, to account for all false alarms following Eq. 4.6. But in the majority of cases, this consideration is not necessary for WS, where low thresholds are used to immediately inform experts about relevant changes and where false alarm should not decrease their willingness to comply (see Chapter 4.1.6). It is also not relevant for FS, where the PFA is not modeled in the BN of the first reliability analysis. Here, the PFA quantified in the second reliability analysis is used as input for the effectiveness analysis.

$$PFA = PFA_1 + PFA_2 \tag{4.6}$$

4.3 Effectiveness Analysis

The effectiveness of an EWS E_w can be quantified in terms of the relative reduction of the overall risk, with R being the overall risk without the EWS and R^w the risk with the EWS installed:

$$E_w = 1 - \frac{R^w}{R} \tag{4.7}$$

Both R and R^w are evaluated according to Eq. 1.1 and 1.2. In many instances, it is not necessary to determine the contribution of all factors to the risk in Eq. 1.1. Instead, it will often be sufficient to assess the effect of the EWS on individual factors as a function of POD and PFA. EWS aim to generate information before a hazard event causes damage; therefore, they reduce the risk primarily by mitigating the exposure probability pe_{ij} of persons and mobile objects i in a hazard scenario j. Only in some cases, e.g., if earthquake AS detect events quick enough to slow down trains, the vulnerability V_{ij} of object i in scenario j is decreased. In the following, an approach in which the EWS decreases the exposure probability pe_{ij} is presented.

With the EWS, the exposure probability is reduced from a value pe_{ij} without warning to a value $pe_{ij}^{(w)}$. Combining Eq. 4.7 with Eq. 1.1 and 1.2, the warning effectiveness for this case becomes

$$E_w = 1 - \frac{\sum_{j=1}^{n_{scen}} \sum_{i=1}^{n_{obj}} p_j \times pe_{i,j}^{(w)} \times V_{i,j} \times A_i}{\sum_{j=1}^{n_{scen}} \sum_{i=1}^{n_{obj}} p_j \times pe_{i,j} \times V_{i,j} \times A_i} \tag{4.8}$$

For those cases, where the EWS is installed to warn people, the n_{obj} are the number of exposed people and it is reasonable to assume that the exposure probability is the same for different i, i.e. $pe_{ij} = pe_j$. For one relevant scenario $j = 1$ the effectiveness of the EWS then reduces to

$$\begin{aligned} E_w &= 1 - \frac{p_j \times pe_j^{(w)} \times \sum_{i=1}^{n_{obj}} v_{ij} \times A_i}{p_j \times pe_j \times \sum_{i=1}^{n_{obj}} v_{ij} \times A_i} \\ &= 1 - \frac{pe_j^{(w)}}{pe_j} \end{aligned} \tag{4.9}$$

The EWS reduces the exposure probability to $pe_j^{(w)}$. This reduction is equal to the probability that a warning is issued, transferred to the target persons and that the affected people comply with the warning. The former corresponds to the POD, the latter to the Probability of Compliance (POC). Therefore:

$$pe_j^{(w)} = pe_j(1 - POD \times POC) \tag{4.10}$$

Inserting in Eq. 4.9, the effectiveness becomes

$$E_w = POD \times POC \tag{4.11}$$

The POC, i.e. the degree to which warnings are followed in practice, is strongly dependent on the PFA and on the lead time (see Chapter 1.2 and Chapter 3.1). POC can be calculated as a result of a basic compliance probability POC_0 and a compliance reduction factor due to false alarms $RF(PFA)$ and a compliance reduction factor due to insufficient lead time $RF(ILT)$:

$$POC = POC_0 \times RF(PFA) \times RF(ILT) \tag{4.12}$$

The basic compliance rate POC_0 depends on several factors such as the type of intervention measures, its environment and human decision-making. If, for example, barriers are closed on a road, car drivers have to comply while red lights can be ignored. Moreover, different means of transportation (e.g. walking, cycling, driving) and varying environments (e.g. city, highway, countryside) can influence the willingness to comply with a warning; e.g. a car driver on a main traffic road would be more likely to comply with a red light than pedestrians on a hiking trail. In many instances, the compliance depends on human decision-making, which is influenced by the cost of damage associated with the hazard, the cost associated with the intervention measure as well as the hazard awareness. If regular training is conducted and persons educated on the potential hazard and associated risks, a higher compliance rate may be achieved.

The reduction factor due to false alarms $RF(PFA)$ depends, among other factors, on the recipient of the information and must be approached case-specifically. For the Illgraben case study (see Chapter 5), values were adopted from a case study by Bliss et al. (1995). For the Preonzo case study (see Chapter 6) the effect of false alarms was neglected, because warning information is send to system operators who appreciate regular feedback from the WS.

In certain cases, EWS have to be constructed in a way that the available lead time may not be sufficient and those willing to comply cannot successfully evacuate. Especially, in the case of AS, lead times are often in the range of seconds and limited through the distance of the release area to endangered objects. If, for example, an AS is installed to protect trains, the stopping distance of an arriving train could be too long to prevent the train from entering the endangered sector. In that case, the probability of a collision or direct hit must be considered. This effect on risk reduction should be included as a compliance reduction factor due to insufficient lead time $RF(ILT)$ to quantify the overall effectiveness.

4.4 Summary

A novel framework approach for the evaluation of EWS comprising three main parts was introduced. In the first part, the reliability of automated EWS is quantified in terms of POD and PFA. In the second part, the reliability of the non-automated part of WS and FS is quantified in the same terms. In both parts, the reliability assessment is conducted in several steps addressing both the technical and the inherent reliability. For the reliability evaluation of automated parts of EWS, a method including six steps is provided, in which a BN is applied to probabilistically model POD and PFA. For the evaluation of complex model-based decision-making in the non-automated part of EWS, five steps are presented summarizing those factors that have a main influence on the reliability. In the last part, the effectiveness can be derived from the reliability. To this end, POD, PFA and the lead time are used to quantify the reduced risk achieved with the EWS. In the illustrated approach, the POD is used to quantify the reduced exposure probability and PFA and the lead time are expressed as compliance reduction factors to estimate the compliance to a warning.

Chapter 5

Illgraben Case Study

In the present chapter, results of the Illgraben case study, in which we assess and optimize the reliability and effectiveness of the Illgraben debris flow AS, are presented. A comprehensive version of this chapter has been published as (Sättele et al., in press).

The overall system evaluation of the Illgraben AS has been conducted following part I and part III of the framework (see Figure 4.1 in Chapter 4). The system reliability analysis includes both the technical and the inherent system reliability. The system reliability is expressed in terms of POD and PFA, modeled in a BN, including the probability of system component failures and illustrated in ROC curves. Moreover, the BN is extended to an influence diagram, here referred to as decision graph (DG), enabling the identification of optimal system thresholds.

The effectiveness of the Illgraben AS is calculated following Eq. 4.11 and Eq. 4.12. To quantify the effect of false alarms, values for the general compliance rate and the effect of false alarms are estimated. The general compliance rate POC_0 is set to 0.95 and was estimated from traffic analysis (Rosenbloom, 2009; Johnson et al., 2011). One traffic analysis investigated the behavior of pedestrians towards red lights and revealed that 5% ignore red-lights. The second analysis considered the behavior of cyclist, where about 7% ignore red lights. To estimate the compliance reduction factor due to false alarms $RF(PFA)$, results from a case study that assessed the compliance frequency of students as a function of false alarms are adopted (Bliss et al., 1995). The resulting compliance frequencies (corresponding to our RF) at different levels of the False Alarm Ratio (FAR) are shown in Figure 5.1, together with a fitted quadratic function:

$$RF(FAR) = -0.34FAR^2 - 0.66FAR + 1 \tag{5.1}$$

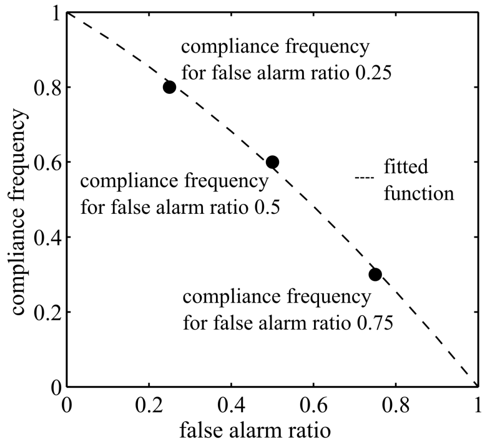

FIGURE 5.1: Compliance Frequency: at different levels of False Alarm Ratio (FAR), according to Bliss et al. (1995).

To incorporate the effect of decreasing compliance for a given number of false alarms in the effectiveness, the FAR is defined as the ratio of false to correct alarms and related to the PFA as:

$$FAR = PFA\frac{Pr(\bar{H})}{Pr(A)} \tag{5.2}$$

$Pr(\bar{H})$ is the probability of no hazard event and $Pr(A)$ is the probability of an alarm (both correct and false) on a given day. For the case study considered here, it is approximately $Pr(\bar{H}) \approx 95\%$ and $Pr(A) \approx 5\%$, therefore $FAR \approx 19$ PFA. Combining Eq. 4.10, 4.11, 4.12, 5.1, 5.2, we obtain the effectiveness as a function of POD and PFA (see also Figure 5.2):

$$\begin{aligned} E_w &= POD \times 0.95(-0.34FAR^2 - 0.66FAR + 1) \\ &= POD \times (0.95 - 116PFA^2 - 11.9PFA) \end{aligned} \tag{5.3}$$

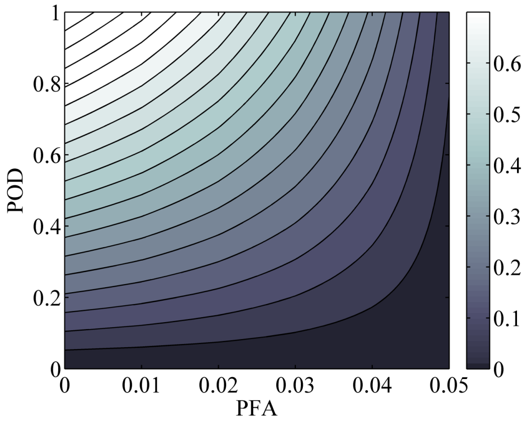

FIGURE 5.2: Effectiveness of the Illgraben Alarm System: as a function of Probability of Detection (POD) and Probability of False Alarms (PFA) for the case study.

5.1 The Illgraben Alarm System

The system under investigation is located at the Illgraben catchment in the western part of the Swiss Alps. The catchment ranges in elevation from 610 m a.s.l. to 2716 m a.s.l. and half of the catchment area (4 km^2) is covered by bedrock and debris deposits. Due to the geological conditions, there is a remarkably high occurrence rate of debris flows. A debris flow is a spontaneous, fast-flowing mixture of water and solid particles, which typically consists of surges (Badoux et al., 2009). In 2006, the Swiss Federal Institute for Forest, Snow and Landscape Research WSL designed an AS to protect local residents and tourists frequently crossing the catchment.

The monitoring unit includes five sensors that are located close to the release area to detect events in real-time (Figure 5.3). In the upper catchment, one single sensor, geophone 1, continuously monitors ground vibrations. Further down in the catchment, some hundred meters below, two geophones, 2 and 3, measure ground vibrations and two radar devices, 1 and 2, measure the flow depth in the river bed. The upper geophone is controlled by one logger and the remaining four sensors are controlled by a second logger. The power at these remote locations is supplied via solar panels and batteries. The loggers build an interface between the monitoring unit and the data interpretation unit. If predefined threshold values in the data loggers are exceeded, an alarm call is automatically activated via modem and transmitted to the valley. The incoming alarm calls are forwarded via two communication devices to the information dissemination unit. To release the alarm information to endangered persons in the catchment, three alarm

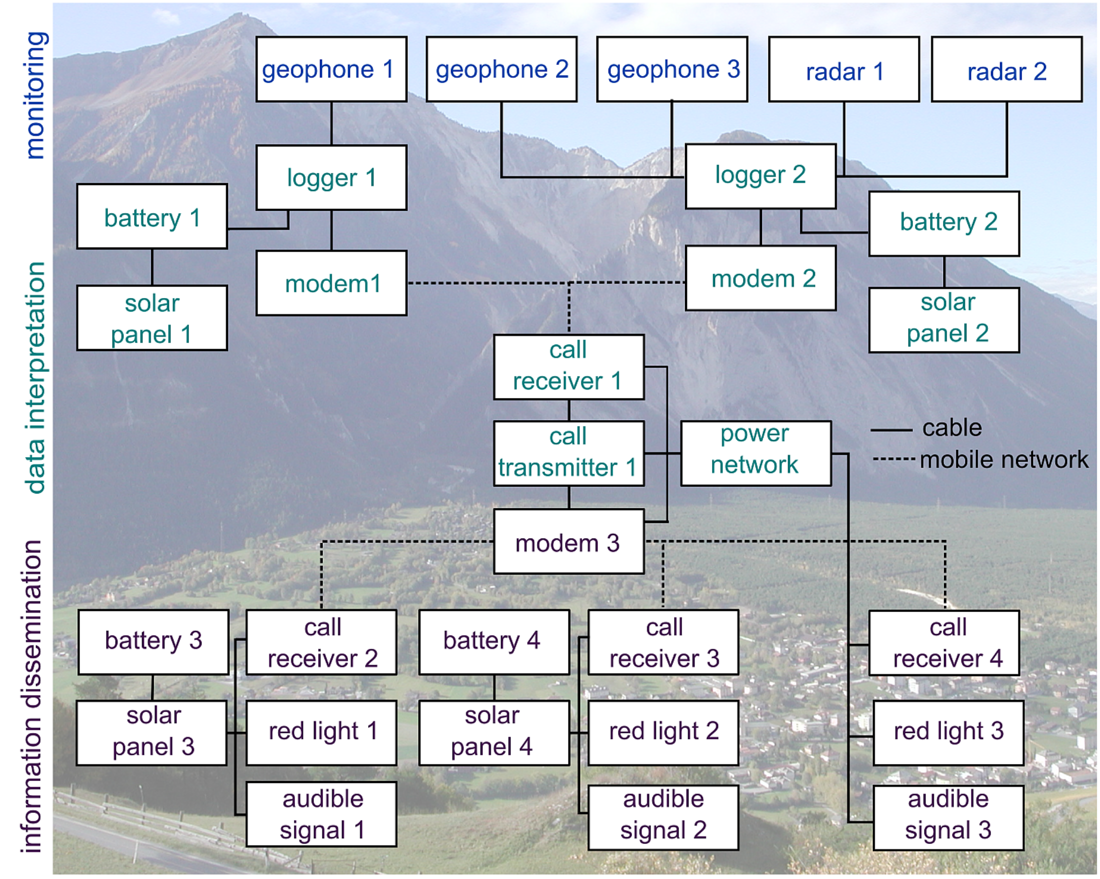

FIGURE 5.3: System Sketch of the Illgraben Alarm System: illustrates the fully automated procedures and components (underlying picture by Graf).

stations are located close to three crossings of the streambed. Each station consists of an audible signal and a red light. The lead time of the AS is determined by the velocity of the debris flow and the runtime between the lower sensor units and the upper crossing and is in the range between five and fifteen minutes.

5.2 BN to Model the Reliability of the Illgraben Alarm System

To probabilistically model the system reliability for varying warning thresholds of the Illgraben debris flow AS and to identify the threshold combination that implies the optimal effectiveness, we design a BN and an associated DG.

By applying the BN (Figure 4.4) to the system sketch of the Illgraben AS (Figure 5.3), the BN model of the debris flow AS depicted in Figure 5.4 is obtained. The BN is implemented with the free GeNIe software (DSL, 2013) and can be downloaded under the following link: $http://abnms.org/bnrepo/bn.php?bnId = 100$.

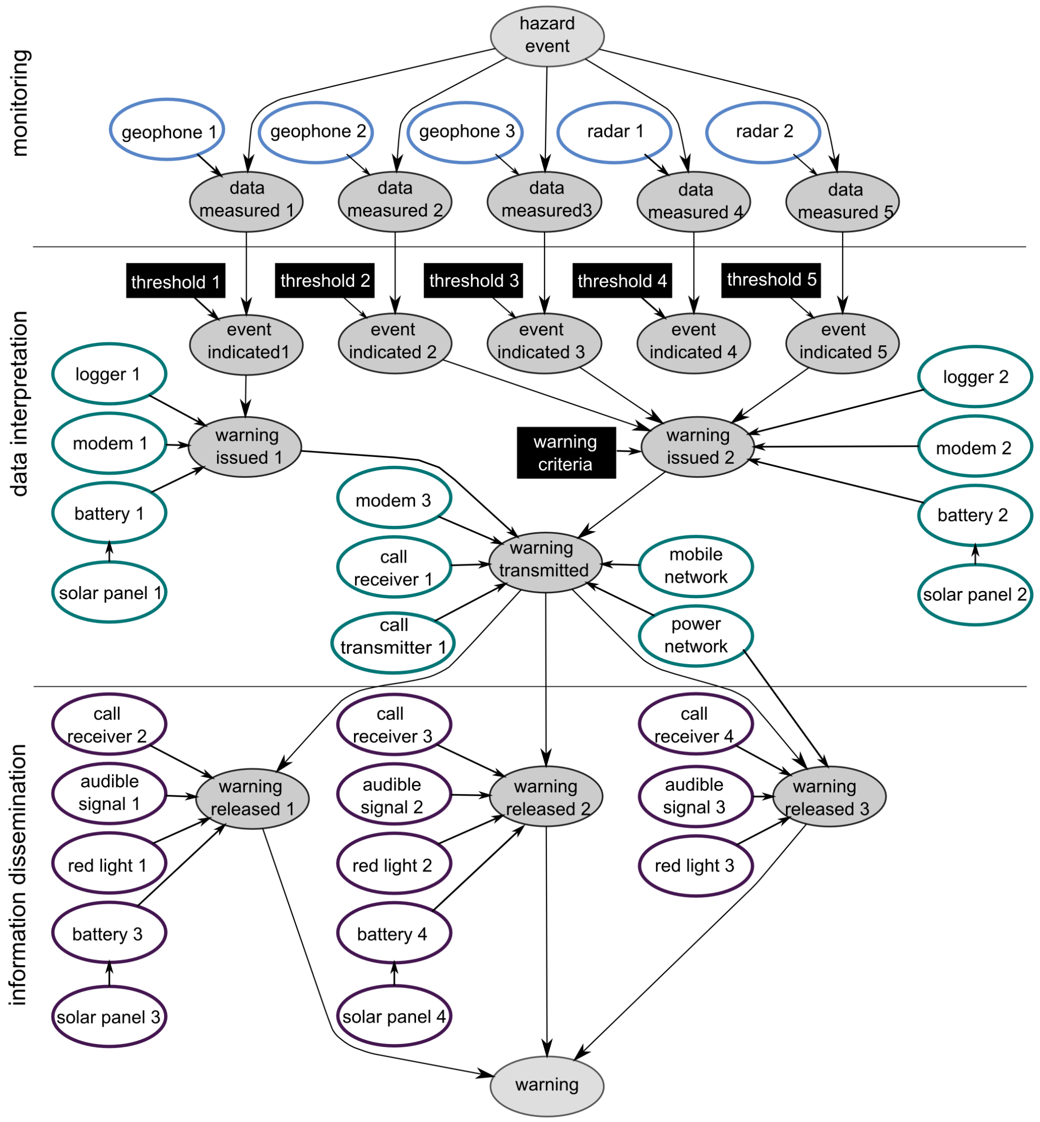

FIGURE 5.4: Bayesian Network for the Illgraben Alarm System: can be obtained by applying the BN (Figure 4.4) to the system sketch (Figure 5.3).

The dark-grey nodes in the BN represent the causal chain from the *hazard event* to the *warning*. This chain can also be interpreted as the information flow. For each sensor, a local interpretation is made in the node *event indicated*, which is in state *true* only if the sensor signal exceeds the corresponding threshold. The information from sensors in the lower catchment (geophone 2, 3 and radar 1, 2) is merged in the node *warning issued 2*, where it is decided whether or not to issue a warning, following the selected criterion defined in the node *warning criteria*. The node *warning transmitted* is in state *true* if either of the two warnings is issued (OR connection). If the warning is transmitted, a warning is released at each of the three stations, given that no component failures occur. Therefore, the final node *warning* should in principle have four states 0, 1, 2, 3, corresponding to the number of stations where warnings are released. However, to comply with the binary definition of POD and PFA, this node has only two states (*yes* and *no*). To account for the number of warnings released, the conditional probability of *warning* = *yes* is 0.33 if two stations release a warning respectively and 0.67 if only one station releases a warning.

5.3 Technical Reliability Analysis

The failure probabilities for components of the Illgraben AS are calculated with Eq. 3.4, 4.3 and 4.4, and incorporated in the white nodes, including both internal failures and failures caused by external influences.

The internal failure rate λ_{IF} is directly derived from the MTTF or, for repairable parts, from the MTBF, as specified by the suppliers. As an example, for radar devices, the MTTF is sixty years and the corresponding internal failure rate is $\lambda_{IF} = 4.5 \times 10^{-5}$ per day. If MTTF or MTBF are not specified by the supplier, expert judgment is used to estimate λ_{IF}.

To estimate λ_{EF}, we consult experts and evaluate historical data from repair records. Since the installation of the Illgraben debris flow AS in 2006, one solar panel was destroyed by a rockfall. In the Illgraben, rockfall is common and we assume the failure rate to be $3 \times 10^{-4} d^{-1}$, which corresponds to a return period of ten years. System failure due to extreme floods, lightning, animals, vandalism and extreme temperatures have not occurred yet, but should be considered as possible failure causes. We assume a failure rate of $3.0 \times 10^{-5} d^{-1}$ for each external failure, which corresponds to a return period of 100 years. Summing up these rates, an overall $\lambda_{EF} = 4.5 \times 10^{-4} d^{-1}$ is computed for all system components. This is in good agreement with available repair records.

In the Illgraben AS, $E[T_r]$ is one day for all system components, because a diagnostic tool is incorporated into the system to ensure that failures are detected within one day.

If the failures cannot be repaired immediately, additional operational measures are taken to ensure detection of an event.

To quantify the effect that technical failures have on the overall system reliability, we incorporate technical failure rates λ for all system components in the BN. In doing so, the maximum POD (achieved with the optimal thresholds described later in the paper) is decreased by 0.34%. Thereof, 0.12% are due to internal failures (λ_{IF}) and 0.22% are due to external failures (λ_{EF}). The technical reliability modeled for the Illgraben AS is very high.

5.4 Inherent Reliability Analysis

The inherent reliability of the Illgraben AS, as expressed through POD and PFA, depends on the selected threshold for each sensor signal. To analyze the influence of these thresholds, decision nodes representing varying thresholds are included in the DG of Figure 5.4. In addition, a decision node *warning criteria* allows various criteria to be analyzed for issuing warnings based on the indications from the individual sensors, e.g., a warning is issued if at least two sensors indicate an event.

Each of the five signal nodes in the monitoring unit are described by the conditional PDF of the maximum measured signal during a day, conditional on whether or not a debris flow event occurs during that day. These conditional probability distributions correspond to those of the signal detection theory as illustrated in Figure 3.2. To estimate them, recorded sensor data from the period between 1st of May 2008 and 24th September 2012 are used. During this period, forty-four debris flow events were recorded on 883 days. For each of the five sensors, a probability distribution is fitted to the observed signals for days with and without events, as displayed in Figure 5.5 for Geophone 2. For inclusion in the BN, the signal is discretized in ten classes, as shown in Table 5.1 for Geophone 2.

To quantify the inherent reliability of individual sensors, POD and the PFA are evaluated from the conditional distributions of the signal following Eq.3.1 and 3.2. The resulting ROC curves that represent the reliability of individual sensors for varying thresholds are presented in Figure 5.6. They indicate that the inherent reliability of the individual sensors varies strongly. Geophone 1 performs best and reaches a reliability close to the optimum with $POD = 0.992$ and $PFA = 10^{-4}$, whereas the remaining sensors have a

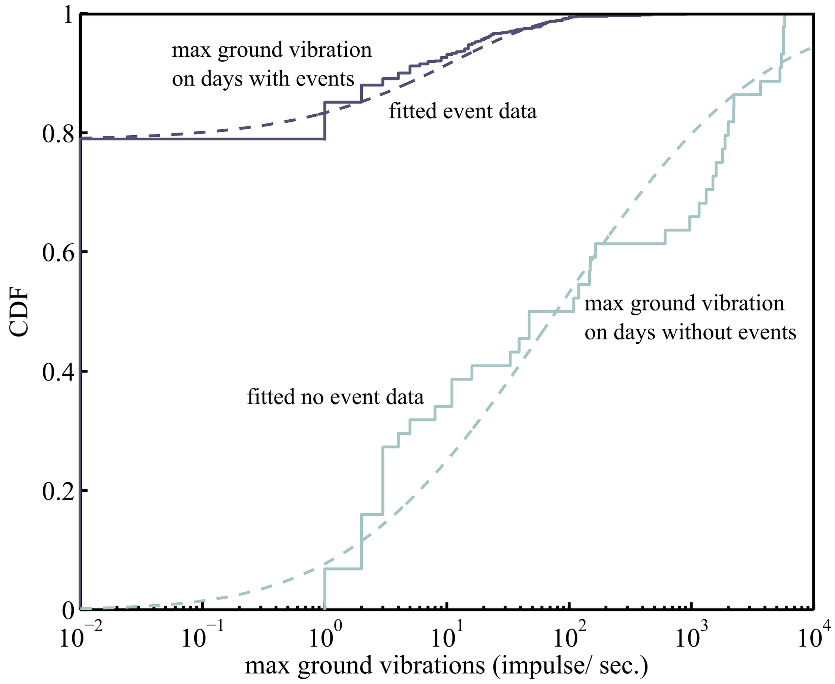

Figure 5.5: Signal Geophone 2, Illgraben: Cumulative distribution functions (CDF) represent observed data (solid lines) and the fitted probability distributions (dashed lines).

much lower inherent reliability. The difference among the reliabilities of the sensors is mainly due to the positioning of the sensors in the field, which influences their sensitivity to the debris flow events and the amount of external disturbances, e.g., from animals, humans and rockfalls.

5.5 Decision Graph to Identify Optimal Threshold Combinations

With five sensors, and all the signals discretized in ten classes, there are $9^5 = 59 \times 10^3$ possible threshold combinations, each of which leads to a POD and a PFA. Furthermore, different warning criteria for combing the individual sensor results can be defined, which further increase the number of possible warning strategies. For the Illgraben case study, two such warning criteria are considered. Either one individual sensor can issue a warning individually or a warning is issued when geophone 1, or at least one geophone and one radar device in the lower catchment, indicates an event. The optimal warning criterion in all instances for the Illgraben case study is the second criterion.

TABLE 5.1: Discretized Probability Distribution: of signals measured by Geophone 2 on days with and without event.

class	impulses/sec	no event	event
1	≤ 1	0.8332	0.0767
2	$> 1 \leq 5$	0.0512	0.1071
3	$> 5 \leq 10$	0.0295	0.0663
4	$> 10 \leq 20$	0.0305	0.0772
5	$> 20 \leq 30$	0.0163	0.0492
6	$> 30 \leq 40$	0.0102	0.0362
7	$> 40 \leq 50$	0.0069	0.0286
8	$> 50 \leq 200$	0.0208	0.1789
9	$> 200 \leq 500$	0.0014	0.1075
10	> 500	0.0001	0.2713

Most of the possible warning strategies will be sub-optimal. Of interest are only the Pareto optimal warning strategies, for which it holds that no other strategy exists with simultaneously higher POD and lower PFA. To identify the Pareto optimal solutions, we employ a DG of Figure 5.4. By adding a utility node, the BN is extended to a DG, which can automatically identify the optimal warning threshold. This is of particular use when multiple sensors are installed. In this case, thresholds must be set for all sensors and combination rules (logic operators) must be defined, e.g., that a warning is issued only if more than x sensors have a signal above their threshold. This leads to a high-dimensional optimization problem, which can be effectively solved with the DG.

In the utility node, we modify the ratio of cost of false alarm to cost of a missed event and use the DG to identify the optimal threshold combination and warning criterion for each ratio. In this way, we obtain a set of Pareto optimal solutions, which allow the construction of the system ROC curve. In Table 5.2, the optimal threshold combinations for twenty utility ratios are presented, together with the corresponding POD, PFA and effectiveness, as computed with Eq. 5.3. The results are also graphically illustrated in

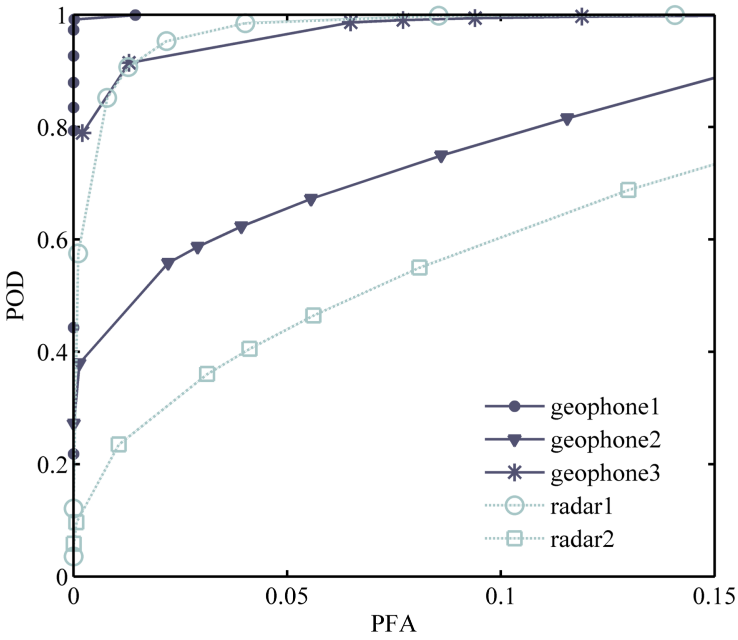

FIGURE 5.6: ROC Curves for Individual Sensors: illustrating the reliability of sensors for nine predefined thresholds. The highest threshold is represented by operation points left. Geophone 1 shows the best performance.

Fig. 5.7. Here, the technical reliability is already included, i.e., the results show the overall system reliability and effectiveness.

5.6 Reliability and Effectiveness of the Illgraben Alarm System

The POD and PFA of the Pareto optimal warning strategies for the Illgraben AS are summarized in Table 5.2 and Figure 5.7. Using these values, the overall ROC curve of the system is constructed, as depicted in Figure 5.8. This ROC curve is overlaid with the system effectiveness, following Figure 5.2.

Overall, the reliability of the Illgraben debris flow AS is high, and so is its efficiency. According to Table 5.3, the warning strategy that maximizes the effectiveness of the system is the one found with utility ratios $0.7, 0.8$ and 0.9. This warning strategy has low thresholds for sensors geophone 1 and radar 1, whereas the thresholds of the remaining three sensors, geophone 2, 3 and radar 2, are set to their maximum. Geophone 3 still has a POD of 0.79 even with the largest threshold (see also Figure 5.6). For geophone

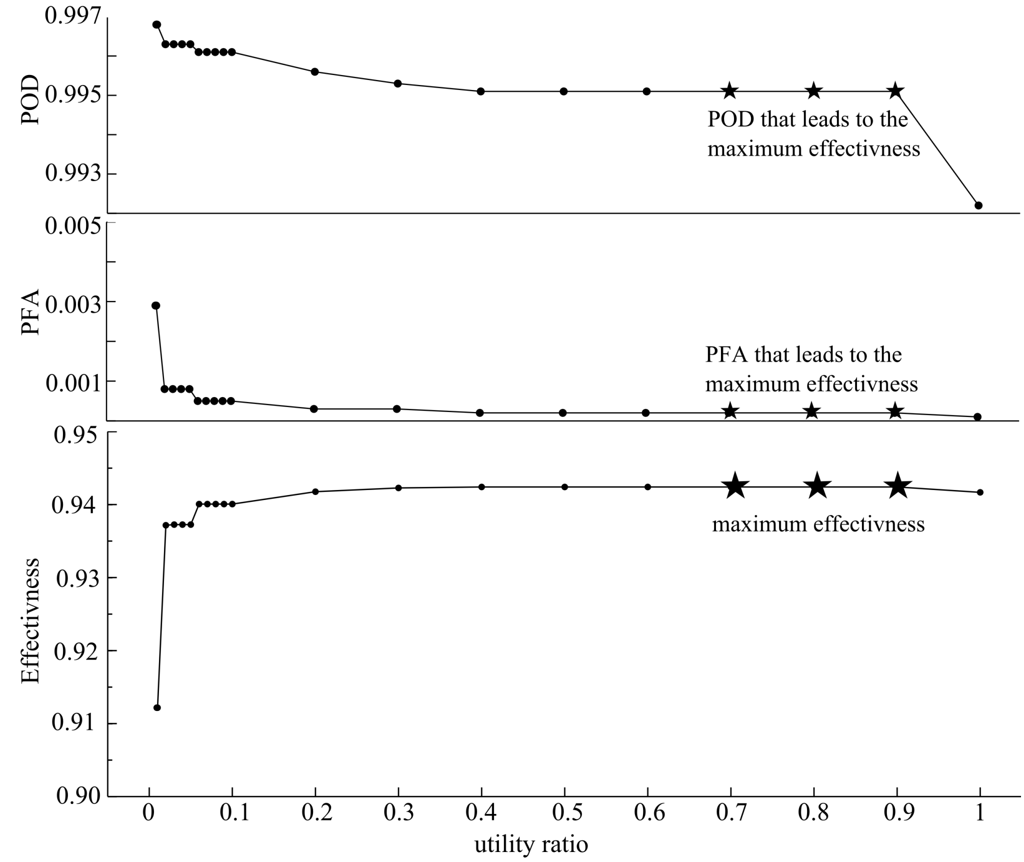

FIGURE 5.7: Reliability and Effectiveness, Illgraben: of Pareto optimal warning strategies, as shown in Table 5.2.

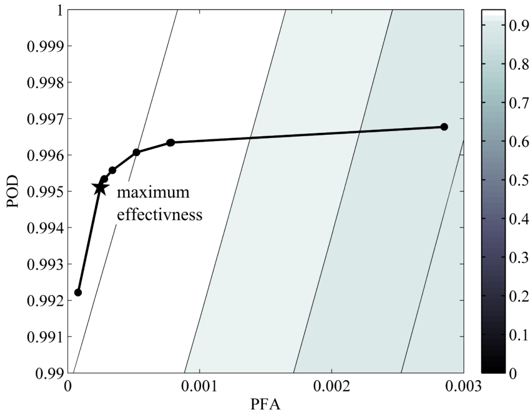

FIGURE 5.8: ROC Curve and Effectiveness of the Illgraben Alarm System: overlaid.

Table 5.2: Pareto Optimal Solutions for Varying Utility Ratios: and the corresponding POD, PFA and effectiveness.

utility ratio	thresholds					POD	PFA	Effectiveness
	G1	G2	G3	R1	R2			
0.009/0.01	2	8	7	3	9	0.996772	0.002851	0.912171
0.02	2	8	8	3	8	0.996342	0.000783	0.937166
0.03/0.04/0.05	2	8	8	3	9	0.996336	0.000775	0.937260
0.06/0.07/0.08/0.09/1	2	8	8	4	8	0.996072	0.000520	0.940068
0.2	2	8	9	3	9	0.995582	0.000339	0.941772
0.3	2	8	9	4	8	0.995339	0.000277	0.942281
0.4/0.5/0.6	2	9	9	4	8	0.995125	0.000248	0.942423
0.7/0.8/0.9	2	9	9	4	9	0.995110	0.000247	0.942424
1	3	8	9	4	8	0.992215	0.000078	0.941680

2 and radar 2, these optimal maximum thresholds indicate that these sensors do not contribute to the system reliability and may even decrease the overall effectiveness of the Illgraben debris flow AS.

To assess the influence of individual technical system components on the overall system reliability and the resulting effectiveness, an elementary sensitivity analysis is conducted. For each technical system component i, the system effectiveness with the optimal warning strategy is recalculated once by assuming that the technical system component i failed and once by assuming that the system component i is perfectly reliable. This is done by simply setting the node of technical system components i to *functioning* or *failure* respectively. The difference in effectiveness between the system with the perfectly reliable technical system component i and the original system is called Effectiveness Achievement Worth, as it corresponds to the Risk Achievement Worth sensitivity measure (Vesely et al., 1983). Accordingly, the difference in effectiveness between the original system and the one with technical system component i failed is called Effectiveness Reduction Worth, corresponding to the Risk Reduction Worth sensitivity measure. The results are summarized in Table 5.3, where technical system components are ordered according to their importance. Overall, the Effectiveness Achievement Worth of all technical system components is small, indicating that little can be gained from improving the reliability of individual technical system components. On the other hand, the Effectiveness Reduction Worth of the technical system components that are responsible for the data transmitting within the Illgraben system (modem 3, call receiver 1, call transmitter 1, mobile network or power supply), is large (9.42×10^{-1}). Upon failure of any of these technical system components, the Alarm System will not work, which is a consequence of the missing redundancy of the system with respect to these technical system components. Redundantly constructed data transmitting devices would therefore improve the system reliability and so its effectiveness considerably. However, as the Effectiveness Achievement Worth shows, the effect would be limited. For a further analysis of possible modifications in the system configuration, a cost-benefit analysis should be conducted.

The non-redundant technical system components in the information dissemination unit (call receiver 2, 3, 4, battery 3, 4) are the most critical components and so their Effectiveness Reduction Worth (3.10×10^{-1}) is largest. All three warning stations are equipped with redundant warning release devices, an audible signal and a red light, which are less critical (1.82×10^{-4}).

The overall high system effectiveness is mainly a consequence of the high reliability of geophone 1 in the upper catchment. If that single geophone 1 or the technical system components essential for its functioning (logger 1, modem 1, battery 1) fail, the loss in effectiveness is large (1.77×10^{-1}). The influence of this individual sensor exceeds the joint influence of all four sensors in the lower catchment. The latter is quantified through the influence of logger 2, modem 2 or battery 2, whose failures would render all four sensors in the lower catchment useless. The influence of the individual sensors varies drastically. While geophone 3 and radar 1 have a considerable effect on the effectiveness of the Illgraben AS, geophone 2 and in particular radar 2 are assumed to be sensors with minor significance. Nevertheless, the positioning of the four sensors in the lower catchment is limited. The position is chosen to detect debris flow events that could enter the main channel below the upper geophone at the earliest possible moment.

TABLE 5.3: Sensitivity of the Effectiveness: to individual technical system components.

	system component	Effectiveness component functioning	Effectiveness Achievement Worth	Effectiveness component failure	Effectiveness Reduction Worth
1	modem 3 call receiver 1 call transmitter power network mobile network	0.943741	1.32×10^{-3}	0.0	9.42×10^{-1}
2	battery 3,4 call receiver 2,3,4	0.942581	1.57×10^{-4}	0.632004	3.10×10^{-1}
3	geophone 1 logger 1 modem 1 battery 1	0.942509	8.45×10^{-5}	0.764853	1.77×10^{-1}
4	modem 2 logger 2 battery 2 radar 1	0.942427	3.30×10^{-6}	0.935417	7.01×10^{-3}
5	radar 1	0.942427	3.24×10^{-6}	0.935876	6.55×10^{-3}
6	geophone 3	0.942426	2.19×10^{-6}	0.937827	4.60×10^{-3}
7	solar panel 3,4	0.942426	1.45×10^{-6}	0.939547	2.88×10^{-3}
8	solar panel 1	0.942425	8.31×10^{-7}	0.940781	1.64×10^{-3}
9	geophone 2	0.942424	2.34×10^{-7}	0.942048	3.77×10^{-4}
10	red light 1,2,3 audible signal 1,2,3	0.942424	1.04×10^{-7}	0.942242	1.82×10^{-4}
11	solar panel 2	0.942424	3.51×10^{-8}	0.942359	6.50×10^{-5}
12	radar 2	0.942424	8.16×10^{-9}	0.942405	1.91×10^{-5}

5.7 Summary

We propose a framework to quantify the reliability of AS for natural hazards based on BN, accounting for both technical failures and the inherent system ability. The reliability is expressed in terms of POD and PFA. To find a warning strategy that offers an optimal trade-off between these two, we define the system effectiveness as a function of POD and PFA as a measure of risk reduction. The optimal warning strategy is the one maximizing the system effectiveness. We show that by enhancing the BN to a DG, one is able to automatically identify an optimal warning strategy for systems with multiple sensors, where the decision on whether or not to issue an alarm is based on a combination of signals from all these sensors. By implementing the framework for a debris flow AS, we are able to demonstrate the applicability and usefulness of the framework in Chapter 4 for real AS installed in practice.

Chapter 6

Preonzo Case Study

In this chapter, results of the Preonzo case study, in which the reliability and effectiveness of a rockfall warning system (RWS) before and during a past rockfall event on May 15, 2012 in Preonzo has been assessed, are presented. Through a hypothetical predictive analysis, we investigate the influence of human decision-making and the number of sensors on the system effectiveness and the intervention cost. A comprehensive version of this chapter has been published as (Sättele et al., accepted,b).

The reliability of the Preonzo RWS is expressed as the probability of the timely set-up of an evacuation before the event (POD) and addresses both the technical and the inherent reliability of the RWS (see Chapter 4). In this case study, we did not address the PFA because automated warnings are sent to experts whose compliance should not be decreased due to frequent false alarm. For the Preonzo RWS, the technical and inherent reliability are analyzed separately for the detachment phase and the acceleration phase. In the detachment phase, the EWS is fully automated and the reliability assessed following part I of the framework approach. Here, the RWS constantly monitors velocity patterns of the unstable rock mass to send warning information instantaneously if predefined thresholds are exceeded. Higher-magnitude rock slope failures characteristically evolve over long periods of time, typically weeks to several years, until a critical path of detachment is developed. Failure slopes show early signs of deformations, such as tension cracks, movements and increasing rockfall activity (Hungr and Evans, 2004). This progressive failure includes daily fluctuations and depends on temperature, rain, snow melt and long-term stress-strain behavior of slopes which control fracture propagation.

Rainfall, earthquake and snow melting, weathering and aging can be important triggers or driving factors that weaken the rock mass during the first phase (Lacasse et al., 2008). In the detachment phase, the technical reliability remains constant and can be modeled with BN. The inherent reliability in the detachment phase depends preliminarily on the warning thresholds, the measured sensor data and their positioning in the field. All these aspects can also be modeled in the BN.

In the acceleration phase, the non-automated part of the RWS is assessed as described in part II of the framework. In this phase, the final failure occurs after an acceleration in which rock bridges are destroyed, often preceded by sub-critical fracture propagation and stress corrosion, especially in brittle rock mass (Petley et al., 2005b,a; Petley and Petley, 2006). To forecast the event time and execute appropriate intervention measures, experts analyze sensor data and apply models. The time of failure can be forecasted using measured velocity data (Fukuzono, 1990). Figure 6.1 illustrates how the inverse velocity ($1/v$) is plotted against time in a linear $1/v$ model to obtain an event forecast (Saito, 1969; Hashimoto et al., 1982). In the acceleration phase, the technical reliability of the system is no longer constant, but decreases over time, because sensors reach their mechanical limits or are likely to be destroyed by environmental impacts. Additionally, power support and communication lines may be interrupted on purpose to prevent additional consequences in case of a direct hit. Thus, the power supply of the RWS becomes less reliable close to the event. We propose to address these increasing failure probabilities of technical failures through inhomogeneous Poisson processes. The inherent reliability in the acceleration phase addresses the ability of the RWS and the decision-makers to set up an evacuation before the event. The forecast ability depends on the ability of the $1/v$ model to forecast the event time and on the risk tolerance of the decision-maker. To assess the inherent reliability achieved with the RWS, event forecasts are calculated and summarized graphically.

The effectiveness of EWS is a function of the achieved risk reduction (Eq. 4.8). RWS reduce the risk primarily by decreasing the exposure probability pe_{ij} of persons and mobile objects i in a hazard scenario j (see Eq. 4.9). Accurate forecasts necessary to generate timely information are still a major challenge for the foreseeable future. Finding the trade-off between an early and safe evacuation and cost caused by unnecessary intervention measures remains crucial for experts and decision-makers. To support

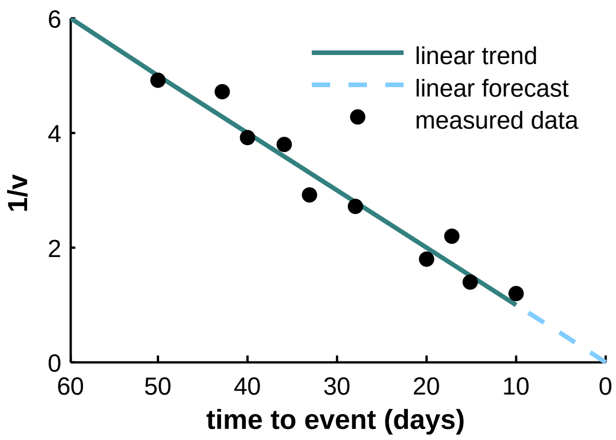

FIGURE 6.1: Sketch of a $1/v$ Model: to predict the event date of brittle rock slope failure based on a measured kinematic time series.

decision-makers in designing an optimal RWS, the effectiveness and the cost of alternative measures are quantified here and compared in a hypothetical predictive Monte-Carlo analysis.

6.1 The Preonzo Rockslide Warning System

Since decades, an unstable rock mass is reported, which potentially threatens the community of Preonzo (Switzerland). Since the eighteenth century, several slope failures occurred (Willenberg et al., 2009; Loew et al., 2012). Here, we investigate the latest event, which took place on May 15, 2012. The entire spring period of 2012 was characterized by unusually high displacement rates. At the beginning of May, local authorities were informed of critical displacements from the geologist operating the warning system. Immediately, a crisis team was established comprising local authorities, safety officers and geologists operating the RWS. After several days of heavy rainfall, the velocity of the rock mass increased significantly and on May 6, the crisis team evacuated people from the underlying factories and closed the nearest road. On May 8, the rain stopped, the velocity decreased and intervention measures were discontinued to avoid loss and business interruption. On May 12, the velocity increased again and a second evacuation was initiated. In the early morning of May 15, approximately 3×10^5 m^3 detached from the rock face. Fortunately, the rock mass stopped on the slope and did not harm any infrastructures or persons.

Between 1999 and May 2012, a RWS was installed at the Preonzo site (6.2). The system was operated and maintained by local geologists, who are in charge of natural hazards management in the Canton Ticino. From 1999 onwards, five extensometers were continuously measuring the rock movements to detect accelerations and to automatically generate warning information. To increase the system reliability, an automated total station with fourteen reflectors was set up in summer 2010 (Loew et al., 2012). The configuration of the Preonzo RWS can be described with three units for monitoring, data interpretation and information dissemination.

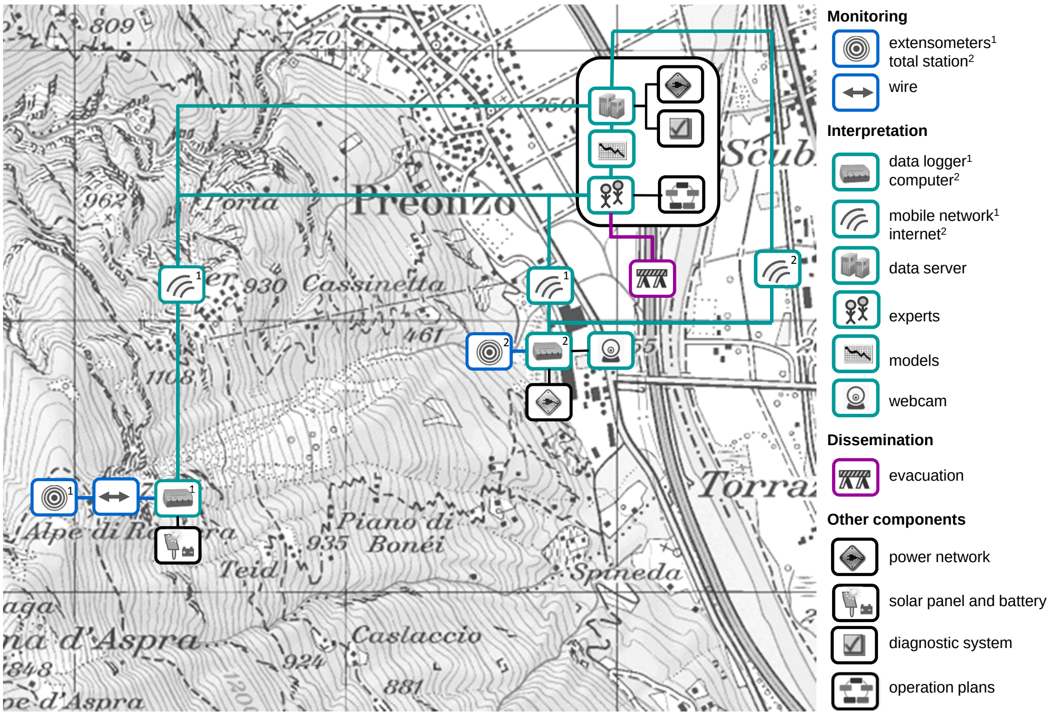

Figure 6.2: System Sketch of the Preonzo Warning System: illustrates the partly automated procedures and components, based on pixmaps©2015 swisstopo (5704 000 000).

The monitoring unit incorporated two sensor technologies. In the tension crack of the northern section, five extensometers monitored the displacement (Figure 6.3a). The extensometer measurements (every 15 - 60 minutes) were controlled by a remote data logger. Sensors and logger communicated via protected cable connections. The power supply was provided by a battery, recharged by a solar panel. In addition to the extensometers, an automated total station measured the relative distance to fourteen reflectors at the front face of the slope (Figure 6.3b). The total station in the valley was connected to a computer that initiated regular measurements every twenty minutes. The power was provided by the power network and the system was located in a heated cabin, which was built on a concrete foundation to avoid movements.

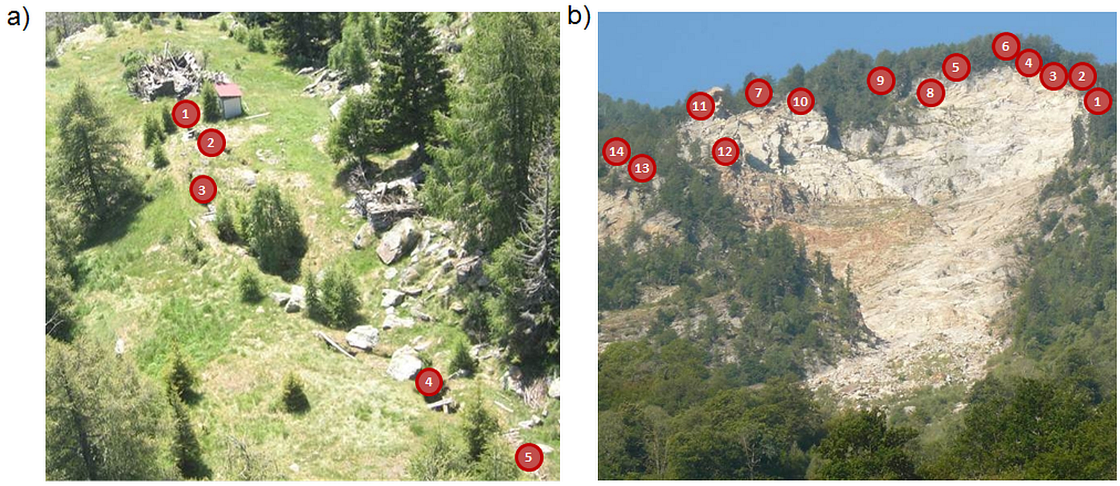

Figure 6.3: Monitoring Technologies of the Preonzo Warning System: a) positioning of the five extensometers in the tension cracks and b) fourteen reflectors in the front face which were regularly recorded by an automated total station (underlying picture by Valenti).

The data interpretation unit included two main decision levels; one in the displacement and one in the acceleration phase. In the detachment phase, warnings were automatically generated if predefined warning thresholds were exceeded; in the acceleration phase, the crisis team analyzed the data to decide on intervention measures. To generate automated warning information, three threshold levels were defined for each extensometer in the tension crack (1 mm/d, 3 mm/h and 5 mm/h) and one threshold for the total station (50 mm/d). The threshold for the total station was higher, because measured displacements were generally higher at the front face. Whenever a threshold for an extensometer was exceeded, the remote data logger issued warning information via the mobile network to the geologists. Independently, the computer connected to the total station in the valley issued a warning if the threshold was exceeded. While data from the remote data logger was transmitted via mobile network, data from the total station was sent via cable connection. Whenever the system operators received automated warning information, they analyzed sensor data to decide on further activities. All data was collected, processed and visualized on a central server and the event date was forecasted by the application of the $1/v$ model. The final decision about an evacuation was made within the crisis team and was based on the calculated forecasts. The RWS was equipped with a diagnostic system, which observed the availability of individual sensors, the status of the remote batteries and the availability of the mobile network at regular intervals. Consequently, system failures could be detected intermediately to implement alternative temporary risk mitigation measures.

The information dissemination unit of the Preonzo RWS consisted of intervention plans, which summarized mitigation measures and responsibilities. The intervention was planned and coordinated by the crisis team to protect the underlying factories and roads. The evacuation of the factories could be initiated through an activation of acoustic signals and was led by the police, who were responsible of closing the underlying roads.

6.2 Quantifying the Reliability of the Preonzo Warning System

This section describes the reliability analysis of the RWS installed before and during the event in 2012, considering both the technical and the inherent reliability. The reliability analysis is presented separately for the detachment and the acceleration phase. In each phase, factors that determine the system reliability are described, selected methods used to assess the reliability are presented and the main results are summarized.

6.2.1 Technical Reliability during the Detachment Phase

Accurate automated warning information to system operators can only be generated if technical system components work properly. In Preonzo, the RWS is equipped with a diagnosis system that sends information when system components fail. In this situation, experts are warned and should assess the situation on-site. Due to this fail-safe system configuration, technical failures of the RWS will not lead to events being missed. Nevertheless, to avoid high costs due to unnecessary interventions because of frequent alarms, the technical reliability is relevant and should be maximized. The BN to model the technical reliability of the Preonzo RWS consists of two different types of nodes (Figure 6.4).

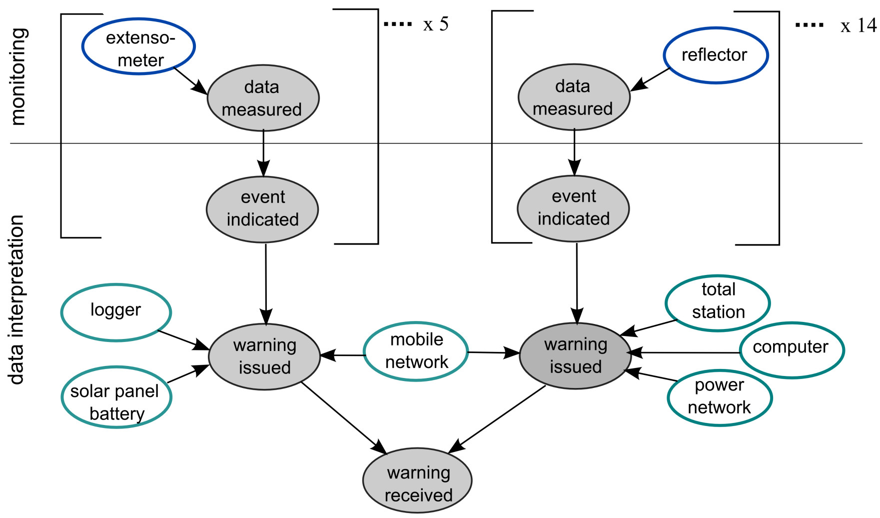

Figure 6.4: Bayesian Network for the Preonzo Warning System: to model the technical reliability in the detachment phase. The monitoring unit incorporates five extensometers and fourteen reflectors; and the data interpretation includes components to initiate and transfer warnings.

Grey nodes represent the causal chain from measured sensor data to the warning provided to system operators. White nodes in the BN specify the failure probabilities of system components and were adapted from the results of the Illgraben case study (see Chapter 5). They are estimated for individual components as $Pr(F(t)) \sim 5 \times 10^{-4}$/day. Only the failure probability of the mobile network is significantly higher, at 1.2×10^{-2}/day, according to a study conducted by the Swiss Federal Office for Civil Protection (FOCP, 2013a).

The analysis shows that the technical reliability achieved with the Preonzo RWS is high, due to multiple and redundant sensor units. The system is equipped with two sensor technologies that both incorporate redundant sensors. The limiting factor for the technical reliability is the availability of the mobile network, which is not redundant. This results in a technical system failure probability of $Pr(F(t)) = 1 - 1.2 \times 10^{-2} = 0.988$.

6.2.2 Inherent Reliability during the Detachment Phase

The inherent reliability of the RWS is its ability to interpret the measured sensor data, to distinguish between noise and hazard and to inform system operators before the event occurs. In the detachment phase, the relation between the POD and PFA is determined by the predefined warning threshold. To achieve a large POD, thresholds for the Preonzo

RWS are set low by design. However, the warning thresholds are high enough to avoid perpetual false alarms due to displacement rates that arise from daily fluctuations, e.g., due to temperature changes. Existing movement records summarize the displacement rates measured by the extensometers and the total station between August 2010 and May 2012. Dilatations measured by extensometers positioned in the northern section are higher (extensometers 3-5) than those measured by similar sensors in the southern section (Figure 6.5). A few hours before the event, extensometers 4 and 5 reach their technical limits and fail. The reflectors show similar displacement characteristics as the extensometers (Figure 6.6). Reflectors 1-7 and 9 are mounted in the northern sector and show large displacement rates. The remaining reflectors (7, 11-14) are installed in the southern section and do not indicate any discernable acceleration. Reflector 10 failed already in summer 2011.

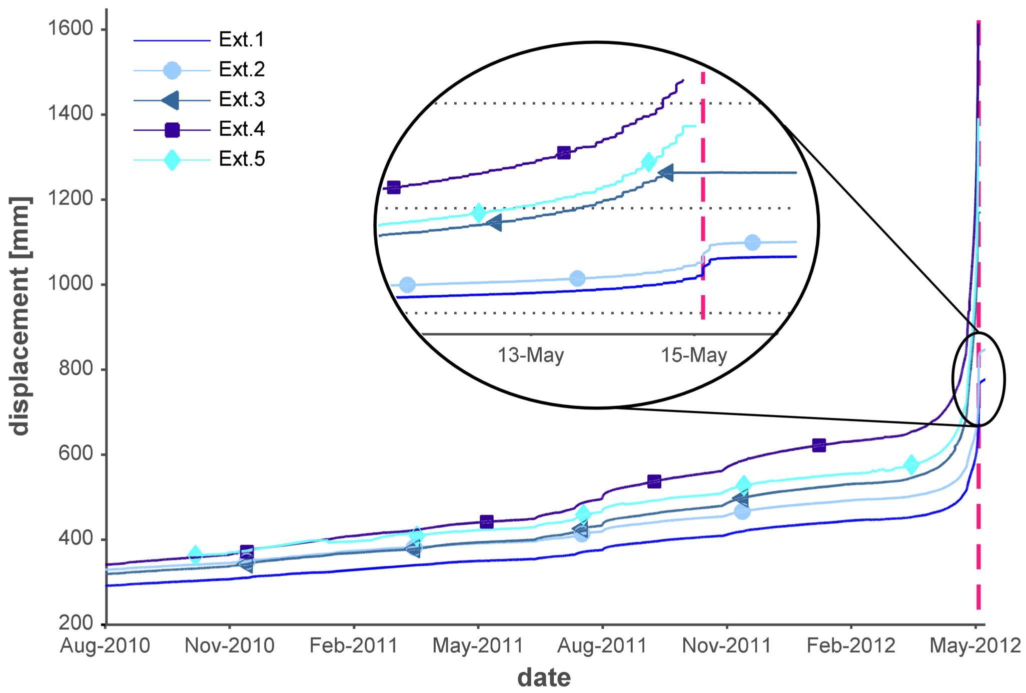

FIGURE 6.5: Displacements Measured by Extensometers: in the tension cracks between August 2010 and May 2012. Extensometers positioned in the northern section (3-5) indicate higher acceleration before the event.

In Figure 6.7, the sensor data measured by extensometer 5 from January to May 2012 is compared to the lowest warning level. The lowest warning threshold (1 mm/d) is regularly exceeded by those sensors installed in the northern section from the beginning of March onwards. Starting in early April, the warning threshold is constantly exceeded

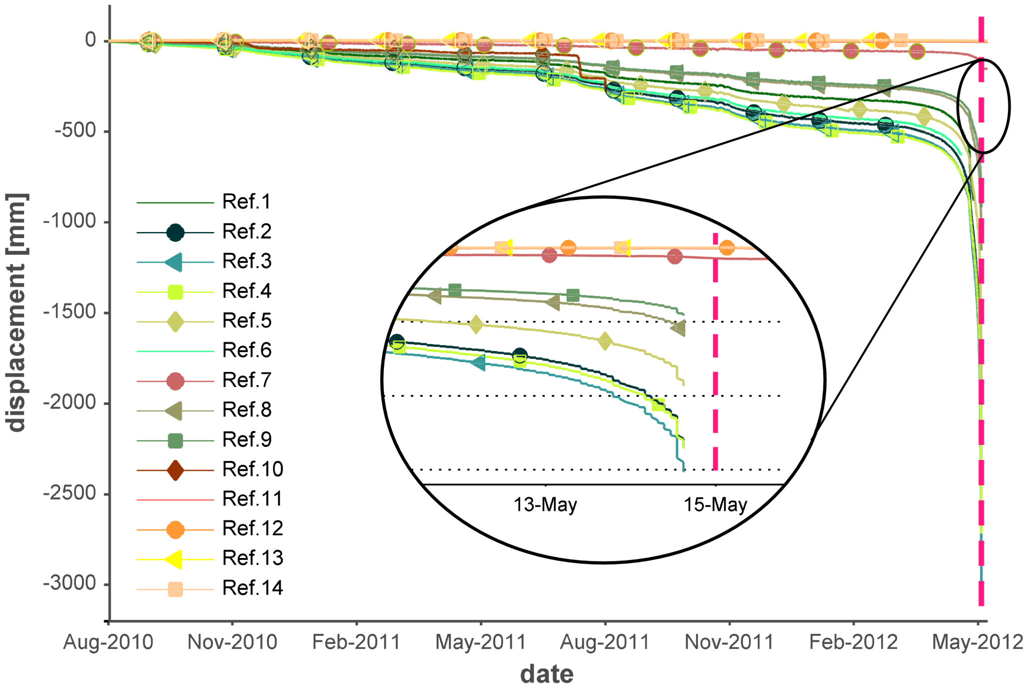

FIGURE 6.6: Displacements Measured by Reflectors: at the front face of the slope between August 2010 and May 2012. Reflectors positioned in the northern section (1-7, 9) indicate acceleration before the event.

and system operators start to analyze the sensor data at more frequent intervals, independent of automated warning information. The two upper thresholds (3 mm/h and 5 mm/h) are reached several days before the event occurs. Other extensometers in the northern section show similar results. The only warning level defined for the reflectors (50 mm/d) is also exceeded before the event by those reflectors installed in the northern section.

The influence of warning thresholds on the system reliability can be modeled within the BN, by making the conditional probability of the nodes *event indicated* dependent on the *threshold*. Such an approach was followed for the Illgraben analysis (see Chapter 4). However, in the detachment phase, a low threshold can be generally chosen, which leads to a POD that is essentially one. This is because the effect of false alarms is less relevant in this phase, as the warning information is sent to system operators and not to endangered persons directly. System operators should be interested in receiving information of every unexceptional displacement. In combination with the fail-safe configuration of the technical system components, the overall probability of identifying an event in the

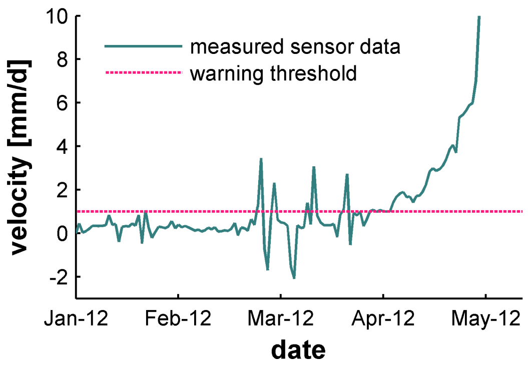

FIGURE 6.7: Velocities Exceed Thresholds of Extensometer 5: velocities temporarily exceed the lowest warning threshold in March and then constantly from beginning of April.

detachment phase is very close to one. The large reliability of the Preonzo RWS also leads to a number of false alarms to system operators that is reasonably small.

6.2.3 Technical Reliability during the Acceleration Phase

In the acceleration phase, geologists analyze the sensor data to forecast the event time and support the crisis team in planning appropriate intervention measures. The technical reliability in the acceleration phase influences the RWS's ability to support the crisis team in creating an accurate event forecast. The forecast of the event time depends directly on the availability and quality of the measured sensor data. Power interruptions due to safety reasons or sensor failures due to large movements in the surrounding area occur more frequently close to the event. The effect of increasing system failure probabilities on the forecast accuracy should therefore be considered in technical reliability analyses of RWS. In the northern section of the Preonzo rock face, the majority of sensors fail in the hours before the event (Figure 6.8). Three out of five extensometers and all reflectors positioned in the fast-moving slope are destroyed.

To quantify the accelerating destruction of sensors in Preonzo before the event in 2012, a function describing the probability of failure is fitted to the observed number of sensors that failed in the northern section (extensometer 1-5; reflectors 1-6 and 8, 9, 10). The failure probability P_f for Δt days to the event in Preonzo is modeled as:

$$P_f(\Delta t) = p_{basic} + p_{end} \times exp(-b \times \Delta t) \tag{6.1}$$

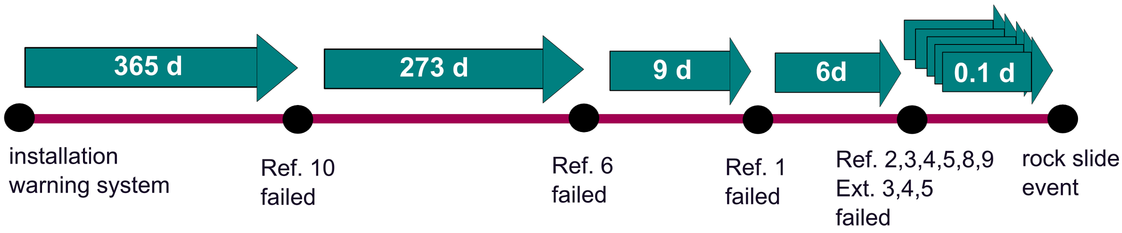

FIGURE 6.8: Increasing Failure Rates of Sensors: shortly before the event on May 15, 2012 many sensors are destroyed due to the fast-moving slope.

The basic failure probability of technical system components p_{basic} is 5.0×10^{-4} (Section 6.2.1). To obtain values for p_{end} and b, a likelihood function describing the observed number of failures is established. The probability of n_F failures out of n sensors on a given day is described by a binomial distribution as:

$$Pr(N_F = n_F) = \binom{n}{n_F} \left\{ P_f(\Delta t)^{n_F} \times [1 - P_f(\Delta t)]^{n-n_F}] \right\} \tag{6.2}$$

The parameters b and p_{end} are found by maximizing the log-likelihood function, which is defined as:

$$lnL(p_{end}, b) = \sum_{t=1}^{44} lnPr(N_F = n_F(t)|P_{end}, b) \tag{6.3}$$

$n_F(t)$ are the observed failures on forty-four days before the event. By maximizing Equation 6.3, maximum likelihood estimates for p_{end} and b are calculated as $p_{end} = 0.689$ and $b = 0.510$. In Figure 6.9, the percentage of sensors that failed in the northern section and the calculated failure probabilities using Equation 6.1 for days 1-44 before the event are summarized.

6.2.4 Inherent Reliability during the Acceleration Phase

The inherent reliability in the acceleration phase is a function of the available sensor data, the accuracy of the $1/v$ model and the expert's ability to forecast the event based on this data. The decision about an evacuation depends on their risk tolerance. Due to the dependence on the available sensor data, the inherent reliability is related to the technical reliability of the RWS. An increasing number of sensor failures can reduce the forecast ability. To assess the inherent reliability of the Preonzo system, we apply

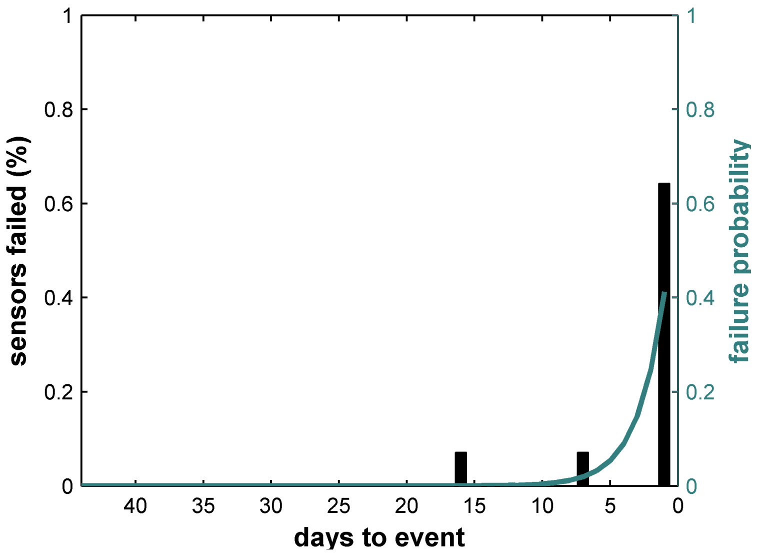

FIGURE 6.9: Modeled and Observed Failures: in the acceleration phase, an increasing number of sensors fail just before the event. The bars (left axis) show the observed percentage of sensors that fail; the line (right axis) depicts the failure probabilities according to Eq. 6.1.

a linear $1/v$ model using measured sensor data to obtain event forecasts. The inverse velocity at time t is calculated as following:

$$\frac{1}{v(t)} = a + b \times t \tag{6.4}$$

a and b are modeled parameters and t is the time expressed in days. To avoid large scatter generated by small velocity values deteriorating the accuracy of the forecast, the parameters are fitted to the measured velocity rather than to its inverse. Specifically, a least-squares fit of a and b to measured values of $v(t)$ is carried out through the following relationship:

$$v(t) = \frac{1}{a + b \times t} \tag{6.5}$$

Figure 6.10a illustrates the velocities measured by extensometer 1 in the ten days before May 14 and the model fit. To obtain a forecast of the event time, the inverse velocities ($1/v$) are calculated according to Equation 6.4 for dates t in the future. The event date forecasted with the $1/v$ model is the day where the inverse velocity ($1/v$) cuts the x-axis. In Figure 6.10b, the inverse velocity corresponding to Figure 6.10a is shown. On May

14, the forecast of the event with extensometer 1 is made for May 16, one day later than the event actually happened.

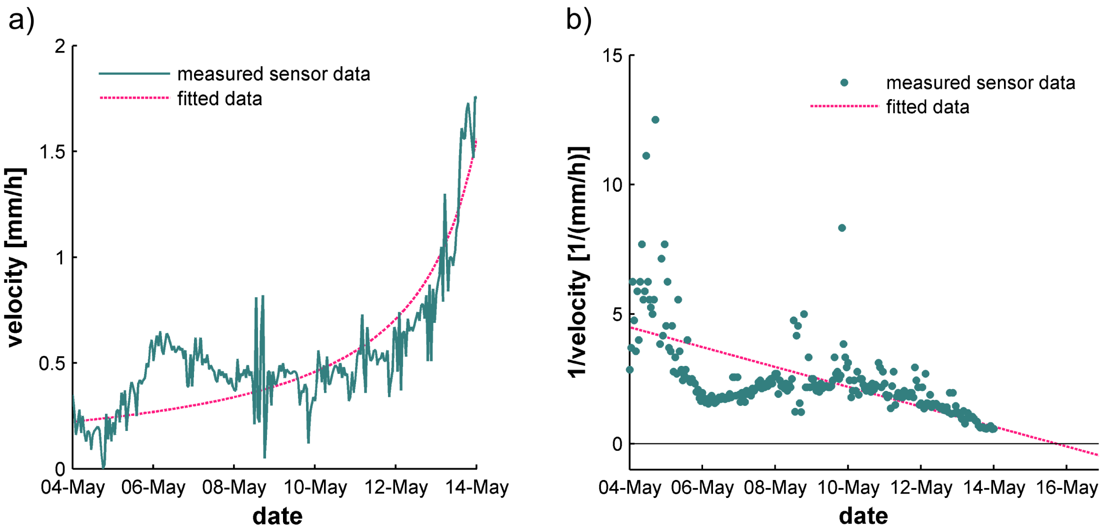

FIGURE 6.10: Application of 1/v Model: a) velocity recorded by extensometer 1 from May 4 to May 14 and fitted function; b) $1/v$ versus time using data from extensometer 1. On May 14, the $1/v$ model forecasts the event to occur on May 16, which is one day later than the observed event.

Following the approach illustrated above for extensometer 1 and data available before May 15, event forecasts were made for every sensor and each day between April 1 and May 14. Figure 6.11a, displays the forecasted event dates using data of different sensors installed in the northern section as a function of the date on which the prediction is made. In April, the forecasts made by different sensors vary significantly, but they become more aligned by the end of April. In this final phase, the predictions based on extensometer data show larger scatter than those based on reflector data. On May 14, the majority of sensors provide velocity data that indicated a hazardous event for the next day. Extensometer 1 and 2 are located further south, where the measured displacements are less significant. They forecast the event with a delay of one day. Nevertheless, ten out of twelve sensors lead to an accurate event forecast.

The inherent reliability in the acceleration phase depends on the risk tolerance of the decision-makers. To understand the human impact on the inherent reliability, the forecasted number of days to the event is plotted for days between April 1 and May 14 (Figure 6.11b) for all relevant sensors. There are several days in April on which some sensors forecast the event for the following day. Here, different experts may come to different conclusions and decisions. In May, the forecasts vary less and the influence of human decision-making becomes less important. It can be assumed that even decision-makers with different risk tolerances would come to the same decision in this period (which is the one that was actually taken by the crisis team in Preonzo).

6.3 Hypothetical Analysis: Optimizing Warning Systems

Based on a hypothetical analysis, the effect of those parameters that influence the reliability of the Preonzo RWS is investigated. To this end, the number of sensors as well as the decision criteria for the evacuation of buildings and closure of roads (hereafter denoted as evacuation criteria) are modified. Such analysis will allow the evaluation of the effectiveness and the cost of varying system configurations in the design phase and will answer questions, such as: would a RWS with less redundant sensor technologies deliver a similar probability of detection? And to what degree does the human risk tolerance influence the reliability and intervention cost of the RWS?

To compare the effectiveness and the cost for varying designs of the Preonzo RWS, the POD achieved with the system and the expected cost arising from the intervention measures are estimated in a hypothetical analysis. Since the actual decision on intervention measures is based on expert assessments, which can include more information than only sensor data, the analysis is simplified and likely to under-estimate the true capacities of the RWS. To assess the effect of the number of initially installed sensors on the reliability, it is varied between five and fifty in the hypothetical analysis. To investigate the effect of human decision-making, we specify two decision-makers with different risk types. They are associated with different evacuation criteria (Table 6.1). A technical evacuation criterion determines the minimum numbers of sensors that must be available for a forecast. Whenever fewer sensors are functioning, the crisis team initiates an evacuation and the closure of the road. The inherent evacuation criterion defines the minimum percentage of sensors that must forecast a hazardous event for the next day in order to initiate an evacuation and road closure.

With a Monte Carlo (MC) analysis, we estimate the POD and intervention cost for the specified risk types and modified numbers of initial sensors. In the MC analysis, the investigated Preonzo rockfall event is randomized, as is the response of the individual

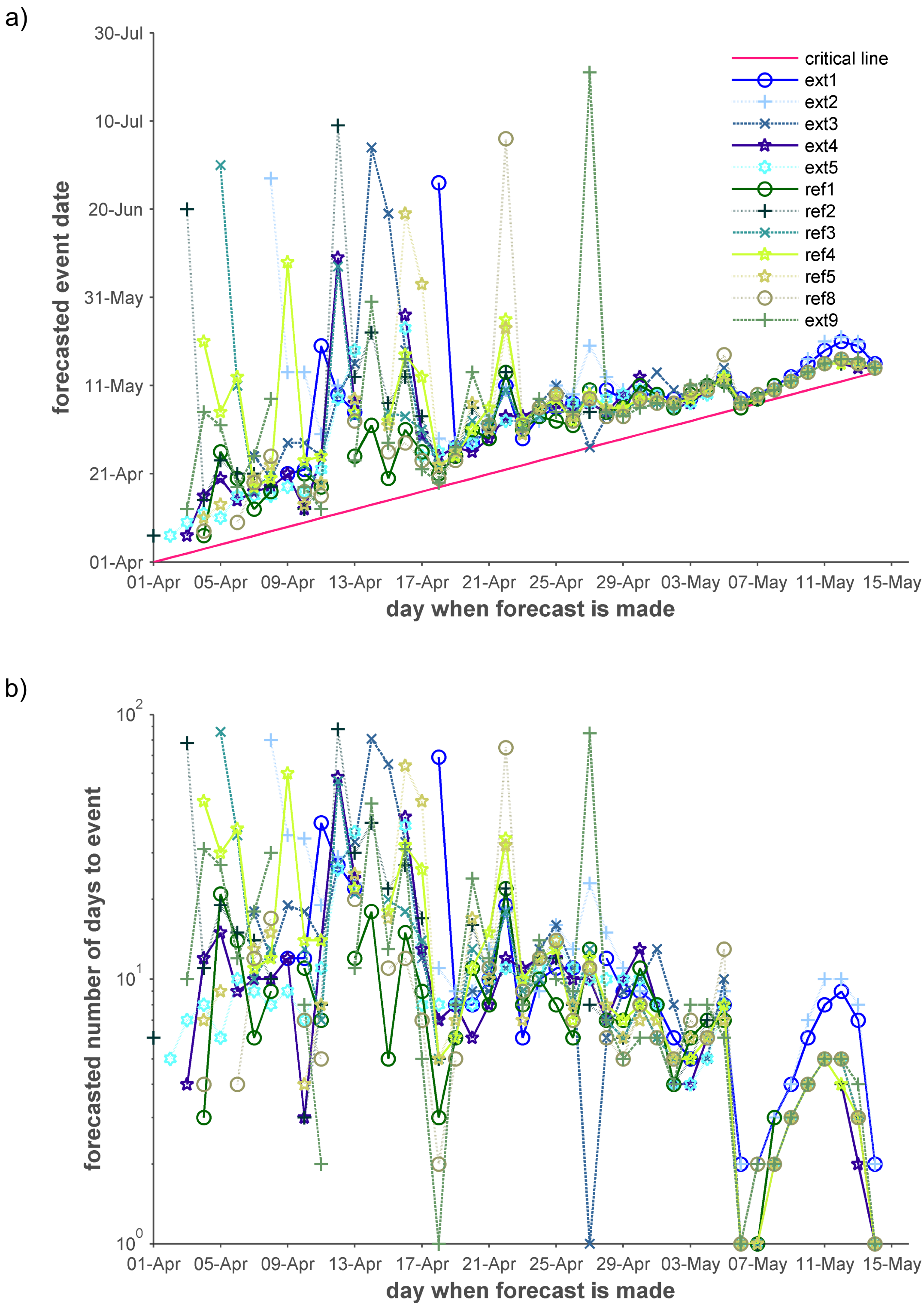

FIGURE 6.11: Forecasted Event Dates: a) calculated with the $1/v$ model for the sensors in the northern section on every day between April 1 and May 14; b) forecasted number of days to the event calculated with the $1/v$ model for sensors in the northern section on every day between April 1 and May 14.

Table 6.1: Evacuation Criteria: used to define risk types.

risk type		technical evacuation criterion	inherent evacuation criterion
conservative	less risk tolerant decision-maker	fewer than six sensors are functioning	20% of the sensors forecast the event for the next day
cowboy	more risk tolerant decision-maker	fewer than three sensors are functioning	50% of the sensors forecast the event for the next day

sensors. We use $n_S = 10'000$ random realizations (run) of the process. For each run if and when evacuations would be initiated is checked, based on the technical and the inherent evacuation criteria. In each run, the number of functioning sensors for all days between April 1 and May 14 is simulated and compared to the minimal required number to investigate whether the technical evaluation criterion is fulfilled. The number of functioning sensors on each day is simulated based on a binomial distribution (Eq. 6.1) with parameters determined following Section 6.2.1.

To assess whether the inherent evacuation criteria is fulfilled, the percentage of simulated positive event forecasts for the next day is compared to the specified percentage. The number of available event forecasts on each day depends on the remaining number of sensors. The forecasts for the group of sensors are modeled by a probability distribution, wherein no distinction is made between individual sensors (i.e. they are considered as statistically independent and identically distributed). To obtain probability distributions for forecasts on each day between April 1 and May 14, lognormal distributions are fitted to sensor forecasts calculated for extensometers 1-5 and reflectors 1-5, 8 and 9 (Figure 6.11b). Figure 6.12 shows the empirical and the fitted CDF of the forecasted days to event calculated on April 18 and May 14. The fitted distributions are applied in the MC analysis to randomly generate forecasts for each day. The percentage of sensors that forecast an event for the next day is calculated and compared to the percentage defined by the inherent evacuation criterion.

Intervention cost arises whenever an evacuation is initiated. This cost is primarily caused through interruptions of business processes in the subjacent factories and are estimated as 100,000 CHF/ day based on the information of local experts. If the technical evacuation criterion is fulfilled, a five-day evacuation is necessary to install a replacement

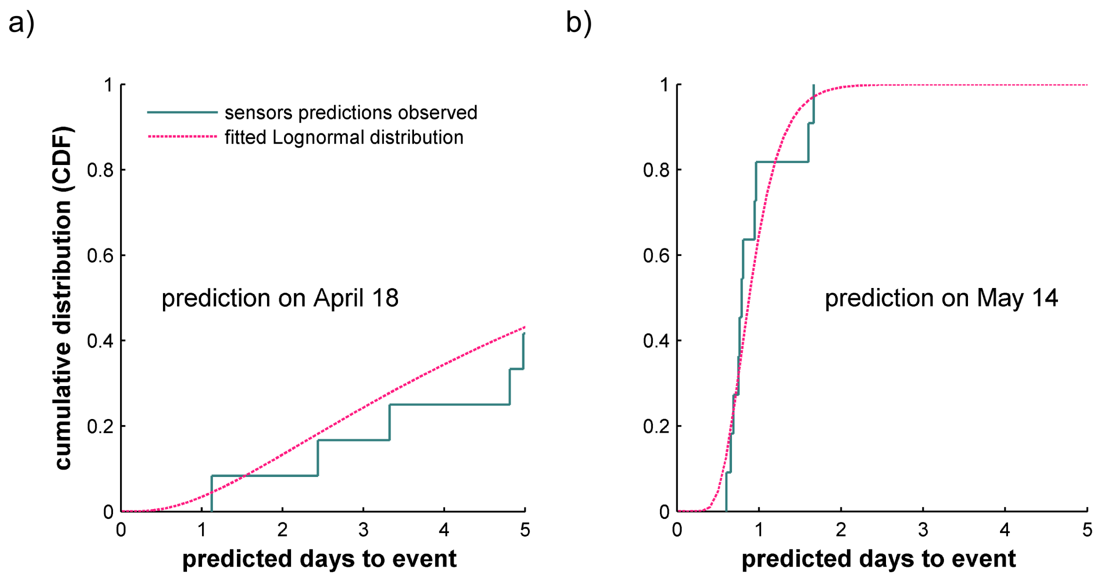

FIGURE 6.12: Forecast with Group of Sensors: the empirical (observed) and the fitted cumulative probability distribution function (CDF) of the forecasted days to the event for the group of sensors. The observed sensor forecasts are those shown in Figure 12b; a) on April 18 the probability of an event on the next day is estimated as 0.034 and for an event in five days as 0.43; b) on May 14, the probability of an event to occur within the next day is estimated as 0.65 and for the second day 0.99.

system. In this time, a temporary monitoring system (e.g. interferometric radar) must be installed to decide if the access for installation to the area is safe. The total cost of intervention is estimated as 800,000 CHF, whereof 500,000 CHF is due to the five days of evacuation and the remaining 300,000 CHF is the investment cost for the replacement system, including the cost of temporary monitoring measures. To not complicate the analysis, we do not separate the individual costs to different stakeholders. If the inherent evacuation criterion is fulfilled, an evacuation for two days is initiated and the corresponding cost is 200,000 CHF. In this analysis, the POD is the probability that the evacuation and road closure are in place on May 15, the day of the actual event.

Figure 6.13a displays the POD calculated for the different risk types as a function of the number of initially installed sensors. For the conservative decision-maker, the POD is close to one, only slightly depending on the number of sensors. The more risk-tolerant decision-maker cowboy achieves a POD between 0.65 and 0.85 which reaches its minimum at eleven sensors. Fig. 6.13b displays the expected intervention cost calculated for both risk types as a function of the initially installed sensors. As expected, the conservative decision-maker creates a higher expected intervention cost, especially with a small number of initial sensors. In this case, large costs for evacuation and replacement systems are generated. With a highly redundant sensor unit (around thirty sensors), the expected cost for the conservative decision-maker reaches its minimum at 400,000 CHF. The expected cost for intervention incurred by the more risk-tolerant cowboy reaches minimal costs (215,000 CHF) at twenty. For a larger number of sensors, the expected cost increases slightly up to a maximum of 236,000 CHF. It is pointed out that this sum does not include the cost for installing the initial sensors. In a comprehensive cost analysis, one should also include the acquisition cost of the RWS, which increases with a rising number of sensors, to determine the optimal number of sensors.

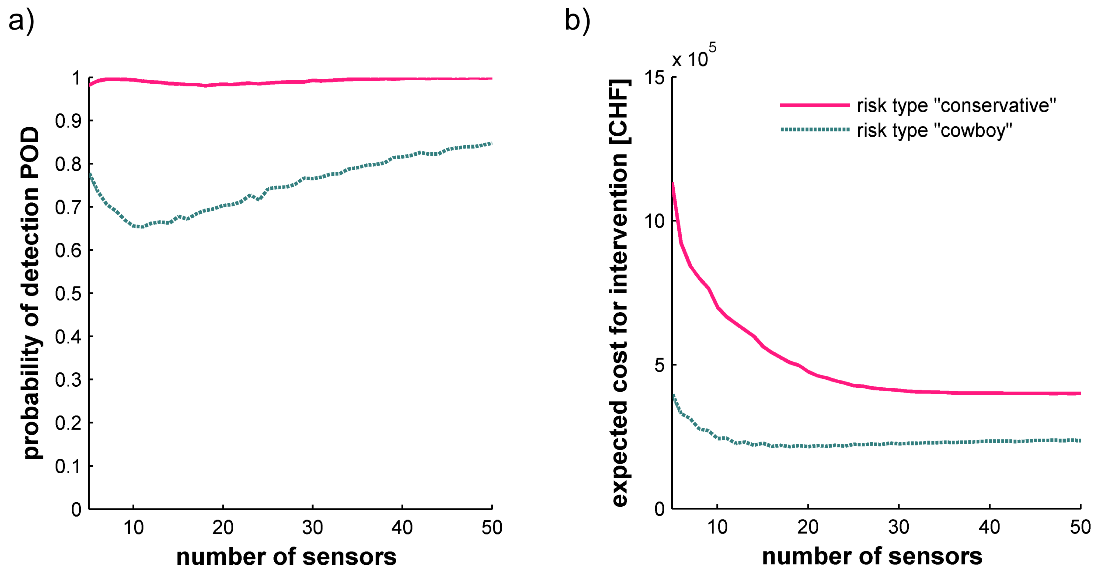

FIGURE 6.13: POD and Intervention Costs Achieved with Different System Designs: a) the POD as a function of the decision-maker and the number of initially installed sensors; b) the expected cost for intervention (evacuation, road closure) as a function of the decision-maker and the number of initially installed sensors.

The intervention on the day of the event, May 15, either occurred because the event was correctly forecasted (inherent reliability) or because the failure of multiple sensors triggered an intervention (technical failures). In Figures 6.14 and 6.15, the PODs and expected intervention cost obtained with the inherent evacuation criterion and the technical evacuation criterion are shown individually for both risk types. To this end, both evacuation criteria are checked on each day, independent of whether or not the other criterion is already fulfilled and an evacuation may already be in place. For this reason, the sum of the two individual PODs may be larger than one. The quality of the inherent forecasts during the time of reinstalling the system after technical failures may be poor, since only a few sensors are left during that period. If no more sensors are available one day before the event occurred, zero forecasts can be made and the POD associated with the inherent evacuation criteria becomes zero.

The POD achieved because of technical failures decreases with an increasing number of initial sensors (Figure 6.14). Evacuations due to an insufficient number of sensors are less likely to occur when the decision-maker is the cowboy. For the conservative decision-maker, an interesting peak is formed around seven sensors. For a minimal numbers of sensors (5-6) an evacuation because of technical failures is low, because the RWS was already substituted before the event. For 7-9 sensors, the probability that the system fails during the event is maximal and so is the POD achieved with the technical evacuation criterion. The POD because of an accurate event forecast increases with the increasing number of sensors and is close to one for RWS with at least twenty sensors for the conservative decision-maker. The POD achieved by the more risk-tolerant cowboy is never exceeding the POD reached by the conservative decision-maker and never exceeds 0.84.

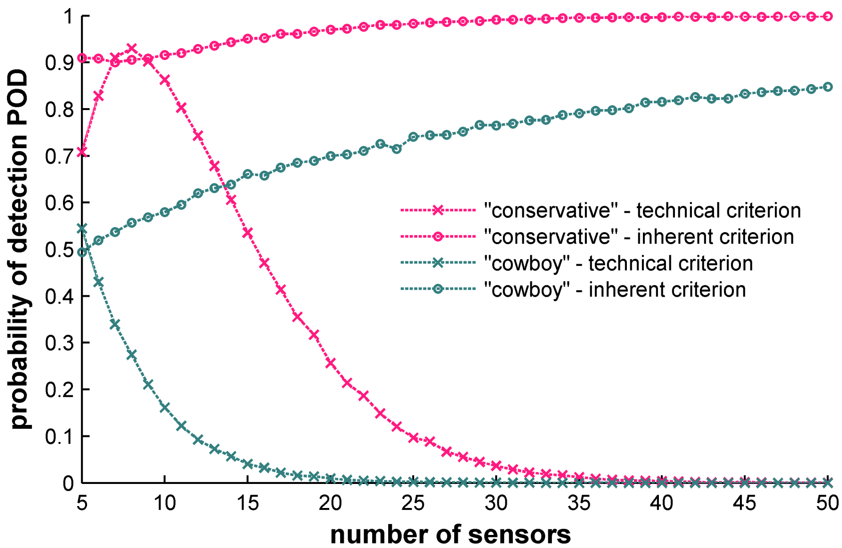

FIGURE 6.14: POD for Inherent and Technical Evacuation Criteria: individually shown for both risk types.

In Figure 6.15, the expected intervention cost created through the inherent and technical evacuation criteria are separately illustrated for both risk types. The expected cost, in accordance with the technical evacuation criterion, decreases when the number of initial sensors increases, because system failures become less likely. In particular, the conservative risk type generates immense costs with a small number of sensors. The expected intervention cost generated by event forecasts becomes constant for more than ten sensors and is higher for the conservative decision-maker.

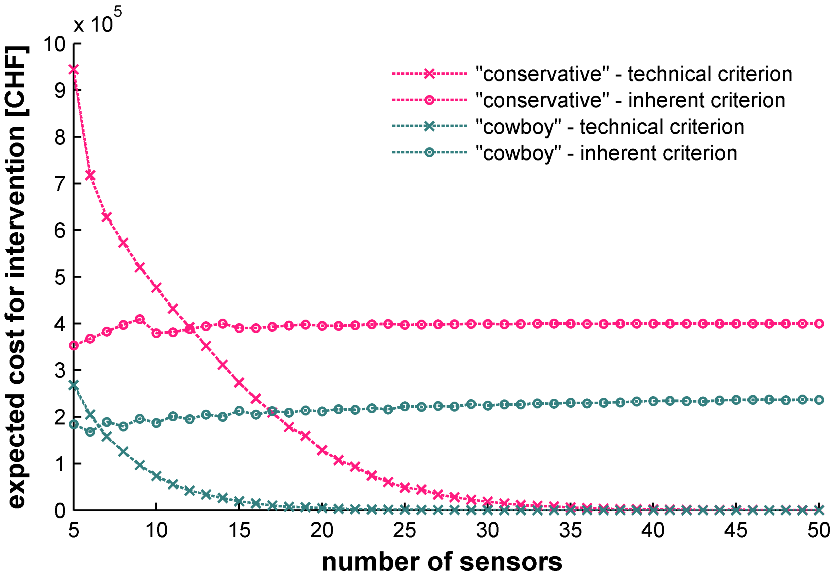

FIGURE 6.15: Cost for Inherent and Technical Evacuation Criteria: expected intervention costs are individually shown for both risk types.

To understand how the intervention cost arises, the probability of an evacuation being mandated due to sensor forecasts (inherent evacuation criterion) is illustrated in Figure 6.16 for the last forty-four days before the event, with ten sensors (a) and thirty sensors (b). The cowboy would evacuate on three days with a significant probability, namely on days 8, 9 and 1 before the event. When comparing 6.16a with 6.16b, it is clear that the forecast accuracy increases with more sensors. The probability of the cowboy proposing an evacuation due to sensor signals on the day of the event is 0.59 with ten sensors and 0.76 with thirty sensors. The probability of wrongly initiating an evacuation on days 8 and 9 stays between 0.37 and 0.35 when increasing the number of sensors from ten to thirty. The same tendencies are observed for the conservative decision-makers, whose evacuation probabilities are significantly higher. With thirty sensors instead of ten, the POD increases from 0.91 to 0.99.

6.4 Summary

The reliability of RWS should be quantified for the displacement and acceleration phase. The reliability analysis confirms that the Preonzo rockfall warning system (RWS), as it

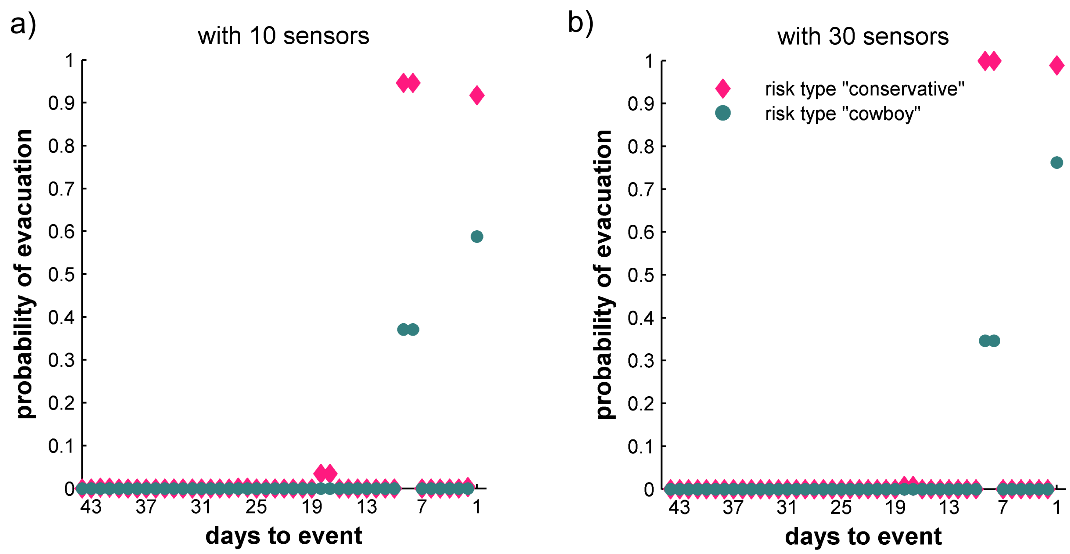

FIGURE 6.16: Probability of Evacuation: due to sensors forecasts (inherent evacuation criteria) calculated for ten (a) and thirty (b) initial sensors and different risk types for forty-four days before the event.

was installed to detect the event in May 2012, was highly reliable. We showed that with BN one can assess the RWS's ability to generate automated warnings in the detachment phase. A highly reliable system includes redundant and multiple sensor technologies, an area-wide sensor positioning, low warning thresholds in combination with a diagnostic system. In the acceleration phase, a maximal probability of evacuation on the day of the event is achieved with a sufficient number of sensors and conservative decision-makers. Both factors have a considerable effect on the system effectiveness and on the related intervention cost. The effect of human decision-making is here modeled with rule-driven decision criteria.

Chapter 7

Guideline for Practitioners

In practice, decision-makers have to identify optimal risk mitigation measures to reduce the risk imposed by natural hazards to an acceptable level. Whenever EWS are a potential mitigation measure, their reliability and effectiveness have to be analyzed and optimized before they can be compared to alternative mitigation measures. To support practitioners in the evaluation of EWS, major findings of the thesis have been summarized in a guideline (Sättele and Bründl, in print) published in German, French and Italian. The guideline supports experts in the field of natural hazards employed by authorities, engineering offices and private companies in developing and operating reliable EWS. The focus of the guideline is set on site-specific AS and WS installed for gravitationally driven alpine processes, namely flash floods, debris flow, snow avalanche, small-magnitude rockfalls to high-magnitude rockfalls and other slope failures. It consists of an introduction followed by three main parts: A - Theoretical Background, B - Decision Tools, C - EWS Examples, which are briefly introduced in the following.

7.1 Theoretical Background

The first part summarizes knowledge and provides the theoretical background. First, natural hazard process types, their monitoring possibilities and associated EWS classes are introduced (see Chapter 2). Second, a structured overview of components for different EWS classes is provided. The overview includes components in three main units of an EWS (monitoring, interpretation and a dissemination unit) in addition to components for power supply, system diagnostic tools and operation plans. Finally, the reliability and factors that have a major influence on the reliability of EWS are discussed for each system unit.

7.2 Decision Tools

In the second part, a decision graph and checklists are provided to support decision-makers in identifying, developing and operating optimal EWS.

The decision graph is a valuable tool for an integrative planning procedure of mitigation measures, whenever an EWS is a potential measures for a specific problem. The decision graph enables the decision-maker to evaluate if an EWS is an appropriate mitigation measure for a specific case and if so, which system type is practicable (Figure 7.1). Compared to the framework approach presented in Chapter 3, the evaluation of EWS and comparison to alternative mitigation measures are highly simplified in this qualitative approach. Such a simplified consideration does not replace a detailed cost-effectiveness analysis, but it enables a rough evaluation on the applicability of EWS.

In addition, two checklists summarize questions that are relevant for the assessment and comparison of the reliability achieved with different EWS configurations from competitive suppliers. Questions are selected to ensure that practitioners do not overlook major factors that influence the reliability and effectiveness of EWS that could be identified in the case studies (see Chapter 5 and 6).

7.3 System Examples

In the last section, six active EWS operated in Switzerland for a GLOF, a debris flow, snow avalanche, small-magnitude rockfall, a mid-magnitude rockslide and a deep-seated landslide are presented. Similar descriptions of EWS are presented in Chapter 2.4. For each EWS, the underlying natural hazard process, its frequency, the potential damage and the available lead time are explained. System relevant information such as the duration of the installation, the decision criteria for the choice of a certain EWS class, reliability related experiences with EWS, associated costs and contact persons are

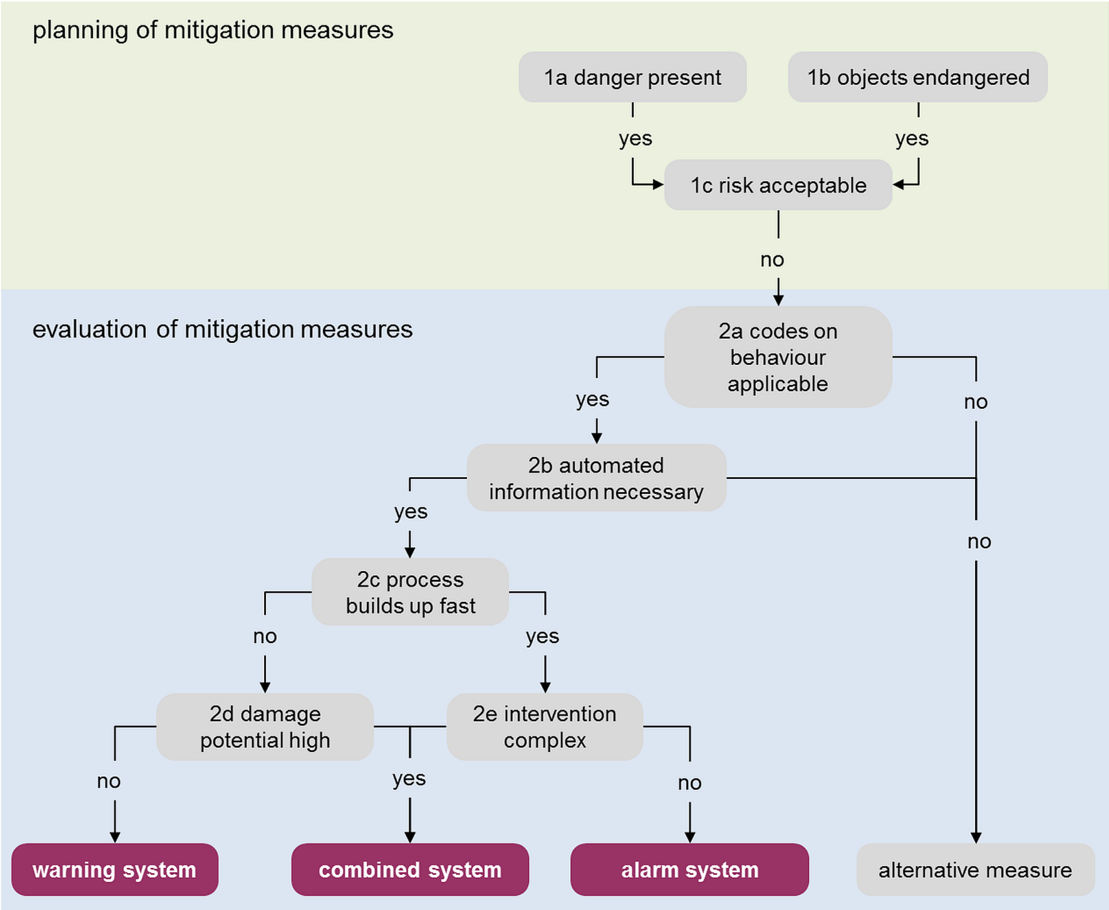

FIGURE 7.1: Decision Graph EWS: supports decision-makers in planning intervention measures and identifying the appropriate EWS class, modified from (Sättele and Bründl, in print).

provided. Each EWS, its components and dependencies among them are graphically illustrated in system sketches and described in detail.

7.4 Summary

The guideline is a simplified version of the framework approach enabling the evaluation of EWS. It includes basic knowledge on EWS, on possible evaluation criteria, such as the reliability and effectiveness ,and summarizes those factors that have a major influence on their performance. With convenient qualitative decision-tools, practitioners without a statistical background are supported in the development and operation of reliable and cost-effective EWS.

Chapter 8

Discussion

In the following, results presented in the last chapters are evaluated with respect to predefined objectives and goals. New contributions to existing knowledge, possible generalizations and practical implications, as well as shortcoming and future needs, are discussed separately for each objective and the overall goal.

8.1 Classification

Objective I - Development and verification of a generic classification for EWS as the basis for a structured evaluation of EWS.

8.1.1 Development of a Generic Classification for EWS

A novel classification, which distinguishes between AS, WS and FS is provided. Following Glantz (2004) and Schmidt (2002), the classification does not include monitoring systems as a standalone EWS class, but as a fix part of EWS, which consists of three main units for monitoring, data interpretation and information dissemination. The classes are selected based on existing definitions and proposals for classifications but also account for the needs of the present thesis. To enable a structured evaluation of EWS, different degrees of automation are defined for each EWS class. As suggested by Bell et al. (2010), fully automated, threshold-based EWS are classified as AS. Partly automated WS and FS are further distinguished by their degree of automation.

8.1.2 Verification of a Generic Classification for EWS

The applicability of the novel classification is demonstrated by assigning it to modern EWS operated worldwide. During that assignment, one main shortcoming could be revealed. The differentiation between partly automated WS and FS is often less clear compared to the differentiation with fully automated AS. Nevertheless, a unique assignment to a class is possible for the vast majority of EWS as demonstrated in Chapter 2, where WS and FS use different decision-instances (thresholds vs. human) and spatial scales (local vs. regional). The assignment to existing EWS, moreover, demonstrated that one EWS can include several sub-system classes. For example, modern severe weather EWS use thresholds to generate automated alarm information directly to persons at risk (AS) and provide daily bulletins in which danger levels are assigned to specify the probability of hazardous processes on a regional scale (FS). This multi-class EWS assignment does not limit the applicability of the classification to EWS, but enables a more specific evaluation of EWS in the framework approach. To support researchers and practitioners in structured development, management and assessment of EWS, this novel classification should be established in the field of EWS.

8.1.3 Basis for a Structured Evaluation of EWS

The novel classification enables a structured consideration of all factors that influence the reliability and effectiveness of different EWS classes. The reliability of AS depends on thresholds and the technical functionality of the automated system components. The reliability of partly automated WS depends additionally on the ability of models and humans to forecast events. These model based human decisions are the only decision-instance used in FS. The classification is, moreover, used in the framework approach for a structured evaluation of EWS.

8.2 Case Studies

Objective II - Quantification and optimization of the reliability and the effectiveness achieved with EWS in two detailed case studies to identify class-specific needs.

8.2.1 Reliability Analysis of Alarm Systems

In the Illgraben case study, a BN is constructed to quantify the reliability of a fully automated debris flow AS in terms of POD and PFA as a function of the thresholds set for all sensors. The flexibility of the BN made it straightforward to assess not only the ability of the system to distinguish between hazard and noise (inherent reliability), but also to address potential technical failures of system components (technical reliability). By extending the BN to an influence diagram, an effective way to identify the optimal warning strategy with multiple sensors, i.e., the determination of the optimal combination of signal thresholds at the individual sensors, was identified. The Illgraben case study demonstrates that the inherent reliability has a significantly higher influence on the AS performance than technical failures of components. Thresholds, the type and number of sensors and their positioning in the field should be a central part of every reliability analysis for AS. The POD achieved with individual sensors and thresholds varies significantly and should be maximal. The associated PFA should be minimal and can be reduced when thresholds from different senors are combined as decision criteria for a warning. The evaluation of the inherent reliability was based on measured sensor data recorded for a great amount (forty-four) of past events. Such a detailed database is not always available in the planning phase of EWS. In those cases, experts have to estimate threshold exceeding probabilities and use existing records from similar sites. The technical reliability of the Illgraben AS is high due to redundancies and an integrated diagnosis system. A sensitivity analysis showed that the majority of the individual technical components have little impact on the reliability, with the exception of the non-redundant communication system and the most important sensors. The case study demonstrated difficulties that are associated with the estimation of failure rates arising from external factors. While internal failure rates can often be derived from MTTF or MTBF values specified by the suppliers, external failure rates have to be estimated by experts or derived from repair records.

8.2.2 Reliability Analysis of Warning Systems

The comprehensive reliability analysis of the Preonzo WS before and during a major rockslide in May, 2012 demonstrates the importance of assessing the reliability of WS for automated and non-automated parts individually. The reliability of the automated WS depends on the technical and inherent reliability and can in some cases be expressed as POD alone. The effect of false alarms (PFA) can be ignored, if warnings are sent to WS operators, who want to receive timely information on precursors, such as increased displacement rates, before major rockfall events. Thresholds of WS are set low to achieve a maximal inherent POD and thus, the influence of the threshold is less crucial and can be neglected in the reliability analysis of automated WS. In common with the Illgraben case study, the technical reliability of the automated part is modeled in a BN. The technical reliability here is also high due to redundant sensor units and a diagnosis system. The reliability analysis of the non-automated part is conducted to assess the ability of models and humans to forecast the event time. By applying the inverse velocity model to data recorded before the 2012 event, reliable forecasts could only be made from sensors located very close to the release area. This case study and past events, such as in Vajont, show that the model accuracy can vary strongly depending on the rock characteristics and should be evaluated case-specifically through a reliability analysis. The Preonzo case study, moreover, demonstrates that a high number of sensors and a low-risk tolerance of human decision-makers lead to a high POD. To assess the influence of human decision-making, the behavior of the experts are replicated through simple, rule-driven decisions, specified in evacuation criteria. Such an approach is novel, facilitates the quantitative assessment of expert-driven WS and could also be used to describe human-decision in FS. Presently, it is unknown if precursory information and lead time are sufficient for the prediction of all mid-magnitude failure types since data is derived from a restricted data set.

8.2.3 Effectiveness Analysis of Alarm Systems

In the Illgraben case study, it is demonstrated that the effectiveness of AS can, under some conditions, be quantified as a function of POD and PFA alone. In the Illgraben, the exposure probability of persons to hazardous events is reduced through timely information (Dai et al., 2002; SafeLand, 2012). To quantify the reduced exposure probability, both positive effects and negative consequences associated with EWS are considered. While an increased POD directly decreases the exposure probability, the PFA accounts for the negative effect on the compliance with warnings due to false alarms, as suggested by Pate-Cornéll (1986); Schröter et al. (2008); Rogers and Tsirkunov (2010). The Illgraben case study demonstrated that the effect of false alarms on the compliance probability is hardly quantified in existing studies and should be investigated in future case studies for different scenarios. Negative effects on the compliance with warnings associated with lead times that are too short are not relevant in the Illgraben analysis, although recommended by Pate-Cornéll (1986). Here, lead times are long enough and enable endangered persons in the catchment to escape from dangerous debris flow events. Nevertheless, such an additional evaluation is relevant for the effectiveness evaluation of certain other AS, e.g., those installed to stop trains with long braking distances from entering rail sections affected by a landslide.

8.2.4 Effectiveness Analysis of Warning Systems

For Preonzo, the effectiveness of the WS is measured in terms of POD alone, because endangered persons typically comply with well-organized evacuations conducted in the underlying factories. Instead, intervention costs, which include the PFA, are compared with the achieved POD. This consideration is relevant for WS, where intervention costs can become very large when several or long evacuations are set up during extended lead times. This is particularly relevant when WS are designed as fail-safe systems and evacuations are set up more frequently to prevent damage as soon as the system fails. A hypothetical analysis demonstrated that the POD increases with increasing number of sensors and for risk-conservative decision-makers. These less risk -tolerant decision-makers will create larger costs for intervention with a small number of sensors, but achieve acceptable costs with a highly redundant sensor configuration. These additional considerations are valuable for the evaluation of WS and thus, cost-effectiveness analyses should be conducted in the planning phase of the WS.

8.3 Framework Approach

Objective III - Development of a novel framework approach for the evaluation of EWS that is generically applicable to different EWS classes.

8.3.1 Development of a Novel Framework Approach

For the first time, a framework approach enables the quantification of the effectiveness achieved with EWS. The framework is a valuable tool for decision-makers to evaluate EWS, to compare EWS to alternative mitigation measures and to identify optimal risk mitigation strategies. It comprises three main parts to quantify the effectiveness from the reliability of the EWS. To account for needs associated with different EWS classes two different reliability analyses are provided.

The reliability of AS and the automated part of WS and FS is expressed in terms of POD and PFA in the first analysis. For this consideration, a tailored method is developed, in which the inherent and technical reliability are probabilistically modeled with a six-step BN. In published reliability analyses, the technical and the inherent reliability have not been evaluated together for EWS. The new method is presented in three slightly adapted versions to account for needs associated with different EWS classes. Critical steps are the evaluation of the probability that measured sensor signals exceed thresholds, conditional on the occurrence of an event and the definition of component failure probabilities (see Chapter 8.2.1). In addition, it should be noted that the BN can get very large when the reliability of sensor networks is modeled.

The reliability of the non-automated part of WS and FS is also measured in terms of POD and PFA, for a fixed lead time Δt in the second reliability analysis. This simplification is necessary because the reliability typically increases when the lead time decreases, see Grasso et al. (2007) and Schröter et al. (2008). This is particularly relevant to WS and FS installed for processes that evolve slowly, such as floods or high-magnitude rockfalls, which provide lead times in the range of days and are associated with large changes of reliability. To obtain the reliability as a function of the lead time, the reliability analysis needs to be performed for different lead times. In contrast to the first reliability analysis, a tailored method is not provided, but factors that influence the technical and the inherent reliability are summarized in five steps. To develop a more comprehensive framework, a tailored method considering of, among other factors, human decision-making and the prediction ability of models should be provided in the future.

The effectiveness of an EWS is equal to the risk reduction achieved with the EWS and quantified from the reliability, following existing approaches published by Margreth and Romang (2010) and Balbi et al. (2014). In the novel framework approach, the exposure probability of persons and mobile objects is reduced through timely information generated by the EWS (Dai et al., 2002; SafeLand, 2012). For some EWS, e.g., in the case of earthquake AS, the vulnerability is reduced by slowing down trains in endangered areas (Einstein and Sousa, 2006). Such cases are not explicitly included in the framework, but should be assessed in future case studies to be added to the framework approach. To account for both positive and negative consequences associated with EWS, the effectiveness is modeled as a function of the POD and the probability that persons comply with the warning (POC). The POC depends on a basic compliance rate and reduction factors associated with PFA and the lead time. The probability of compliance with warnings depends on human decision-making and is complex to estimate. In the future, studies need to be conducted to be able to quantify the basic compliance rate and both reduction factors necessary for the effectiveness evaluation.

8.3.2 Applicability on all EWS Classes

The novel framework approach delivers an accurate basis for the evaluation of all kinds of EWS. Together with the classification and due to its high flexibility, it is extendable to cover all future needs associated with EWS. Even for EWS, which comprise the functionalities of several EWS classes, all sub-systems can be evaluated in either both or one part of the reliability analysis in a structured manner to quantify the effectiveness. The framework is designed in a way that it can be easily adapted to future needs that may come along with different EWS classes. To this end, steps in each of the three parts can be added or skipped.

8.4 Synoptic Discussion

With this thesis, an important basis for the evaluation of complex and often human-centered EWS is provided. For the first time, the effectiveness and reliability of EWS is evaluated in a generically applicable , comprehensive framework approach. In published literature, either single EWS are investigated in detailed case studies or rather superficial approaches for the evolution of EWS are presented. Besides this novel framework approach, major results are provided in a simplified form as a guideline for practitioners.

In the framework, the effectiveness is measured as a function of the reliability, which is quantified in two parts. Two reliability analyses are necessary to enable a structured evaluation of different EWS classes. The novel classification is a valuable basis enabling a straightforward selection of the right kind of reliability analysis. To establish this classification in the field of natural hazard risk management, it must be accepted, applied and published by others. To increase the attention and demonstrate associated benefits, this classification will be published together with the novel framework in conference and journal papers, which will be proactively provided to risk managers and other stakeholder of EWS.

To provide a convenient framework approach, a simplified binary evaluation of the reliability in terms of POD and PFA is chosen in both reliability analyses. In this binary evaluation, the system ability in distinguishing between hazard and noise, but not its ability to correctly predict the real extent of the event, is assessed. If an AS, for example, detects the occurrence of an avalanche correctly, this is classified as a hit regardless of whether the avalanche reaches the road section underneath. A more detailed evaluation of the reliability should assess this ability of the EWS to predict the real extent, such as the severity or the run-out distance of the hazard events, as recommended Grasso et al. (2007) and SafeLand (2012). Such a detailed consideration would be especially valuable for WS and FS. In Preonzo, the WS was, for example, able to correctly predict the event timing, but not the affected area. In retrospect, the evacuation was not necessary because the rockslide did not reach the underlying factories. Although a more detailed reliability analysis would increase the quality of the reliability analysis, it would also require a more complex effectiveness analysis; at least when the effectiveness is calculated as a function of the reliability.

The effectiveness of EWS is derived from the reliability and accounts for both positive effects and negative consequences that are associated with EWS. In the presented framework approach, it is extensively illustrated how POD and PFA can be used to calculate the risk reduction. The effect of the lead time on the effectiveness is only sparsely explained and should be further investigated in future research works. To enable the demonstration of a comprehensible framework, assumptions are made. The effectiveness calculation is, for example, limited to one scenario and elements at risk with the same probability of exposures. In the future, a more detailed effectiveness analysis, in which different scenarios and exposure probabilities are presented, should be conducted and included in the framework approach. Moreover, the effectiveness evaluation is based on the assumption that EWS reduce the exposure probability in a scenario and not for EWS that reduce the vulnerability (Einstein and Sousa, 2006), such as earthquake AS, which reduce the vulnerability in rail traffic by slowing down the trains. In such a case, POD could be used to determine the degree to which the vulnerability is reduced through timely detection. Finally, the Preonzo case study demonstrated the need to evaluate and optimize the effectiveness of EWS with respect to cost, such as the acquisition and intervention cost of the EWS. In such a comprehensive cost-effectiveness analysis, risk mitigation strategies can be compared and the optimal strategy can be identified.

To increase the applicability of the framework approach for all EWS classes, a tailored method should be provided for the second reliability analysis. Hereby, additional case studies assessing the inherent and technical reliability of the non-automated part of WS and FS should be conducted. This method should cover, among other factors, the influence of the model accuracy and of human decision-making on the system reliability, and express the reliability in terms of POD and PFA. In published case studies, the accuracy of different models used for tornado and flood warning is expressed as POD and PFA for past events (Simmons and Sutter, 2009; Liechti et al., 2013). However, the POD and PFA achieved with different models on varying sites are hardly summarized in published literature and should be further investigated. Similarly, the ability of humans to make accurate decisions should be quantified. When decision-making can be described by certain decision rules, different risk types can be specified through evacuation criteria (see Chapter 6). However, in most cases, human decision-making is complex and evaluation methods have to address psychological factors, such as risk-tolerance, experiences and group dynamics. The current trend towards an increased automation of EWS, e.g., within Meteo FS, where forecasters are supported with warning proposals (Reichert, 2010; Neal et al., 2013), will reduce the influence of humans and increase the influence of models in reliability analyses for EWS. But as long as models cannot replace the additional value gained through expert knowledge and experience, human decision-making has to be considered as an integral element of WS and FS.

Finally, the user-friendliness of the framework approach could be strongly improved by the introduction of a software tool. This software tool comprises the same three parts as the framework approach, enabling the quantification of the effectiveness from the reliability. It could, moreover, provide optimization possibilities for EWS and account for the life-cycle costs associated with different system designs. In this optimization, the costs that are caused by false alarms should be considered. To identify necessary steps and input parameters for each step, the user has to specify the class and case-specific requirements of the EWS, such as the endangered persons and the minimal required lead time. In the first part, the reliability of automated EWS could be modeled in an underlying BN that is computed in the six steps. To implement the second reliability analysis in the software tool, a comprehensive method accounting for all factors, such as the model accuracy and complex human decision-making, should be developed. In this method, the reliability should be expressed as a measure of POD and PFA for a fixed lead time, so that results of both reliability analyses can be merged and the effectiveness can be calculated as a function of the reliability and the lead time. Finally, this software tool could be embedded in a software environment in which EWS can be compared to alternative measures of an integrated risk management approach. For example, in Switzerland, the tool EconoMe currently enables the comparison of varying mitigation measures expect of EWS (Bründl, 2012) and should be enhanced to provide a comprehensive selection of optimal risk mitigation strategies.

Chapter 9

Conclusion and Outlook

9.1 Conclusion

In this thesis, a novel, comprehensive framework approach for the evaluation of EWS is developed. This framework will support decision-makers in evaluating and optimizing the effectiveness and the reliability achieved with EWS. For the first time, EWS become comparable to alternative risk mitigation measures, and optimal risk mitigation strategies can be identified.

The novel framework approach enables a structured evaluation of EWS. It includes two parts to analyze the reliability as a basis for the last part, in which the effectiveness is quantified. Dependent on the degree of automation, different reliability analyses need to be conducted for an EWS. To specify different degrees of automation, a novel classification for EWS into alarm systems (AS), warning systems (WS) and forecasting system (FS) is developed and verified by a successful application to modern, active EWS. In the framework approach, reliability is calculated in predefined steps and expressed in terms of POD and PFA. The effectiveness is the risk reduction due to the EWS and can be calculated as a function of the POD and the PFA, i.e., the reliability. In this evaluation, both positive effects and negative consequences associated with EWS are considered. To develop such as framework approach, two detailed case studies are conducted. In these case studies, the reliability and effectiveness of an AS and a WS are assessed and optimized to identify class-specific factors with a major influence on the effectiveness, and to develop methods for the evaluation of EWS. The reliability of the automated debris flow AS Illgraben is modeled in a Bayesian network (BN) and depends significantly on the sensor technology (including the number, the positioning and the type of sensors), the predefined thresholds and the failure probability of components and their dependencies among each other. The reliability achieved in the automated part of the Preonzo rockfall WS is also modeled in a BN and can, under most instances, be expressed as POD alone, because false alarms should not reduce the willingness of system operators to comply with warnings. The reliability evaluation in the non-automated part is complex and has to consider, among other factors, the accuracy of models and human decision-making.

Together, the classification and the framework approach enable a structured evaluation of EWS operated worldwide and provide a basis that is flexible enough to cover all needs associated with future developments in the field of EWS.

9.2 Outlook

In the future, two main areas should be further developed to improve the applicability and benefits of the framework approach.

First, the framework approach should be enhanced with a method enabling the quantification of the reliability achieved with non-automated EWS parts. Such a method should consider all major factors that influence the reliability, such as human decision-making and the model accuracy that increases when the lead time decreases. The method should express the reliability in terms of POD and PFA. Moreover, it should consider both the inherent and technical reliability. The technical reliability is less relevant for non-automated parts, but should be considered because the availability of sensors determines the quality of the database and of the associated model accuracy. Although a trend towards increased automation of decision procedures can be observed, human decision-making should, besides the model accuracy, be a central part for the assessment of the inherent reliability.

A second major area of future works should aim at the development of a software tool that enables a convenient evaluation of the reliability and effectiveness achieved with EWS. The software tool can be developed following the steps defined in the three parts of the framework approach. The reliability for automated system parts of EWS could be assessed with a BN in the background. The user would have to specify the class of EWS and those parameters that influence the reliability of the system. This would include the system components, their estimated failure probabilities, redundancies and dependencies, thresholds and probabilities that those thresholds are exceeded given an event or not. The software could also provide the opportunity to identify the optimal decision criteria of an EWS. In this case, the user would have to assign costs for false alarms, misses, hits and correct detections. To develop a comprehensive software tool, results gained in work area one, the method enabling the quantification of automated parts, would have to be translated in the same software environment. Such a software tool would support decision-makers in quantifying and optimizing the effectiveness of EWS to compare them with alternative measures of an integrated risk management approach and to identify optimal risk reduction strategies.

Bibliography

AGS: Landslide Risk Management Concepts and Guidelines, Australian Geomechanics Society, 2000.

Aguilera, P. A., Fernández, A., Fernández, R., Rumí, R., and Salmerán, A.: Bayesian networks in environmental modelling, Environmental Modelling and Software, 26, 1376–1388, 2011.

Alfieri, L., Burek, P., Dutra, E., Krzeminski, B., Muraro, D., Thielen, J., and Pappenberger, F.: GloFAS - global ensemble streamflow forecasting and flood early warning, Hydrology and Earth System Sciences, 17, 1161–1175, 2013.

Allen, R. M.: The ElarmS earthquake early warning methodology and application across California, in: Earthquake early warning systems, pp. 21–43, Springer, 2007.

Arattano, M. and Marchi, L.: Systems and sensors for debris-flow monitoring and warning, Sensors, 8, 2436–2452, 2008.

Badoux, A., Graf, C., Rhyner, J., Kuntner, R., and McArdell, B. W.: A debris-flow alarm system for the Alpine Illgraben catchment: design and performance, Natural Hazards, 49, 517–539, 2009.

Balbi, S., Villa, F., Mojtahed, V., and Giupponi, C.: Estimating the Benefits of Early Warning Systems in Reducing Urban Flood Risk to People: A Spatially Explicit Bayesian Model, in: Proceedings of the 7th International Congress on Environmental Modelling and Software, San Diego, edited by Ames, D., Quinn, N., and Rizzoli, A., 2014.

Bell, R., Mayer, J., Pohl, J., Greiving, S., and T., G.: Integrative Frühwarnsysteme für gravitative Massenbewegungen (ILEWS): Monitoring, Modellierung, Implementierung, Klartext Verlag, 2010.

Bensi, M., Kiureghian, A. D., and Straub, D.: Efficient Bayesian network modeling of systems, Reliability Engineering & System Safety, vol. 112, 200–213, 2012.

Blake, E. S. and Kimberlain, T.: Eastern North Pacific Hurricane Season of 2011, Monthly Weather Review - American Meteorological Society, 141, 1397–1412, 2013.

Blanchard, B. S. and Fabrycky, W. J.: Systems Engineering and Analysis, Prentice Hall International Series in Industrial & Systems Engineering, Pearson Education, Inc., New York, 5th edn., 2011.

Blaser, L., Ohrnberger, M., Riggelsen, C., Babeyko, A., and Scherbaum, F.: Bayesian networks for tsunami early warning, Geophysical Journal International, 185, 1431–1443, 2011.

Blikra, L. H.: The Åknes rockslide; monitoring, threshold values and early-warning, in: Proceedings, 10th International Symposium on Landslides and Engineered Slopes, Xian, China, vol. 2, pp. 1089–1094, 2008.

Bliss, J. P., Gilson, R. D., and Deaton, J. E.: Human probability matching behaviour in response to alarms of varying reliability, Ergonomics, 38, 2300–2312, 1995.

Borga, M., Anagnostou, E., Blöschl, G., and Creutin, J.-D.: Flash flood forecasting, warning and risk management: the HYDRATE project, Environmental Science & Policy, 14, 834–844, 2011.

Böse, M., Erdik, M., and Wenzel, F.: A New Approach to Earthquake Early Warning, in: Earthquake Early Warning Systems, pp. 65–83, Springer, 2007.

Brennan, M.: Tropical Cyclone Report Hurricane Jova, National Hurricane Center, 2012.

Breznitz, S.: Cry wolf: The psychology of false alarms, Erlbaum, Hillsdale, NJ, 1989.

Bründl, M., Romang, H., Bischof, N., and Rheinberger, C.: The risk concept and its application in natural hazard risk management in Switzerland, Natural Hazards and Earth System Sciences, 9, 801–813, 2009.

Bründl, M.: EconoMe-Develop–a software tool for assessing natural hazard risk and economic optimisation of mitigation measures, in: Proceedings, 2012 International Snow Science Workshop, Anchorage, Alaska, 2012.

Bründl, M. and Heil, B.: Reliability analysis of the Swiss avalanche warning system, in: Applications of Statistics and Probability in Civil Engineering - Proceedings of the 11th International Conference on Applications of Statistics and Probability in Civil Engineering, Zürich, edited by Faber, M., Köhler, J., and Nishijima, K., pp. 881–887, CRC Press an imprint of the Taylor & Francis Group, Zürich, 2011.

Brunetti, M., Peruccacci, S., Rossi, M., Guzzetti, F., Reichenbach, P., Ardizzone, F., Cardinali, M., Mondini, A., Salvati, P., Tonelli, G., et al.: A prototype system to forecast rainfall induced landslides in Italy, in: Proceedings of the 1st Italian Workshop on Landslides, edited by: Picarelli, L., Tommasi, P., Urciuoli, G., and Versace, P., Rainfall-Induced Landslides: mechanisms, monitoring techniques and nowcasting models for early warning systems, Naples, vol. 1, pp. 157–161, 2009.

Burkett, E. R., Given, D., and Jones, L.: ShakeAlert-An Earthquake Early Warning System for the United States West Coast: Fact Sheet 2014-3083, U.S. Geological Survey, 2014.

Calvello, M., Piciullo, L., Paes, N., Magalhaes, M., Lacerda Willy, A., et al.: The Rio de Janeiro early warning system for rainfall-induced landslides: Analysis of performance for the years 2010–2013, International Journal of Disaster Risk Reduction, 2014.

Carsell, K., Pingel, N., and Ford, D.: Quantifying the Benefit of a Flood Warning System, Natural Hazards Review, 5, 131–140, 2004.

Clinton, J., Cauzzi, C., Fäh, D., Michel, C., Zweifel, P., Olivieri, M., Cua, G., Haslinger, F., and Giardini, D.: The current state of strong motion monitoring in Switzerland, in: Earthquake Data in Engineering Seismology, pp. 219–233, Springer, 2011.

Cloke, H. and Pappenberger, F.: Ensemble flood forecasting: a review, Journal of Hydrology, 375, 613–626, 2009.

Conedera, M., Pezzatti, G., Calabrese, R., and Brini, M.: Final Report of the Experimental Phase, 2 FireLess 2 System, Enveve and Swiss Federal Institute for Forest, Snow and Landscape Research WSL, 2011.

CSEP: CSEP Tests, Collaboratory for the Study of Earthquake Predictability, URL `http://cseptesting.org/tests`, last accessed: January 2015, 2015.

Cyranoski, D.: Why Japan missed volcano's warning signs, Nature: International Weekly Journal of Science, 29 September, 2014.

Dai, F., Lee, C., and Ngai, Y. Y.: Landslide risk assessment and management: an overview, Engineering Geology, 64, 65–87, 2002.

Davies, D. K., Vosloo, H., Vannan, S. S., and Frost, P. E.: Near real-time fire alert system in South Africa: from desktop to mobile service, in: Proceedings of the 7th ACM conference on designing interactive systems, pp. 315–322, ACM, 2008.

Davies, D. K., Ilavajhala, S., Wong, M., and Justice, C. O.: Fire information for resource management system: archiving and distributing MODIS active fire data, Geoscience and Remote Sensing, 47, 72–79, 2009.

De Groot, W. J., Goldammer, J. G., Justice, C. O., Lynham, T. J., Csiszar, I. A., and San-Miguel-Ayanz, J.: Implementing a global early warning system for wildland fire, in: Proceedings of the VI International Conference on Forest Fire Research, ADAI/CEIF University Coimbra, Portugal, 2010.

Dejoy, D. M., Cameron, K. A., and lindsay, J. D.: Postexposure evaluation of warning Effectiveness: a review of field studies and population-based research, in: Handbook of Warnings (Human Factors & Ergonomics), edited by S.Wogalter, M., pp. 35–48, Lawrence Erlbaum Associates, 2006.

D'Orsi, R., Feijó, R., and Paes, N.: 2.500 Operational days of Alerta Rio System: History and Technical Improvements of Rio de Janeiro Warning System for Severe Weather, in: International Symposium on Landslides, vol. 9, pp. 831–836, 2004.

DSL: GeNIe & SMILE, Decision Systems Laboratory, https://dslpitt.org/genie/, URL `https://dslpitt.org/genie/`, last accessed: June 2014, 2013.

Einstein, H. and Sousa, R.: Warning systems for natural threats, in: Proceedings Geohazards, Engineering Conferences International, edited by Nadim, F., Pöttler, R., Einstein, H., Klapperich, H., and Kramer, S., 2006.

Fawcett, T.: An introduction to ROC analysis, Pattern recognition letters, 27, 861–874, 2006.

Fell, R., Ho, K., Lacasse, S., and Leroi, E.: State of the Art Paper 1: A framework for landslide risk assessment and management, in: Proceedings of the International Conference on Landslide Risk Management, Vancouver, Canada, vol. 31, 2005.

FOCP: Risk Cycle, Swiss Feder Office for Civil Protection, URL `http://www.planat.ch/en/specialists/risk-management/`, last accessed: January 2015, 2012.

FOCP: Project REWARN - Availability of telecommunication systems, Swiss Federal Office for Civil Protection, 2013a.

FOCP: Leitfaden KATAPLAN - Kantonale Gefährdungsanalyse und Vorsorge, FOCP Swiss Federal Office for Civil Protection., 2013b.

Friedl, M. A. and Brodley, C. E.: Decision tree classification of land cover from remotely sensed data, Remote sensing of environment, 61, 399–409, 1997.

Froese, C. R. and Moreno, F.: Structure and components for the emergency response and warning system on Turtle Mountain, Alberta, Canada, Natural Hazards, 70, 1689–1712, 2011.

Fuchs, S., Thöni, M., McAlpin, M. C., Gruber, U., and Bründl, M.: Avalanche hazard mitigation strategies assessed by cost effectiveness analyses and cost benefit analyses-evidence from Davos, Switzerland, Natural Hazards, 41, 113–129, 2007.

Fukuzono, T.: Recent studies on time prediction of slope failure, Landslide News, 4, 1990.

Gasparini, P. and Manfredi, G.: Development of Earthquake Early Warning Systems in the European Union, in: Early Warning for Geological Disasters - Scientific Methods and Current Practice, edited by Wenzel, F. and Zschau, J., pp. 89–102, Springer Verlag, 2014.

GeoNet: Monitoring Methods, GeoNet, http://info.geonet.org.nz/display/volc/Monitoring+Methods, URL `http://info.geonet.org.nz/display/volc/Monitoring+Methods`, last accessed: December 2014, 2014.

GEOPRAEVENT AG: Murgang - Alarmanlage Höfjibach Flüela Passstrasse, Geotest AG, 2009.

GEOPRAEVENT AG: Plaine Morte (Gletscherseen), URL `http://www.geopraevent.ch/messmethoden/gletscherseen-plaine-morte/`, last accessed: March 2015, 2015.

GITEWS: Concept, Helmholtz-Zentrum Potsdam Deutsches GeoForschungsZentrum GFZ, URL `http://www.gitews.org/en/concept/`, last accessed: March 2015, 2015.

Glantz, M. H.: Usable science 8: early warning systems: does and dont's, in: Report of workshop, pp. 20–23, 2004.

Graf, C.: Picture Illgraben, Swiss Federal Institute for Forest, Snow and Landscape Research WSL.

Grasso, V., Beck, J., and Manfredi, G.: Automated decision procedure for earthquake early warning, Engineering Structures, 29, 3455 – 3463, 2007.

Grasso, V. F. and Singh, A.: Early Warning Systems: State-of-Art Analysis and Future Directions, Division of Early Warning and Assessment (DEWA), United Nations Environment Programme (UNEP), 2009.

Groot, W., Wotton, B., and M.D., F.: Wildland Fire Danger Rating and Early Warning Systems, in: Wildfire Hazards, Risks, and Disasters, edited by Paton, D., pp. 207–228, Elsevier, 1 edn., 2015.

Gubler, H.: Five years experience with avalanche-, mudflow-, and rockfall-alarm systems in Switzerland, in: Proceedings of the international snow science workshop (ISSW), Big Sky, Montana, 2000.

Guha-Sapir, D., Santos, I., and Borde, A.: The economic impacts of natural disasters, Oxford University Press, 2013.

Hamilton, R.: Report on Early Warning Capabilities for Geological Hazards, IDNDR Early Warning Programme, 1997.

Hardy, J., Gourley, J. J., Kain, J., Clark, A., Novak, D., and Hong, Y.: Probabilistic Flash Flood Forecasting using Stormscale Ensembles, in: AGU Fall Meeting Abstracts, vol. 1, p. 1582, 2013.

Hashimoto, T., Stedinger, J. R., and Loucks, D. P.: Reliability, resiliency, and vulnerability criteria for water resource system performance evaluation, Water resources research, 18, 14–20, 1982.

Hattenberger, D. and Wöllik, A.: (Naturgefahren-) Mess-und Frühwarnsysteme: Einzelne rechtliche Aspekte, Baurechtliche Blätter: bbl, 11, 89–101, 2008.

Heil, B., Petzold, I., Romang, H., and Hess, J.: The common information platform for natural hazards in Switzerland, Natural Hazards, 70, 1673–1687, 2014.

HEPEX: Operational HEPS systems around the globe, Hydrologic Ensemble Prediction Experiment, URL `http://hepex.irstea.fr/operational-heps-systems-around-the-globe/`, last accessed: December 2014, 2013.

Hess, J. and Schmidt, F.: Towards optimised early warning developments in Switzerland, in: 12th conference INTERPRAEVENT 2012, 2012.

Hilker, N., Badoux, A., and Hegg, C.: The Swiss flood and landslide damage database 1972–2007, Natural Hazards and Earth System Science, 9, 913–925, 2009.

Hincks, T. K., Komorowski, J.-C., Sparks, S. R., and Aspinall, W. P.: Retrospective analysis of uncertain eruption precursors at La Soufrière volcano, Guadeloupe, 1975–77: volcanic hazard assessment using a Bayesian Belief Network approach, Journal of Applied Volcanology, 3, 1–26, 2014.

Huggel, C., Clague, J. J., and Korup, O.: Is climate change responsible for changing landslide activity in high mountains?, Earth Surface Processes and Landforms, 37, 77–91, 2012.

Hungr, O. and Evans, S.: The occurrence and classification of massive rock slope failure, Felsbau, 22, 16–23, 2004.

IEEE: Std1413.1-2002 Guide for Selecting and Using reliability Prediction based on 1413, The Institute of Electrical and Electronics Engineers, Inc., 2002.

IEEE: Std 1413-2010 - Standard Framework for Reliability Prediction of Hardware, The Institute of Electrical and Electronics Engineers, Inc., 2010.

Intrieri, E., Gigli, G., Mugnai, F., Fanti, R., and Casagli, N.: Design and implementation of a landslide early warning system, Engineering Geology, 147, 124–136, 2012.

Intrieri, E., Gigli, G., Casagli, N., and Nadim, F.: Brief communication "Landslide Early Warning System: toolbox and general concepts", Natural Hazards and Earth System Sciences, vol. 13, pp. 85–90, 2013.

IRV: Durchschnittlicher Anteil der Ursachen an der Schadenhöhe im Zeitraum 2004 - 2013, Interkantonale Rückversicherungsverband, URL `www.irv.ch/IRV/Services/Statistik/Elementar/Ursachen.aspx`, last accessed: October 2014, 2014.

Jackson, P.: Introduction to expert systems, Addison-Wesley Longman Publishing Co., Inc., 1990.

Jensen, F. V. and Nielsen, T. D.: Bayesian networks and decision graphs, Information Science and Statistics, Springer Science + Business Media, New York, 2 edn., 2007.

JMA: Earthquake Early Warning System, Japan Meteorological Agency, URL `http://www.jma.go.jp/jma/en/Activities/earthquake.html`, last accessed: December 2014, 2014.

Johnson, M., Newstead, S., Charlton, J., and Oxley, J.: Riding through red lights: The rate, characteristics and risk factors of non-compliant urban commuter cyclists, Accident Analysis & Prevention, 43, 323–328, 2011.

Krautblatter, M. and Moore, J. R.: Rock slope instability and erosion: toward improved process understanding, Earth Surface Processes and Landforms, 39, 1273–1278, 2014.

Krautblatter, M., Funk, D., and Günzel, F. K.: Why permafrost rocks become unstable: a rock ice mechanical model in time and space, Earth Surface Processes and Landforms, 38, 876–887, 2013.

Krähenbühl, R.: Der Felssturz, der sich auf die Stunde genau ankündigte, Bull. Angew. Geol, 11, 49–63, 2006.

Kristensen, L., Blikra, L., and Hole, J.: Åknes: State of instrumentation and data analysis, Åknes/Tafjord Early Warning Centre, 2010.

Krzysztofowicz, R., Kelly, K., and Long, D.: Reliability of Flood Warning Systems, Journal of Water Resources Planning and Management, 120, 906–926, 1994.

Lacasse, S., Eidsvik, U., Nadim, F., Hoeg, K., and Blikra, L. H.: Event tree analysis of Åknes rock slide hazard, in: 4th Canadian conference on geohazards, pp. 20–24, 2008.

Lall, S. V. and Deichmann, U.: Density and disasters: economics of urban hazard risk, The World Bank Research Observer, 2011.

Langseth, H. and Portinale, L.: Bayesian networks in reliability, Reliability Engineering and System Safety, 92, 92–108, 2007.

Lauterjung, J., Münch, U., and Rudloff, A.: The challenge of installing a tsunami early warning system in the vicinity of the Sunda Arc, Indonesia, Natural Hazards and Earth System Sciences, 10, 641–646, 2010.

Legg, T. P. and Mylne, K. R.: Early warnings of severe weather from ensemble forecast information, Weather Forecasting, 19, 891–906, 2004.

Lehning, M., Bartelt, P., Brown, B., Russi, T., Stöckli, U., and Zimmerli, M.: A network of automatic weather and snow stations and supplementary model calculations providing snowpack information for avalanche warning, in: Proceedings of the International Snow Science Workshop: a merging of theory and practice, September, vol. 27, pp. 225–233, 1998.

Leonard, G. S., Johnston, D. M., Paton, D., Christianson, A., Becker, J., and Keys, H.: Developing effective warning systems: ongoing research at Ruapehu volcano, New Zealand, Journal of Volcanology and Geothermal Research, 172, 199–215, 2008.

Liechti, K., Zappa, M., Fundel, F., and Germann, U.: Probabilistic evaluation of ensemble discharge nowcasts in two nested Alpine basins prone to flash floods, Hydrological Processes, 27, 5–17, 2013.

Loew, S., Gischig, V., Moore, R. J., and Keller-Signer, A.: Monitoring of potentially catastrophic rockslides, in: Proc. of 11th Int. and 2nd North Am. Symp. on Landslides and Engineered Slopes, vol. 1, pp. 101–116, 2012.

Margreth, S. and Romang, H.: Effectiveness of mitigation measures against natural hazards, Cold Regions Science and Technology, 64, 199–207, 2010.

Martina, M., Todini, E., and Libralon, A.: A Bayesian decision approach to rainfall thresholds based flood warning, Hydrology and earth system sciences, 10, 413–426, 2006.

Marzocchi, W., Sandri, L., and Selva, J.: BET_EF: a probabilistic tool for long-and short-term eruption forecasting, Bulletin of Volcanology, 70, 623–632, 2008.

Mass, C.: Nowcasting: The Next Revolution in Weather Prediction, Bulletin of the American Meteorological Society, 2011.

McClung, D. and Schaerer, P. A.: The avalanche handbook, The Mountaineers Books, 2006.

Medina-Cetina, Z. and Nadim, F.: Stochastic design of an early warning system, Georisk: Assessment and Management of Risk for Engineered Systems and Geohazards, 2, 223–236, 2008.

MetOffice: Weather warnings guide, URL `http://www.metoffice.gov.uk/guide/weather/warnings`, lastaccessed: December 2014, 2014a.

MetOffice: First steps, Met Office, URL `http://www.metoffice.gov.uk/learning/science/first-steps`, last accessed: December 2014, 2014b.

Michoud, C., Bazin, S., Blikra, L., Derron, M.-H., and Jaboyedoff, M.: Experiences from site-specific landslide early warning systems, Natural Hazards and Earth System Sciences, 13, 2013.

Moran, S. C., Freymueller, J. T., LaHusen, R. G., McGee, K. A., Poland, M. P., Power, J. A., Schmidt, D. A., Schneider, D. J., Stephens, G., Werner, C. A., et al.: Instrumentation recommendations for volcano monitoring at US volcanoes under the National Volcano Early Warning System, US Geological Survey, 2008.

Nakamura, H., Horiuchi, S., Wu, C.and Yamamoto, S., and Rydelek, P. A.: Evaluation of the real-time earthquake information system in Japan, Geophysical Research Letters, 36, 2009.

Nakamura, Y. and Saita, J.: UrEDAS, the earthquake warning system: Today and tomorrow, in: Earthquake Early Warning Systems, pp. 249–281, Springer, 2007.

NASA: FIRMS Web Fire Mapper, URL `https://firms.modaps.eosdis.nasa.gov/firemap/`, last accessed: February 2015, 2015.

Neal, R., Boyle, P., Grahame, N., Mylne, K., and Sharpe, M.: ensemble based first guest support towards a risk-based severe weather warning service, Meteorological Applications, 21, 563–577, 2013.

Obrusnik, I.: Early warning for flash floods, Proceedings of International Workshop 2010, Czech Hydrometeorological Institut and Czech National Committee for Disaster Reduction, 2011.

Oliveros, A. Q., Carniel, R., Tárraga, M., and Aspinall, W.: On the application of hidden markov model and bayesian belief network to seismic noise at las canadas caldera, tenerife, spain, Chaos, Solitons & Fractals, 37, 849–857, 2008.

Ozaki, T.: Outline of the 2011 off the Pacific coast of Tohoku Earthquake (M (w) 9. 0) -Tsunami warnings/advisories and observations, Earth, planets and space, 63, 827–830, 2011.

Pate-Cornéll, M. E.: Warning Systems in Risk Management, Risk Analysis, 6, 223–234, 1986.

Penning-Rowsell, E., Johnson, C., Tunstall, S., Tapsell, S., Morris, J., Chatterton, J., and Green, C.: The Benefits of Flood and Coastal Risk Management: A Handbook of Assessment Techniques, Middlesex University Press, 2005.

Peterson, W., Birdsall, T., and Fox, W.: The theory of signal detectability, IRE Professional Group on Information Theory, 4, 171–212, 1954.

Petley, D. and Petley, D.: On the initiation of large rockslides: perspectives from a new analysis of the Vaiont movement record, in: Landslides from Massive Rock Slope Failure, edited by Evans, S., Scarascia Mugnozza, G., Strom, A., and Hermanns, R. L., pp. 77–84, Springer, 2006.

Petley, D., Higuchi, T., Dunning, S., Rosser, N., Petley, D., Bulmer, M., and Carey, J.: A new model for the development of movement in progressive landslides, in: International conference on landslide risk management. Taylor & Francis Ltd., Vancouver, pp. 350–358, 2005a.

Petley, D. N., Higuchi, T., Petley, D. J., Bulmer, M. H., and Carey, J.: Development of progressive landslide failure in cohesive materials, Geology, 33, 201–204, 2005b.

Poolman, E., Rautenbach, H., and Vogel, C.: Application of probabilistic precipitation forecasts from a deterministic model towards increasing the lead-time of flash flood forecasts in South Africa, Water SA, 40, 729–738, 2014.

Price, D. A., Wynn, A., Harrison, T., Pollard, O., Pierce, C., Cole, S. J., and Moore, R. J.: Operational flash flood forecasting in England: quantifying flood risk using radar-based nowcasts and high resolution NWP forecasts, in: 2014 International Weather Radar and Hydrology Symposium, 2014.

Rageth, T., ed.: Frühwarndienste Stand der Kenntnisse und Anwendungsbeispiele, FAN, Forstliche Arbeitsgruppe Naturgefahren, 1998.

Rappaport, E. N., Franklin, J. L., Avila, L. A., Baig, S. R., Beven II, J. L., Blake, E. S., Burr, C. A., Jiing, J.-G., Juckins, C. A., Knabb, R., Landsea, C. W., Mainelli, M., Mayfield, M., McAdie, C. J., Pasch, R., Sisko, C., Stewart, S. R., and Tribble, A. N.: Advances and challenges at the national hurricane center, Weather Forecasting, 24, 395–419, 2009.

Reichert, B.: AutoWARN - Automatische Unterstützung der Herausgabe von Unwetterwarnungen, promet, 35, Nr.1/2, 98–103, 2010.

Reiweger, I., Mayer, K., Steiner, K., Schweizer, J., and Dual, J.: Measuring and localizing acoustic emission events in snow prior to fracture, Cold Regions Science and Technology, 2014.

Rheinberger, C. M.: Learning from the past: statistical performance measures for avalanche warning services, Natural Hazards, 65, 1519–1533, 2013.

Rogers, D. and Tsirkunov, V.: Global Assessment Report on Disaster Risk Reduction. Costs and Benefits of Early Warning Systems, ISDR and World Bank, 2010.

Romang, H.: Wirkung von Schutzmassnahmen, Nationale Plattform für Naturgefahren PLANAT, Bern, 2008.

Rose, N. D. and Hungr, O.: Forecasting potential rock slope failure in open pit mines using the inverse-velocity method, International Journal of Rock Mechanics and Mining Sciences, 44, 308–320, 2007.

Rosenbloom, T.: Crossing at a red light: Behaviour of individuals and groups, Transportation research part F: traffic psychology and behaviour, 12, 389–394, 2009.

Rossi, M., Peruccacci, S., Brunetti, M., Marchesini, I., Luciani, S., Ardizzone, F., Balducci, V., Bianchi, C., Cardinali, M., Fiorucci, F., et al.: SANF: National warning system for rainfall-induced landslides in Italy, in: 11th Int. Symp. Landslides, 2012.

Safeland: Guidelines for landslide susceptibility, hazard and risk assessment and zoning. Deliverable D2.4, SafeLand Project - Living with landslide risk in Europe: Seventh Framework Programme for research and technological development (FP7) of the European Comission, 2011.

SafeLand: Quantitative risk-cost-benefit analysis of selected mitigation options for two case studies. Deliverable 5.3, SafeLand Project - Living with landslide risk in Europe: Seventh Framework Programme for research and technological development (FP7) of the European Comission, 2012.

Saita, J. and Nakamura, Y.: UrEDAS: the early warning system for mitigation of disasters caused by earthquakes and tsunamis, in: Early Warning Systems for Natural Disaster Reduction, pp. 453–460, Springer, 2003.

Saito, M.: Forecasting time of slope failure by tertiary creep, in: Proceedings of the 7th International Conference on Soil Mechanics and Foundation Engineering, vol. 2, pp. 677–683, 1969.

Sättele, M. and Bründl, M.: Praxishilfe für den Einsatz von Frühwarnsystemen für gravitative Naturgefahren, WSL-Institut für Schnee-und Lawinenforschung SLF, Bundesamt für Bevölkerungsschutz, in print.

Sättele, M. and Meier, L.: Elektronisch warnen, TEC21, 31-32, 16–21, 2013.

Sättele, M., Bründl, M., and Straub, D.: A classification of warning system for natural hazards, in: 10th International Probabilistic Workshop, edited by Moormann, C., Huber, M., and Proske, D., pp. 257–270, Institut für Geotechnik der Universität Stuttgart, Stuttgart, 2012a.

Sättele, M., Bründl, M., and Straub, D.: Warning and alarm systems for natural hazards - A classification and generic system break-down, in: Academia Raetica (ed) Program & Abstracts, p. S. 29, 2012b.

Sättele, M., Bründl, and Straub, D.: Bayesian Networks to Quantify the reliability of a debris flow alarm system, in: Proc. 11th International Conference on Structural Safety & Reliability, edited by Deodatis, G., Ellingwood, B., and Frangopol, D., 2013a.

Sättele, M., Bründl, M., and Straub, D.: Early warning, warning or alarm systems for natural hazards? A generic classification, in: Geophysical Research Abstracts Vol.15, 2013b.

Sättele, M., Bründl, M., and Straub, D.: Reliability analyses provide guidance to cost-efficient early warning systems for natural hazards, in: Academia Raetica (ed) Program and Abstracts, 2014a.

Sättele, M., Bründl, M., and Straub, D.: Early Warning Systems for Natural Hazards: Reliability Analyses and Guidance for Decision Makers, in: Proc. INTERPRAEVENT 2014 in the Pacific Rim - Natural Disaster Mitigation to Establish Society with the Resilience, edited by Fujita, M., 2014b.

Sättele, M., Bründl, M., and Straub, D.: Quantifying the effect of early warning systems on natural hazard risk, in: Inproceedings ICASP 2015, accepted,a.

Sättele, M., Krautblatter, M., Bründl, M., and Straub, D.: Forecasting rock slope failure: How reliable and effective are warning systems?, Landslides, accepted,b.

Sättele, M., Straub, D., and Bründl, M.: A framework approach for quantifying the effectiveness of early warning systems for natural hazards, in preparation.

Sättele, M., Bründl, M., and Straub, D.: Reliability and effectiveness of warning systems for natural hazards: concept and application to debris flow warning, Reliability Engineering and System Safety, in press.

SBB: Naturgefahrenanlagen - kurze Information über die NGA Anlagen, Swiss Federal Railway Company SBB, 2011.

Schanze, J.: Flood risk management: a basic framework, in: Flood risk management: hazards, vulnerability and mitigation measures, edited by Schanze, J., Zeman, E., and Marsalek, J., pp. 1–20, Springer, 2006.

Schleiss, M. and Berne, A.: Stochastic space–time disaggregation of rainfall into DSD fields, Journal of Hydrometeorology, 13, 1954–1969, 2012.

Schmidt, R.: Warnsysteme in Wildbacheinzugsgebieten, Ph.D. thesis, Institut für Alpine Naturgefahren und Forstliches Ingenieurwesen, Universität für Bodenkultur, Wien, 2002.

Schröter, K., Velasco, C., Nachtnebel, H. P., Bianca, H., Beyene, M., Rubin, C., and Gocht, M.: Effectiveness and Efficiency of Early Warning Systems for Flash-Floods (EWASE), CRUE Funding Initiative on Flood Risk Management Research, 2008.

Shachter, R. D.: Evaluating influence diagrams, Operations research, 34, 871–882, 1986.

Sherburn, S. and Bryan, C.: The Eruption Detection System: Mt. Ruapehu, New Zealand, Seismological Research Letters, 70, 505–511, 1999.

Simmons, K. M. and Sutter, D.: False Alarms, Tornado Warnings, and Tornado Casualties, Weather, Climate, and Society, 1, 38–53, 2009.

SKYE: Hydrological observations, Finnish Environment Institute, URL `http://www.environment.fi/en-US/Maps_and_statistics/Hydrological_observations`, last accessed: December 2014, 2013.

Smith, K.: Environmental Hazards Assessing Risk and Reducing Disaster, Routledge, 6 edn., 2013.

Špačková, O. and Straub, D.: Cost-benefit analysis for optimization of risk protection under budget constraints, Risk Analysis, 2014.

Spreafico, M.: Automatische Fernmelder im Stationsnetz der Landeshydrologie, Wasser Energie Luft, 3, 1972.

Spreafico, M., Weingartner, R., and Auer, M.: The Hydrology of Switzerland: Selected Aspects and Results, Federal Office for Water and Geology, 2005.

Stewart, M. G. and Melchers, R. E.: Probabilistic Risk Assessment of Engineering Systems, Chapman and Hall, 1997.

Stähli, M., Sättele, M., Huggel, C., McArdell, B. W., Lehmann, P., Van Herwijnen, A., Berne, A., Schleiss, M., Ferrari, A., Kos, A., Or, D., and Springman, S.: Monitoring and prediction in Early Warning Systems (EWS) for rapid mass movements, Natural Hazards and Earth System Sciences, 2015.

Straub, D.: Natural hazards risk assessment using Bayesian networks, in: 9th International Conference on Structural Safety and Reliability ICOSSAR, edited by Augusti, G., Schuëller, G. I., and Ciampoli, M., Millpress, Rome, 2005.

Straub, D.: Lecture Notes Engineering Risk Analysis: Part E: Probabilistic models, Technische Universität München, 2012.

Straub, D. and Der Kiureghian, A.: Bayesian network enhanced with structural reliability methods: Methodology, Journal of engineering mechanics, 136, 1248–1258, 2010.

Sturny, R. A. and Bründl, M.: Reliability Analysis of a Glacier Lake Warning System Using a Bayesian Net, in: EGU General Assembly Conference Abstracts, vol. 15, p. 6750, 2013.

Sturny, R. A. and Bründl, M.: Bayesian Networks for Assessing the Reliability of a Glacier Lake Warning System in Switzerland., in: Extended Abstracts of the INTERPRAEVENT2014 in the Pacific Rim - Natural Disaster Mitigation to Establish Society with the Resilience, edited by Fujita, M., 2014.

Swets, J. A.: Signal detection theory and ROC analysis in psychology and diagnostics: Collected papers, Lawrence Erlbaum Associates, Inc, New Jersey, 1996.

SwissRe: Sigma: Natural catastrophes and man-made disasters in 2013: large losses from floods and hail; Haiyan hits the Philippines, Swiss Re Ltd Economic Research and Consulting, 2014.

SYKE: Hydrological forecasts and maps, Finnish Environment Institute, URL `http://www.environment.fi/en-US/Waters/Hydrological_situation_and_forecasts/Hydrological_forecasts_and_maps`, last accessed: December 2014, 2013.

Taylor, S. J., Bright, D., G., C., Bothwell, P., and R., N.: Using short range ensemble model data in national fire outlooks, in: Preprints, 4th Symp. Fire and Forest Meteor., 2003.

Techel, F. and Darms, G.: Schnee und Lawinen in den Schweizer Alpen - Hydrologisches Jahr 2012/13, WSL-Institut für Schnee- und Lawinenforschung SLF, 2014.

Thiebes, B.: Landslide analysis and early warning - Local and regional case study in the Swabian Alb, Germany, Ph.D. thesis, Universitat Wien, 2011.

Thielen, J., Bartholmes, J., Ramos, M.-H., and Roo, A.: The European flood alert system–Part 1: concept and development, Hydrology and Earth System Sciences, 13, 125–140, 2009.

UNDRO: Natural disasters and vulnerability analysis - Report of Expert Meeting, Office of the United Nations Disaster Relief Co-ordinator UNDRO, Geneva, 1980.

UNISDR: Hygo Framework for Action 2005-2015: Building the Resilience of nations and Communities to Disaster, United Nations Office for Disaster Risk Reduction (UNISDR), 2007a.

UNISDR: Terminology, The United Nationa Office for Disaster Risk Reduction, URL `http://www.unisdr.org/we/inform/terminology`, last accessed: November 2014, 2007b.

USGS: U.S. Geological Survey's Alert-Notification System for Volcanic Activity, U.S. Geological Survey's, 2014.

USGS: Lahar-Detection System, U.S. Geological Survey, URL `http://volcanoes.usgs.gov/activity/methods/hydrologic/lahardetection.php`, last accessed: January 2015, 2015a.

USGS: How We Monitor Volcanoes, U.S. Geological Survey, URL `http://volcanoes.usgs.gov/activity/methods/index.php`, last accessed: January 2015, 2015b.

Valenti, G.: Picture Preonzo, Sezione Forestale Ticino.

Van Aalst, M. K.: The impacts of climate change on the risk of natural disasters, Disasters, 30, 5–18, 2006.

Van Herwijnen, A. and Schweizer, J.: Monitoring avalanche activity using a seismic sensor, Cold Regions Science and Technology, 69, 165–176, 2011.

Vellinga, P. and van Verseveld, W. J.: Climate Change and Extreme Weather Events, WWF - World Wide Fund For Nature, 2000.

Vesely, W., Davis, T., Denning, R., and Saltos, N.: Measures of risk importance and their applications (NUREG/CR-3385, BM-2103), Office of Nuclear Regulatory Research, 1983.

Villagrán de Leon, J. C., Pruessner, I., and Breedlove, H.: Alert and Warning Frameworks in the Context of Early Warning Systems. A Comparative Review, Intersections No. 12. Bonn: United Nations University Institute for Environment and Human Security, 2013.

Vogel, K.: Applications of Bayesian networks in natural hazard assessments, Ph.D. thesis, Universitätsbibliothek, 2014.

Wegmann, M., Funk, M., Flotron, A., and Keusen, H.: Movement studies to forecast the time of breaking off of ice and rock masses, in: Early Warning Systems for Natural Disaster Reduction, edited by Zschau, J. and Küppers, A., pp. 565–568, Springer, 2003.

Wei, Y., Chamberlin, C., Titov, V. V., Tang, L., and Bernard, E. N.: Modeling of the 2011 Japan tsunami: Lessons for near-field forecast, Pure and Applied Geophysics, 170, 1309–1331, 2013.

Wetterhall, F., Pappenberger, F., Cloke, H. L., Thielen-del Pozo, J., Balabanova, S., Daňhelka, J., Vogelbacher, A., Salamon, P., Carrasco, I., Cabrera-Tordera, A., et al.: Forecasters priorities for improving probabilistic flood forecasts, Hydrology and Earth System Sciences Discussions, 10, 2215–2242, 2013.

Willenberg, H., Eberhardt, E., Loew, S., McDougall, S., and Hungr, O.: Hazard assessment and runout analysis for an unstable rock slope above an industrial site in the Riviera valley, Switzerland, Landslides, 6, 111–119, 2009.

WMO: Tropical Cyclone Forecaster Website - Advisory and Warning Centres, World Meteorological Organization, URL `http://severe.worldweather.wmo.int/TCFW/`, last accessed: January 2015, 2014.

Yang, T.-H.and Yang, S., Ho, J., Lin, G.-F., Hwang, G.-D., and Lee, C.-S.: Flash Flood Warnings Using the Ensemble Precipitation Forecasting Technique: A Case Study on Forecasting Floods in Taiwan Caused by Typhoons, Journal of Hydrology, 2014.

Zimmermann, M., Mani, P., Gamma, P., Gsteiger, P., Heiniger, O., and Hunziker, G.: Murganggefahr und Klimaänderung: ein GIS-basierter Ansatz: Projektschlussbericht im Rahmen des Nationalen Forschungsprogrammes" Klimaänderungen und Naturkatastrophen", Schlussbericht NFP 31, vdf Hochschulverlag AG an der ETH, 1997.